Phage Encapsulation as a Treatment for Vibriosis in Oyster Aquaculture

Submitted by Lucy Christine Witherall to the University of Exeter as a thesis for the degree of

Master's by Research in Biological Sciences

in September 2019

I certify that all material in this thesis which is not my own work has been identified and that no material has previously been submitted and approved for the award of a degree by this or any other university.

Signature: Lucy Witherall

Acknowledgements

I would like to thank Ben Temperton and Charles Tyler for their support and supervision during this degree. Thanks also to Ula Lapinska for her huge help in getting me started.

A special thanks to the members of the Temperton Lab and everyone in GP 211 for welcoming me and keeping me sane throughout. Thanks also to Caius Constable.

Finally, thanks to my family and Elliot for their never-ending support and encouragement.

Abstract

With our global population expected to increase to as much as 9.8 billion by 2050, strategies for obtaining worldwide food security become increasingly important. The oceans act as a generous resource for reaching our global nutrition targets, yet overfishing in recent decades has caused great harm, including localised population extinction, to fish and shellfish stocks. Aquaculture, the act of maintaining and farming marine or freshwater animal organisms, has become a popular alternative to wild fisheries. However, with a high demand for food sources, comes a move towards more intensive farming practices, whereby denser communities of farmed animals are kept in waters with high nutrient input. Such farming practices can favour pathogenic bacterial communities, which can cause disease in farmed animals and consequently lead to reduced stock numbers. Not only does this affect yield, but there can be further economic impacts to the detriment of those whose livelihoods depend on the aquaculture sector.

Traditionally, antibiotics have been used with abundance to treat disease in aquaculture, however overuse and misuse has led to a global rise in antibiotic resistance. This is particularly apparent in aquaculture, where antibiotics can be directly applied to organisms and also, easily accumulate within the water column. Therefore, as the global antibiotic crisis worsens, it has become ever more important to develop novel therapeutic alternatives. One such promising alternative is the use of bacteriophages (phages) – viruses which kill bacteria. However, application of phages requires more research to become commercially viable. Encapsulation of such phages may improve their therapeutic use through increased concentrations during application, improved stability and increased protection. Long term storage of encapsulated phages, e.g. after lyophilisation (freeze drying), would facilitate development of a robust phage library and enable rapid construction of bespoke phage cocktails, whereby distinct phages are combined to combat bacterial resistance. Droplet microfluidics is an emerging field, which can be used for the high-throughput encapsulation of bacteriophages, for use against bacterial infections, not only in aquaculture, but also in clinical settings.

Vibrio parahaemolyticus is a highly pathogenic bacterium, capable of infecting shellfish and subsequently cause gastroenteritis in humans. *V. parahaemolyticus* is commonly isolated from oysters, for example *Crassostrea gigas*, which is the most commonly farmed species of oyster in the UK, and there is increasing evidence of antibiotic resistance in *V. parahaemolyticus*.

This project aimed to evaluate the use of droplet microfluidics and subsequent freeze-drying in order to encapsulate bacteriophages specific for *V. parahaemolyticus,* a highly pathogenic bacterium, capable of infecting shellfish and subsequently cause gastroenteritis in humans. *V. parahaemolyticus* is commonly isolated from oysters, for example *Crassostrea gigas*, which is the most commonly farmed species of oyster in the UK and furthermore, there is increasing evidence of antibiotic resistance in *V. parahaemolyticus*. In order to develop of an encapsulated viral library for phage therapy of *V. parahaemolyticus,* the following four challenges needed to be addressed: (1) isolate novel vibriophages specific for *V. parahaemolyticus*, (2) develop a novel protocol for the synthesis of monodisperse sodium alginate microcapsules, using microfluidics, (3) encapsulate vibriophages in alginate droplets and (4) use such encapsulated phages to treat *V. parahaemolyticus* infection of *C. gigas*.

The genomes of four strains of *V. parahaemolyticus* (EXE V18/004, V12/024, V05/313 and V05/027) were sequenced. In total, 10 dsDNA high quality (category 5) prophage and 5 Inoviruses were detected and manually curated across the four genomes. Furthermore, in this instance the isolation of novel vibriophages was unsuccessful. Despite this, a novel protocol was developed for the synthesis of monodisperse alginate droplets, using a glass microfluidic device. Droplets were synthesised with an alginate concentration of 1 % (w/w) and collected in calcium chloride ($CaCl_2$) solution with a concentration of 2 % (w/w). Bacteriophage T4, vibriophage sm030 and vibriophage sm031 were successfully encapsulated within alginate microcapsules and later lyophilised. Lyophilised droplets containing bacteriophage T4, vibriophage sm030 or vibriophage sm031 were able to cause infection and reduce cell growth in broth cultures of *Escherichia coli* and *V. parahaemolyticus*, respectively. More research is needed into phage encapsulation in bacteriophage therapy before its widespread use.

Table of Contents

List of Figures

Figure 30 - Spot plaque assays carried out using filtrate from two cultures of *Escherichia coli* infected with either un-encapsulated and un-lyophilised T4 phage or encapsulated and lyophilised T4 phage

List of Tables

Abbreviations

AHPND	Acute hepatopancreatic necrosis disease
ARGs	Antibiotic-resistance genes
ATCC	American Type Culture Collection
BATS	Bermuda-Atlantic Time Series
BP	Base pair
CaEDTA	Calcium disodium ethylenediamine tetraacetate
DI	Deionised
dsDNA	Double-stranded DNA
HOT	Hawaii Ocean Time Series
IDs	Taxon identifiers
IMG	Integrated Microbial Genomes System
iTOL	Interactive Tree of Life
JGI	Joint Genome Institute
L	Lyophilised
LB	Lysogeny Broth
MB	Marine Broth
NB	Nutrient Broth
MilliQ	Deionised H_20
NCBI	National Center for Biotechnology Information
NL	Non-lyophilised
PBS	Phosphate-buffered saline
PDMS	Polydimethylsiloxane
rpm	Rounds per minute
ssDNA	Single-stranded DNA
T3SS	Type 3 Secretion System
Tdh	Thermostable direct hemolysin
Tdr	Thermostable direct hemolysin-related hemolysin
WEC	Western English Channel
WGS	Whole genome sequencing
W-O	Water-in-oil
Zot	Zonula occludens toxin

1 Literature Review

1.1 Aquaculture

As our global population continues to expand, with reports estimating an increase to 9.8 billion by 2050, we must develop sustainable methods for providing sufficient nutrition worldwide (UN DESA, 2017). A large proportion of this nutrition is derived from the oceans; 540 million people worldwide depend on either capture fisheries or aquaculture, not only as a source of sustenance but also as a primary source of income (FAO, 2016, 2018). In 2016, global fish production reached an estimated 171-8 million tonnes, with 36-47 % of this total production attributed to the aquaculture industry (FAO, 2018; Schiller *et al.*, 2018). In fact, the aquaculture sector continues to grow at an average annual rate of 5.8 % (Oyinlola *et al.*, 2018) and now provides more marine fish and invertebrates for human consumption than wild fisheries (FAO, 2016). In 2016, 37 countries world-wide produced more fish and marine or freshwater invertebrates from farmed aquaculture than wild fisheries (FAO, 2018).

However, increased demand from aquaculture production is concomitant with a rising pressure on the sector. This pressure has resulted in a shift from extensive farming practises, which involve the removal of predators and competitors, towards those which are intensive or semi-intensive, whereby on top of predator removal, all nutrition is provided and enhanced (Dawood & Koshio, 2016). Intensive practises also tend to favour dense concentrations of fish and invertebrates, with nutrient pollution and waste decreasing water quality. In turn, this escalates the likelihood of pathogen outbreaks and the spread of contagious disease caused by bacterial infection, which often results in large stock losses (ECDC, 2017; Watts *et al.*, 2017). In fact, disease may be considered the principal challenge to aquaculture. For example, recurrent problems with disease outbreaks have occurred recently in Thailand, causing exports in farmed shrimp to decline sharply (FAO, 2018). Since Thailand has been a leading exporter of farmed fish and marine invertebrates for decades, such declines may influence critical economies (USDA Foreign Agricultural Service, 2006).

The need to develop strategies for the successful control of disease in aquaculture is constantly increasing, not only in order to improve animal welfare, quality of fish stocks and increase yield, but also to benefit local, national and even global economies. Antibiotics are often the first port of call in the treatment of disease, yet their continued overuse has resulted in escalating problems with antimicrobial resistance (Watts *et al.*, 2017; FAO, 2018). Whilst research into our growing antibiotic issue is expanding, 90 % of global aquaculture is carried out in developing countries, which lack the resources to enforce limits on antibiotic use (Chuah *et al.*, 2016). Furthermore, there is a severe lack of data regarding antimicrobial use in aquaculture from all countries, meaning it is not possible to know the exact extent of this issue. Therefore, it is imperative that we are able to develop alternative therapeutic strategies for combating bacterial infections of commercially important species in aquaculture. The development of such techniques would not only benefit aquaculture in the Western World, but improve food security across the globe.

1.2 *Crassostrea gigas*

1.2.1 Basic Biology

Crassostrea gigas is an obligate size-selective feeder (Barille *et al*., 1997) that can ingest a wide range of different size particle (Dupuy *et al*., 1999). Most (95%) of particles ingested by *C. gigas* have been found to be in the range 2 – 20 µm (Barille *et al*., 1997) but particles of sizes up to 150 µm in length, width and diameter have been reported to be infested (Cognie *et al*., 2003).

1.2.2 Oyster Aquaculture

More than 60 % of aquaculture production involves the farming of marine molluscs and crustaceans and a number of countries from around the globe are dependent on mollusc mariculture (Forrest *et al.*, 2009; Oyinlola *et al.*, 2018). The European Union is the largest single market for bivalves and within this, oyster cultivation holds notable importance, in particular the farming of the Pacific oyster (*Crassostrea gigas*) (FAO, 2018). In fact, more than 1,000 tonnes of *C. gigas* have been recorded to be produced annually in the UK, with 67 % of this production exported internationally (Herbert *et al.*, 2012). In terms of economic

profit within the UK, *C. gigas* production has an estimated gross output of at least £13 million and a gross value added of £10.14 million, not including seed production (Herbert *et al.*, 2012; Humphreys *et al.*, 2014). These estimates are based on data collected from the 2011/12 UK Pacific oyster market and therefore are likely to have increased somewhat in more recent years. Since there is a lack of data on this matter, more research is necessary to reveal a more accurate representation of the current economic importance of *C. gigas* production in the UK.

C. gigas was first introduced in the UK for aquacultural purposes in 1965, to support the declining native flat oyster (*Ostrea edulis*) industry (Utting & Spencer, 1992). At the time of their establishment, it was considered that the coastal waters of the UK had too low a temperature to facilitate self-sustaining populations of *C. gigas* compared to native species, yet, warming coastal waters have resulted in many now-indigenous populations of *C. gigas* around the UK (Herbert *et al.*, 2012). In fact, estimated figures, which show a continual decline in *O. edulis* landings around the UK, suggest that native oyster populations in the UK are not recovering and regularly make up less than 10 % of total UK oyster production (Humphreys *et al.*, 2014). Contrary to this, over the last decade, farmed *C. gigas* production has seen a general upward trend and alongside mussel production, dominates shellfish aquaculture industry in the UK (Ellis *et al.*, 2012). Despite Wales providing the most tonnage of shellfish production in aquaculture, out of the UK nations, English shellfish industry is reported to have a higher value due to the increased per unit worth of Pacific oysters, further highlighting the economic importance of *C. gigas* to UK aquaculture industry (Ellis *et al.*, 2012).

Outside of economic value, oyster cultivation in the UK has a somewhat historical importance, especially in the South East and South West as improved transport links opened up the country (Neild, 1996). The first record figures in 1886 listed oyster landings in the UK as 3,500 tonnes (Spencer, 2002), yet overfishing resulted in the importation of oyster seed to replace stocks (Humphreys *et al.*, 2014). The oyster industry provided an abundance of work, in otherwise poor seaside towns and to this day, oyster farming is still celebrated, for example during the annually held Oyster Festival in Whitstable, Kent (Hall & Sharples, 2008).

Infectious diseases can be more common in marine environments than in terrestrial ecosystems. This can be seen particularly in aquaculture, where intensive farming conditions often lead to over-crowded areas, with poor water quality and high nutrient inputs. These conditions can result in high incidences of marine disease and therefore can lead to decreases in the economic value of such seafood. In fact, infectious marine diseases can cost billions in losses every year (Lafferty *et al.*, 2015). There is global demand for oysters as a luxury item, which pushes industry prices up and subsequently increases the value of oysters here in the UK (Ervynck *et al.*, 2003). Since the UK contributes to global exports of oysters, improving disease treatment in oyster aquaculture is of importance in its contribution to the UK economy.

1.3 Vibriosis in Aquaculture

With an increased intensity in shellfish farming comes an increased prevalence of disease, often caused by low water quality, due to increased nutrient input (Folke & Kautsky, 1992). In addition to this, changes in climate, which result in global rises in sea surface temperature, favour some pathogenic bacteria. For example, *Vibrio parahaemolyticus*, a Gram-negative, halophilic bacterium, is widely-disseminated throughout marine and estuarine environments and favours warm waters, often 15 °C or higher (Le Roux *et al.*, 2015; Powell *et al.*, 2013; Ceccarelli *et al.*, 2013; Letchumanan, Chan & Lee, 2014). *V. parahaemolyticus* is a human pathogen and the causative agent of acute gastroenteritis (Fujino *et al.*, 1953). Whilst clinical symptoms are non-life threatening, such as nausea, diarrhea and fever, gastroenteritis can lead to septicemia in susceptible patients and burdens the health service annually (Su & Liu, 2007; Nelapati, Nelapati & Chinnam, 2012; Sandmann *et al.*, 2017). Infection is particularly linked to the consumption of raw seafood, and *V. parahaemolyticus* has been isolated from a variety of seafoods globally, from both finfish and shellfish, especially mussels, scallops and oysters (Su & Liu, 2007). In fact, *V. parahaemolyticus* is able to infect all stages of the life-cycle of crustaceans and is highly pathogenic (Kalatzis *et al.*, 2018). Although *V. parahaemolyticus* virulence has traditionally been poorly understood, pathogenic *V. parahaemolyticus* strains isolated from humans often carry one of, or both of, two virulence genes: thermostable direct hemolysin (*tdh*) and *tdh*-related hemolysin (*trh*), although, it should be noted that in rare cases

neither of these genes are present in bacteria isolated from infected patients (Letchumanan, Chan & Lee, 2014). Whilst these virulence markers are often found in the majority of human patients, less than 3% of *V. parahaemolyticus* strains isolated from environmental samples contain these genes (Martinez-Urtaza *et al.*, 2010). *V. parahaemolyticus* also expresses two type III secretion systems (T3SS1 and T3SS2), key virulence factors in the causation of gastroenteritis through interactions with the intestinal epithelia (Makino *et al.*, 2003; Zhang *et al.*, 2019a)). The expression of these virulence factors is tightly regulated through a quorum sensing cascade (Zhang *et al.*, 2019a). T3SS1 is expressed in all strains of *V. parahaemolyticus*, whereas T3SS2 is only expressed in strains determined as human clinical isolates (Angulo *et al.*, 2018).

V. parahaemolyticus has been isolated worldwide from Asia, Africa, America and more recently Europe (Newton *et al.*, 2012; Powell *et al.*, 2013; Ceccarelli *et al.*, 2013; Martinez-Urtaza *et al.*, 2018), with *V. parahaemolyticus* now determined as the lead causative agent for seafood-borne human gastroenteritis globally (Newton *et al.*, 2012; Martinez-Urtaza *et al.*, 2018). Previously, occurrence of *V. parahaemolyticus* infection in Europe has been rare and relative to the rest of the world, incidences have seldom been reported. However, better understanding of *V. parahaemolyticus* virulence, as well as increased global abundance, have caused an increase in reports of infection (Powell *et al.*, 2013; Le Roux *et al.*, 2015; Martinez-Urtaza *et al.*, 2018; Lopatek, Wieczorek & Osek, 2018b). Research suggests that the growth rate of *V. parahaemolyticus* is particularly affected by temperature; seasonal rises in seawater temperature result in increased abundance of *V. parahaemolyticus*, and infection is particularly common in countries that have a tropical climate (Martinez-Urtaza *et al.*, 2010). A warming climate and consequent rising seawater temperatures are likely to influence the distribution and abundance of *V. parahaemolyticus* worldwide. Increased seawater temperatures has been observed at a faster-than-average rate in coastal European seas (Dulvy *et al.*, 2008), which may help to explain the increase in *V. parahaemolyticus* infection. Due to the continuous rise in temperature in UK waters, accompanied with a higher rate of *V. parahaemolyticus* infection, it is therefore important to further understand this pandemic pathogen and develop novel strategies to combat its incidence in shellfish farmed for human consumption.

Aside from vibriosis, *V. parahaemolyticus* has more recently been determined as the causative agent of acute hepatopancreatic necrosis disease (AHPND) in shrimps (Lightner *et al.*, 2012; Tran *et al.*, 2013). AHPND is also often referred to as early mortality syndrome and has observed mortality rates of up to 100 % (Xiao *et al.*, 2017; Angulo *et al.*, 2018). First observed in China in 2009 (FAO, 2012), AHPND has been responsible for large economic losses in shrimp aquaculture across Asia, (Angulo *et al.*, 2018; Prachumwat *et al.*, 2018) due to early mortality in shrimp farms, typically within 20 to 30 days of stocking ponds with postlarvae or juveniles (Lightner *et al.*, 2012). However, losses have been observed as early as 10 days post-stocking (Varela, 2018). AHPND is caused by a unique strain of *V. parahaemolyticus* (Vp_{AHPND}), with a plasmid encoding deadly toxins PirA*vp* and PirB*vp*, which Vp_{AHPND} is able to transfer to other *Vibrio* species (Lai *et al.*, 2015; Devadas *et al.*, 2019). This disease has also been found to have reached Central America, particularly Mexico (Nunan *et al.*, 2014). Whilst no evidence of AHPND has been reported in oysters, it further emphasises the urgent need for the development of novel therapies against *V. parahaemolyticus*.

1.4 Antibiotic Resistance in Aquaculture

The antimicrobial resistance epidemic is a threat to global human health, with an estimated 23,000 deaths attributed to drug-resistant bacteria annually in the USA alone (Centers for Disease Control and Prevention, 2013). Despite this, antibiotic use is regulated differently country-to-country and there is no global standard for their continued use (Aslam *et al.*, 2018). Whilst resistance to antimicrobials, across any sector, is at least partly caused by antibiotic overuse and misuse in clinical settings, naturally-occurring processes, such as horizontal gene transfer, can also contribute to the development of antimicrobial resistance (Watts *et al.*, 2017). There is a multitude of entry sources for antimicrobials into the aquatic environment (Costanzo, Murby & Bates, 2005): clinical use by humans, especially in hospitals, results in antimicrobials entering lakes, rivers and coastal waters through sewage effluent; antimicrobials used in agriculture, including in farm animals, also enter the aquatic environment through sewage effluent, as well as in water run-off from the land (Santos & Ramos, 2018). This means that antibiotics do not necessarily have to be directly applied in aquaculture for there

to be an impact on the health of farmed species. In fact, the practise of aquaculture provides a 'hot-spot' for genetic exchange, primarily due to the release of pathogenic bacteria in waste effluents (Baquero, Martinez & Canto, 2008; Watts *et al.*, 2017). Such pathogenic bacteria often harbour antimicrobial resistance genes within genetic elements that are able to move, for example plasmids or transposons, which can then spread easily through an aquatic environment (Watts *et al.*, 2017). Ultimately, even in countries where antibiotic use in aquaculture farms is limited and highly regulated, external influences may increase the prevalence and impact of antimicrobial resistance to aquaculture

Antibiotic use in aquaculture can be categorised in one of three ways: (i) therapeutic, whereby they are applied to an established infection; (ii) prophylactic, whereby they are used to prevent infection and (iii) metaphylactic, whereby they are not only used to treat sick animals, but to prevent disease in uninfected animals (Chuah *et al.*, 2016). A majority of the antibiotics used in aquaculture are given to the entire population of animals, including sick, carrier and healthy individuals (Santos & Ramos, 2018). That is, most antimicrobial use in aquaculture is metaphylactic, particularly since antimicrobial drugs are most commonly administered through mixing with feed. However, ineffective metabolisation can result in the excretion of antibiotic active substances to the environment, where they are able to readily persist (Romero, Gloria & Navarrete, 2012). When you consider that most of, if not all, antibiotics used in aquaculture share similarities in structure and mode of action as those used clinically in humans, the issue of antibiotic resistance is a major cause for concern; marine and freshwater bacteria may develop resistance to antibiotics in the aquatic environment and then pass these antimicrobial genes on, mother to daughter cell (vertical gene transmission), or to other organisms through horizontal gene transfer. Not only does this increase the likelihood of antimicrobial drugs being unsuccessful in the treatment of disease in aquaculture but complicates the treatment of bacterial disease in humans. There are a number of routes through which humans can come into contact with aquatic pathogens, namely through the consumption of infected seafood, or as food handlers working in aquaculture. In the unfortunate case that an individual becomes infected by a bacterium that has developed resistance to one or multiple antimicrobial drugs,

the chance of successfully treating infection is greatly reduced (Smith, 2008; Done, Venkatesan & Halden, 2015; Watts *et al.*, 2017).

One example of this problem is the increasing resistance of Gram-negative bacteria against the antibiotic colistin. Colistin (otherwise known as polymyxin E) has been used to treat multidrug-resistant bacterial infections in humans for decades, and primarily works through disruption of the outer-cell and cytoplasmic membranes of bacterial targets (Storm, Rosenthal & Swanson, 1977). Although it has been accepted that vertical gene transmission occurs for colistin resistance, there have been little to no previous reports on the horizontal transfer of resistance by mobile genetic elements (Santos & Ramos, 2018). Unfortunately, recent reports provide evidence for the plasmid-mediated transfer of the *mcr-1* gene, which confers resistance to colistin (Hasman *et al.*, 2015; Liu *et al.*, 2016; Yang *et al.*, 2019). Antibiotic resistance in Gram-negative bacteria, such as *V. parahaemolyticus*, is increasing and therefore the need for research into alternative treatments for infection is more urgent than ever.

Since *V. parahaemolyticus* is not only an important human pathogen, but also responsible for extensive stock losses in aquaculture (Prachumwat *et al.*, 2018), antibiotics have been readily applied to combat infection. However, excessive antibiotic use, particularly in aquaculture, has resulted in the development of *Vibrio* spp. which are resistant to specific antibiotics, or even those which develop multidrug-resistance (Madhusudana Rao & Lalitha, 2015). Generally, Gram-negative bacteria have a number of mechanisms which aid in antibiotic-resistance, such as antibiotic deactivation, efflux mechanisms or modification of the target site (Reeve, Lombardo & Anderson, 2015), although mechanisms in *V. parahaemolyticus* are poorly documented and less understood. Despite this, data regarding *V. parahaemolyticus* resistance to antimicrobials has been recorded from all parts of the world (**Table 1**), including the USA and Canada, South America, Europe, Africa, the Middle-East, India, China and Southeast Asia. 75 % of *V*. *parahaemolyticus* isolates from around the world have demonstrated resistance to ampicillin and 68 % to streptomycin (Lopatek, Wieczorek & Osek, 2018a). Instances of resistance, which have been documented in V. parahaemolyticus, have been obtained from environmental, aquacultural, agricultural and clinical isolates (**Table 1**). Despite the current increase in

bacterial resistance to antibiotics, there has been a lack of progress in the discovery of new antimicrobial drugs, further stressing the urgent need for the development of alternatives to antibiotics (Payne *et al.*, 2007).

Table 1: Examples of antibiotic resistance in global *Vibrio parahaemolyticus* isolates.

Location	Antibiotics	References
Brazil	Ampicillin and cephalothin	(Silva *et al.*, 2018)
Canada	Ampicillin, cephalothin, erythromycin, kanamycin, piperacillin and streptomycin	(Banerjee & Farber, 2018)
China	Amikacin, ampicillin, cephazolin, chloramphenicol, streptomycin, tetracycline and trimethoprim	(He *et al.*, 2016; Jiang *et al.*, 2019; Zhang *et al.*, 2019b)
Egypt	Ampicillin, chloramphenicol, gentamicin, kanamycin and tetracycline	(Ahmed *et al.*, 2018)
India	Ampicillin, erythromycin, furazolidone, gentamicin, and streptomycin	(Bhattacharya, Choudhury & Kumar, 2000; Devi, Surendran & Chakraborty, 2009; Silvester, Alexander & Ammanamveetil, 2015)
Iran	Ampicillin, erythromycin, gentamicin and tetracycline	(Raissy *et al.*, 2012; Shakerian *et al.*, 2018)
Italy	Ampicillin	(Zanetti *et al.*, 2001)
Malaysia	Chloramphenicol, erythromycin, kanamycin and sulfamethoxazole	(Letchumanan *et al.*, 2015b; Devadas *et al.*, 2018; Hamdan *et al.*, 2018)
Poland	Ampicillin and streptomycin	(Lopatek, Wieczorek & Osek, 2015)
Saudi Arabia	Ampicillin, carbenicillin and cephalothin	(Ghenem & Elhadi, 2018)
South Africa	Ampicillin and sulfamethoxazole	(Okoh & Igbinosa, 2010)

South Korea	Ampicillin, ceftazidime, chloramphenicol, erythromycin, streptomycin and vancomycin	(Kang *et al.*, 2018; Ashrafudoulla *et al.*, 2019; Lee *et al.*, 2019; Di *et al.*, 2019)
United Kingdom	Cefazolin, gentamicin, kanamycin and tetracycline	(Daramola, Williams & Dixon, 2009)
United States of America	Ampicillin, amoxicillin, apramycin, ceftazidime, cephalothin, penicillin, and streptomycin	(Han *et al.*, 2007; Baker-Austin *et al.*, 2008; Elmahdi *et al.*, 2018)

1.5 Bacteriophage Therapy

Although there is some debate surrounding the discovery of viruses that infect bacteria, termed bacteriophages (also known as 'phages'), it is generally accepted that phages were first discovered in 1915 and later in 1917, by Frederick W. Twort and Félix d'Hérelle, respectively (Twort, 1915; d'Hérelle, 1917). Following this, phage therapy was first trialled in France in 1919, against avian typhosis (caused by *Salmonella gallinarum*), before going on to have far more widespread therapeutic use in humans in the 1920s and 1930s (Summers, 2012). However, use of phage therapy has always been deemed controversial and post-war discovery of antibiotics, which were broad-spectrum and had the benefit of more convenient administration, led to bacteriophages being disregarded as a primary therapeutic therapy in the West (Clokie *et al.*, 2011). Despite this, phage therapy continued to be employed, albeit at a reduced rate, in certain parts of Eastern Europe, such as Georgia, and in the Soviet Union (Morozova, Vlassov & Tikunova, 2018). Since their discovery, bacteriophages have been isolated using both plate-based and broth culturing methods for decades and nowadays, it is estimated that the global bacteriophage population to be somewhere in the vicinity of 10^{31} phage particles, making them the most abundant organisms on the planet (Comeau *et al.*, 2008). Now, less than a century after the discovery of antibiotics, novel therapies are needed in order to combat global antibiotic resistance and it is being suggested that we are entering a 'post-antibiotic era' (Gordillo Altamirano & Barr, 2019). In the marine environment, antibiotic resistance has been reported to be higher in aquaculture farms than in neighbouring coastal regions (Labella *et al.*, 2013). Therefore, the use of bacteriophages in aquaculture offers the potential of combating bacterial infections and reducing antibiotic levels that enter the human food chain.

Bacteriophages can be divided into two primary groups based on the life-cycle that they undergo. Lytic phages, such as T4, exclusively replicate by releasing new progeny following bacterial cell lysis, whereas temperate phages integrate their genomes into the bacterial chromosome or as a plasmid, without killing the cell and may replicate through cellular division (Weinbauer, 2004). Phage therapy relies on the identification and use of lytic bacteriophages, to infect specific bacterial hosts and lyse the intended cells. Temperate phages are considered a

risk to phage therapy since temperate phages can alter bacterial host fitness, through phage-encoded auxiliary metabolic genes; convert non-pathogenic strains into pathogens through transfer of genomic islands (Warwick-Dugdale *et al.*, 2019a) and contribute to pathogen evolution (Doss *et al.*, 2017). Benefits of using bacteriophages in the fight against antibiotic disease are numerous: (i) vast numbers of viral progeny are rapidly released from infected cells (Skurnik & Strauch, 2006; Doss *et al.*, 2017); (ii) bacteriophages evolve against bacterial resistance, in an arms race under Red Queen dynamics (Paterson *et al.*, 2010; Fortuna *et al.*, 2019); (iii) phages have narrow-host range and therefore are less likely to impact the microbiome of the surrounding environment, for example the human gut (Hyman & Abedon, 2010; Hyman, 2019); (iv) phages have low toxicity, since they are comprised of nucleic acids and proteins and therefore do not present a problem to human or animal health (Kutter *et al.*, 2010); (v) bacteriophages are naturally occurring and ubiquitous in the environment, so there is plenty of scopy for isolation of novel species (Forde & Hill, 2018); (vi) additionally, since phages are naturally occurring and have low-toxicity, they pose little environmental harm, unlike antibiotics which can accumulate in the environment and affect local species (Abedon & Thomas-Abedon, 2010).

Despite the obvious benefits in regards to using phage therapy, there are a number of negatives that must also be considered: (i) narrow host-range, whilst undisruptive to natural flora, can limit the efficacy of treatment to specific strains of pathogen and hence, limit the use of individual phage in treating broad ranges of pathogens (Hyman & Abedon, 2010; Hyman, 2019); (ii) bacteria are able to develop resistance to bacteriophages as rapidly as to antibiotics (Rohde *et al.*, 2018); (iii) and phages can alter the genomes of hosts and pick up host genes during their replication, which can subsequently be spread through the environment (Wang *et al.*, 2018; Calero-Cáceres, Ye & Balcázar, 2019). However, there are potential solutions to such negatives. For example, phage cocktails can be employed, whereby multiple phage types are combined in a single treatment, in order to broaden host-range (McCallin *et al.*, 2018). Bacterial hosts also struggle to develop resistance to multi-phage cocktails and such cocktails act synergistically with antibiotics, hence a combined approach may offer a solution to this problem (Rohde, Wittmann & Kutter, 2018).

Regardless of present limitations, bacteriophage therapy has been investigated in a number of organisms, both in terrestrial environments and in aquaculture farms, with some degree of success. Some examples of bacteriophage therapy in agricultural livestock include the use of phage to treat *E. coli* O157:H7 infection in intensively farmed cattle (Stanford *et al.*, 2010) and to treat *Salmonella* infection and prevent *Salmonella* colonisation in swine (Saez, *et al.*, 2011). There have even been reports of promising phage therapy trials in humans, where bacteriophages have been used in the alleviation of acute lung infections in cystic fibrosis patients (Agarwal *et al.*, 2018). However, there is perhaps the most significant attention on the use of phage therapy in the aquaculture sector, where multidrug resistant bacteria are extremely common, due to the accumulation of antibiotics, or compounds from the breakdown of antibiotic drugs, in the aquatic environment. Here, phage therapy has been trialed in fish (Huang & Nitin, 2019), in shrimp (Vinod *et al.*, 2006; Angulo *et al.*, 2018), as well as in oysters (Rong *et al.*, 2014; Jun *et al.*, 2014b; Zhang *et al.*, 2018). Of particular interest, is the use of bacteriophages against *Vibrio* spp. infections in the aquatic environment. There has been some documented success of bacteriophage treatment in oysters infected with *V. parahaemolyticus*; Rong *et al.* (2014) reported the successful use of vibriophage VPp1 against *V. parahaemolyticus* during the oyster depuration process (Rong *et al.*, 2014). The efficacy of lytic phage VPp1 has been supported by multiple papers (Peng *et al.*, 2013; Jun *et al.*, 2014b). Phage cocktails have also been shown to be effective in the treatment of *V. parahaemolyticus*, for example, the combination of three phages (VP-1, VP-2 and VP-3) was demonstrated to be significantly more infective than any of the single phage alone (Mateus *et al.*, 2014). Furthermore, the occurrence of specific phages has been used to detect the presence of pathogenic *Vibrio* spp. in oysters in Delaware Bay and against *V. parahaemolyticus* biofilm formation (Yin *et al.*, 2019; Richards *et al.*, 2019). Phages have also been used against *V. parahaemolyticus* in the successful treatment of AHPND; phage therapy has prevented early infections of *V. parahaemolyticus* in shrimp (Martínez-Díaz & Hipólito-Morales, 2013; Lomelí-Ortega & Martínez-Díaz, 2014).

1.6 Droplet Microfluidics

As the name of this emerging field suggests, microfluidics involves the manipulation of minute volumes of fluids (10^{-9} to 10^{-18} litres) in channels that are micrometres wide in order to perform laboratory assays (Whitesides, 2006). Microfluidic manipulation enables high numbers of experiments to be performed in parallel and in a fraction of the time of bulk experiments, offering significant advantages to assays such as screening for disease biomarkers, biological assays, single-cell analysis and screening bacterial populations for the presence of persisters and viable but non-culturable cells (Joensson & Andersson Svahn, 2012; Guo *et al.*, 2012; Bamford *et al.*, 2017; Kaushik, Hsieh & Wang, 2018). 'Droplet microfluidics' is a sub-branch of this field, using water-in-oil (W-O) emulsions to encapsulate tissues, cells, viruses or reagents into picolitre volumes, in order to further reduce experiment run times and costs, whilst improving experimental sensitivity (Teh *et al.*, 2008; Guo *et al.*, 2012). Devices used in droplet microfluidics consist of microchannels with cross-junctions or flow-focusing geometric properties to facilitate the mixing of two immiscible liquids, in order to break the aqueous phase into droplets by the outer carrier oil phase (Kaminski, Scheler & Garstecki, 2016). The use of microfluidics in order to encapsulate biomaterials greatly improves the uniformity of droplets, creating vast numbers of monodisperse droplets. Droplet microfluidics has a range of applications including: high-throughput genetic screens (Marcy *et al.*, 2007); single-cell growth assays (Köster *et al.*, 2008); analysis of bacterial persistence and viable but non-culturable populations (Kaushik *et al.*, 2017), viral plaque assays (Chaipan *et al.*, 2017) and using epicPCR to investigate community function at the single-cell level (Spencer *et al.*, 2016).

In the case of bacteriophage therapy, droplet microfluidics can be employed for the high-throughput encapsulation of high concentrations and unique combinations of bacteriophages. Alginate encapsulation is most commonly used for this purpose. Alginate is a polymer derived from brown seaweed (King, 1983) and is favourable to use in droplet microfluidics since it is regarded as having low toxicity and is biocompatible to living cells; it can easily be manufactured into matrices and gels through cationic cross-linking (most commonly Ca^{2+} ions) and

is a relatively cheap resource to use, since it is commonly found in environments across the world (Wee & Gombotz, 1998).

Alginate droplets crosslinked with calcium ions have been used to encapsulate bacteriophage UFV-AREG1 for the treatment of *E. coli* infection (Boggione *et al.*, 2017). This study reported the successful retention of phage UFV-AREG1 within the alginate matrix for up to 21 days and concluded that phage encapsulated in this manner would be fit for use in the food sanitation industry (Boggione *et al.*, 2017). Alginate microdroplets have also been used to encapsulate *Salmonella* phage Felix O1 for delivery to enteric infection sites (Vinner & Malik, 2018). Here, findings reported the diameter of monodisperse alginate droplets can be precisely controlled by adjusting the flow rate of the immiscible aqueous and carrier oil phases, for sizes ranging from 50 μm – 200 μm (Vinner & Malik, 2018). Additional findings stated that increased alginate concentration can provide improved protection in acidic environments, although it should be noted that highly viscous alginate concentrations, for example 2 % w/v, reduced the ease at which droplets formed in-chip (Vinner & Malik, 2018). Bacteriophages specific to *Clostridium difficile* (including phage CDKM9) that have also been encapsulated in alginate droplets, were found to have increased protection in an acidic environment when compared to free phages (Vinner *et al.*, 2017). In this study, researchers were able to trigger phage release in an intestinal pH range by preparing the alginate droplets with Eudragit S100 formulation, which facilitates the use of such droplets in the therapeutic treatment of bacterial infections within the human gut (Vinner *et al.*, 2017).

Aside from alginate, bacteriophages have also been encapsulated into manufactured liposomes, using droplet microfluidics. One paper describes the encapsulation of two *Pseudomonas* phages of different sizes: *Podovirus* PEV2, with an approximately size of 65 nm and *Myovirus* PEV40, with an approximate size of 220 nm (Leung *et al.*, 2018). Using the same microfluidic device, researchers were able to control the diameter of the manufactured liposomes through controlling the flow rate, to encapsulate both phages of different sizes (Leung *et al.*, 2018). Another study highlighted the possibility of using phage-containing liposomes to treat intracellular bacterial infections, such as *Mycobacterium tuberculosis* and *Salmonella* spp. (Cinquerrui *et al.*, 2018). The

same study investigated the encapsulation of *E. coli* phage T3 and *Staphylococcus aureus* phage K, two tailed viruses (Cinquerrui *et al.*, 2018). Here, findings were slightly more pessimistic than previous reports, as to the success of encapsulating tailed phage; findings suggested that tailed viruses have the tendency to aggregate during encapsulation within liposomes, or interact with the lipid bilayer of the liposome (Cinquerrui *et al.*, 2018). Evidently, further research is needed into the encapsulation of bacteriophages in biocompatible materials. Such research is crucial in the fight against antibiotic resistance and the search for novel therapeutic strategies.

1.7 Project Outline

This project aims to use a novel glass microfluidic device for the high-throughput encapsulation of bacteriophages, with the purpose for its use in the specific treatment of a *V. parahaemolyticus* infection in *C. gigas* oyster aquaculture. The project outline is depicted in the flow diagram in **Figure 1**. Briefly, in the first instance, the genomes of multiple strains of *V. parahaemolyticus* were sequenced in order to carry out global abundance analysis and screened for the presence of prophage, which may inhibit infection of lytic phages through superinfection immunity (Abedon & Lejeune, 2007). Following this, vibriophages specific for these strains of *V. parahaemolyticus* were isolated from seawater samples. In parallel, the project sought to develop a novel protocol for the synthesis of monodisperse alginate microcapsules using a glass microfluidic device. The aims of the project were then to encapsulate vibriophages in alginate droplets for use in a series of infectivity assays to determine whether phages were able to (1) exit alginate matrices and (2) remain infective. The process of lyophilisation was then proposed to assess whether encapsulated phages could be made commercially viable. If all of the previous steps were successful, the final objective was to apply vibriophages encapsulated in alginate to *C. gigas* infected with *V. parahaemolyticus*.

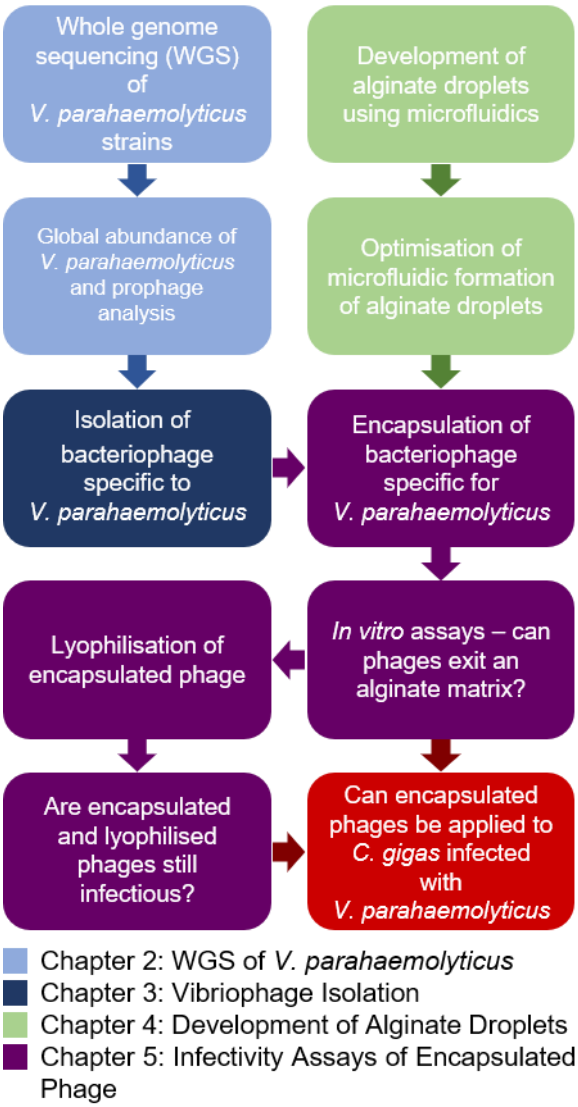

Figure 1: Schematic representation of experimental workflow in this thesis. Steps have been colour coded for each experimental chapter according to the key in the figure. The final step (coloured red) was not achieved in this thesis.

2 Whole Genome Sequencing of *Vibrio parahaemolyticus*

The following chapter has been published: Witherall L, Wagley S, Butler C, Tyler CR, Temperton B. 2019. Genome Sequences of Four Vibrio parahaemolyticus Strains Isolated from the English Channel and the River Thames. *Microbiology resource announcements* 8.

2.1 Prefix

Bioinformatic processing of sequencing reads and assembly in chapter 2. 4. 7. were performed by supervisor Dr Ben Temperton.

2.2 Introduction

It has been decades since the first bacterial genomes were sequenced and the record of genome sequences in GenBank has doubled approximately every 18 months since that time ("GenBank and WGS Statistics"; Fleischmann *et al.*, 1995). Today, whole genome sequencing (WGS) enables us to better understand bacterial populations, how they function and what impact they might have on the environment around them. Furthermore, WGS of bacterial genomes allows for the identification of specific genes of interest, for example antibiotic resistance genes (ARGs) (Tagini & Greub, 2017). Genetic profiles can also provide an insight into the presence of prophages that have been integrated into the bacterial genome. It is not uncommon for bacteria to harbour multiple prophages within their genomes; taking *Vibrio* spp. as an example, most contain at least one fully intact, integrated phage (Canchaya *et al.*, 2003; Millard, 2019). Bacteria containing more than one prophage are generally termed as 'lysogens' and are protected from subsequent infection from closely-related phages (Fortier & Sekulovic, 2013).

WGS has been used in this project to determine (1) whether prophages were present in the strains of *V. parahaemolyticus* (EXE V18/004, V12/024, V05/313, V05/027 and EXE V13/004) used for isolating novel vibriophages for potential use in phage therapy; (2) to estimate strain abundance across global oceans,

using metagenomic data (Biller *et al.*, 2018) to evaluate the scope for phage therapy from this work. Presence of multiple prophage integrated into the genomes may potentially result in the failure of future isolation attempts. Furthermore, since the occurrence of *V. parahaemolyticus* infections is increasing globally (Martinez-Urtaza *et al.*, 2018), understanding the global abundance of this bacterium will provide insight into the spread of disease, in humans and aquaculture. Such data is crucial when developing sustainable therapies with high efficacy.

2.3 Chapter Aims

This chapter set out to sequence the whole genomes of environmental *V. parahaemolyticus* strains, with the purpose of identifying any prophage present within the genomes (**Figure 2**). The presence of prophage may prevent superinfection of novel vibriophages and thus, the identification of any prophage was required to ensure the strains selected were appropriate for future experiments for the isolation of novel vibriophages. Genetic sequences were obtained to also ascertain the abundance of these strains, which were all isolated from the UK, relative to the global metagenomic datasets.

2.4 Materials and Methods

2.4.1 Bacterial Strains

Vibrio parahaemolyticus strains EXE V18/004 and EXE V13/004 were isolated at the University of Exeter from *Ostrea edulis* (Chichester harbour) *and Mytilus edulis* (River Exe estuary) respectively. *V. parahaemolyticus* strain V12/012 was isolated at Cefas Weymouth Laboratories, from *Crassostrea gigas*. *V. parahaemolyticus* strain V05/313 was isolated from *Eriocheir sinensis* (River Thames). *V. parahaemolyticus* strains EXE V18/004, EXE V13/004, V05/313 and V12/024 were all isolated following previously described methods (Wagley, Koofhethile & Rangdale, 2009; Powell *et al.*, 2013). *V. parahaemolyticus* strain V05/027 was donated by Cefas Weymouth Laboratories and was isolated from

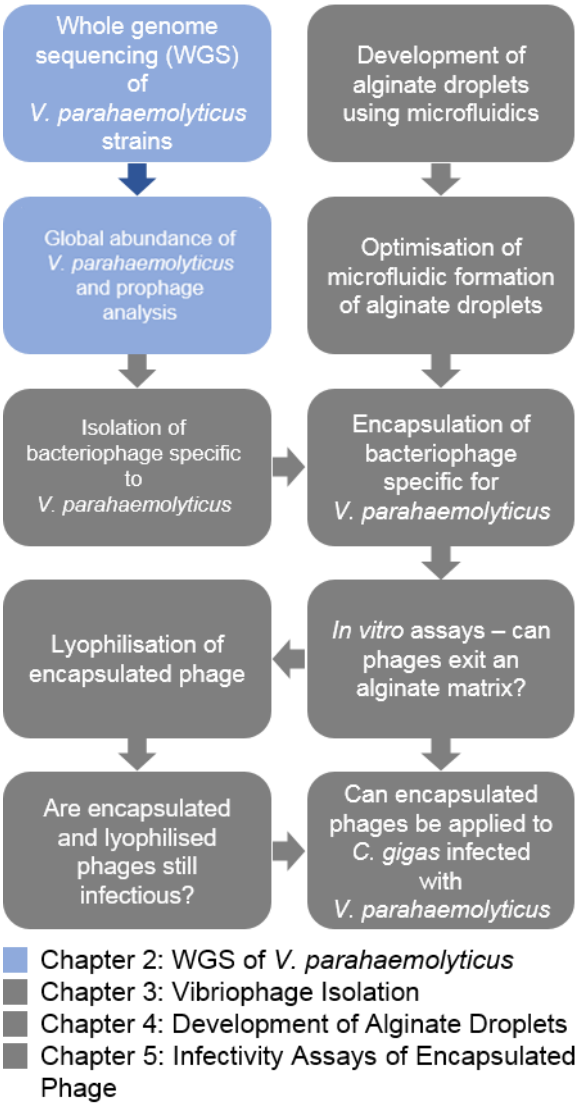

Figure 2: Schematic representation of experimental workflow in Chapter 2. Steps relevant only to Chapter 2 have been highlighted.

an unknown source in Southampton. All strains were kindly provided for sequencing by Dr Sariqa Wagley at the University of Exeter.

2.4.2 Preparation of 1.2 % Marine Agar

All seawater used in this project was collected from the surface water in the Western English Channel (50°15.0'N; 4°13.0'W) using a Niskin bottle aboard the research vessel PML Quest unless otherwise stated. To 400 mL of seawater, which had been filtered through a 0.22 µm pore size polyvinylidene difluoride (PVDF) Durapore® membrane (Millex), was added the following: 2 g bacto-peptone (Oxoid); 0.4 g yeast extract (Oxoid); 4.8 g No. 2 Agar Bacteriological (Lab M), before autoclaving for 15 minutes at 121°C.

2.4.3 Preparation of Marine Broth (MB)

To 400 mL of seawater, which had been filtered through a 0.22 µm pore size PVDF Durapore® membrane (Millex), was added the following: 2 g bacto-peptone (Oxoid); 0.4 g yeast extract (Oxoid), before autoclaving for 15 minutes at 121°C.

2.4.4 Preparation of Bacterial Cultures

Initial streak plates for all *V. parahaemolyticus* strains were provided on marine agar, by Dr Sariqa Wagley, at the University of Exeter. From these, single colonies of each strain were picked and re-plated on marine agar.

For all strains, overnight *Vibrio parahaemolyticus* cultures were prepared by picking a single colony of *V. parahaemolyticus* from a streak plate (prepared on marine agar) and growing it in 10 mL MB, in a shaking incubator at 220 rpm, 37 °C for 18h. Overnight *V. parahaemolyticus* cultures had a cell density of approximately 10^9 CFU mL^{-1}.

2.4.5 DNA Extraction

V. parahaemolyticus isolates EXE V18/004, V12/024, V05/313, V05/027 and EXE V13/004 were grown overnight in marine broth (37 °C, 220 rpm) to a cell

density of approximately 1 x 10^9 cells mL^{-1}. DNA extraction was carried out using a Qiagen DNeasy PowerWater kit (Germany), following the manufacturer's protocol, with the following modification: instead of inserting a 0.2 µm 25 mm Whatman Nuclepore Track-Etch membrane filter (with bacteria) into a PowerWater DNA bead tube, 1 mL of each overnight bacterial culture was centrifuged (4000 x g, 20 °C, 15 min). The pellet of bacterial cells was resuspended in 1 mL MB and added directly into the bead tube. DNA was quantified with the Invitrogen Qubit double-stranded DNA broad-range assay (Thermo Fisher Scientific), using an Invitrogen Qubit 2.0 fluorometer (Life Technologies, Thermo Fisher Scientific).

2.4.6 Library Preparation and Sequencing

Short-read sequencing was provided by MicrobesNG (https://microbesng.uk/). Short-read genomic DNA libraries were prepared using Nextera XT Library Prep Kit (Illumina, San Diego, USA) following the manufacturer's protocol with the following modifications: two nanograms of DNA instead of one were used as input; PCR elongation time was increased to 1 min from 30 seconds. DNA quantification and library preparation were carried out on a Hamilton Microlab STAR automated liquid handling system. Pooled libraries were quantified using the Kapa Biosystems Library Quantification Kit for Illumina on a Roche lightcycler 96 qPCR machine. Libraries were sequenced on the Illumina HiSeq. 2 ng of DNA were required for short-read library preparation and sequencing and because of a low DNA extraction yield, *V. parahaemolyticus* EXE V13/004 was not sequenced.

Long-read sequencing was performed in-house using a multiplexed SQK-LSK108 library preparation kit and sequenced on a MinION FLO-MIN106 flowcell, following Oxford Nanopore Technologies protocol (Oxford Nanopore Technologies, 2018).

2.4.7 DNA Sequence Assembly and Quality Checks

Short-read sequences were adapter trimmed using Trimmomatic 3.0 (Bolger, Lohse & Usadel, 2014), with a sliding window quality cut-off of Q15. Long-read

sequences were base-called using the guppy v2.3.5 FlipFlop algorithm, then de-multiplexed and adapter trimmed using porechop (https://github.com/rrwick/Porechop), with the following settings: '`--require_two_barcodes --discard_unassigned --discard_middle`' to minimise cross-talk between samples.

Whilst long-read sequences were generated for all five isolates of *V. parahaemolyticus* (EXE V18/004, V12/024, V05/313, V05/027 and EXE V13/004), short-read sequencing was not possible for *V. parahaemolyticus*, due to low yield following DNA extraction. Therefore, hybrid genome assembly was not possible for this isolate. For all other isolates, hybrid genome assembly was performed using Unicycler (version 0.4.7) (Wick *et al.*, 2017) and each assembly was uploaded to the Integrated Microbial Genomes (IMG) platform (Chen *et al.*, 2019), developed by the Joint Genome Institute (JGI, USA), for annotation.

Short-read coverage was calculated using bbmap v38.22 (https://sourceforge.net/projects/bbmap/) with the following settings: '`idfilter=0.95 covstats=covstats.txt`'. Long read coverage was calculated by first using minimap2 v2.17 (https://github.com/lh3/minimap2) and samtools v1.9 (http://samtools.sourceforge.net/), as follows, to create a bam file: '`minimap2 -t 16 -ax map-ont <assembly> <long_reads> | samtools view -F 4 -buS | samtools sort - o long.sorted.bam`', then using `bbmap`'s pileup.sh to calculate coverage: '`pileup.sh in=long.sorted.bam ref=ref.fa out=long.covstats.txt`'. Default parameters for software were used unless otherwise noted.

2.4.8 Phylogenetic Tree Construction

A phylogenetic tree for *V. parahaemolyticus* strains EXE V18/004, V12/024, V05/313 and V05/027 was constructed, including reference genomes for the following strains: *V. parahaemolyticus* RIMD 2210633; *Vibrio alginolyticus* NBRC 15630; *Vibrio campbellii* ATCC BAA-1116; *Vibrio cholerae* O1 N16961; *Vibrio tubiashii* ATCC 19109; *Vibrio vulnificus* ASM221513v1; *Aliivibrio fischeri* ES114; *Vibrio anguillarum*; *Vibrio caribbeanicus* ATCC BAA 2122;

Vibrio coralliilyticus; *Vibrio cyclitrophicus* FF75; *Vibrio diabolicus*; *Vibrio fluvialis*; *Vibrio furnissii* NCTC 11218; *Vibrio harveyi*; *Vibrio mediterranei* NBRC 15635; *Vibrio mimicus*; *Vibrio nereis*; *Vibrio nigripulchritudo*; *Vibrio orientalis* ATCC 33934; *Vibrio proteolyticus*; *Vibrio rotiferianus*; *Vibrio splendidus*; *Vibrio tasmaniensis* LGP32; *Escherichia coli* K 12 and *Pseudomonas aeruginosa* PAO1. All genomes were acquired from the National Center for Biotechnology Information (NCBI). Strains were chosen to include a range of *Vibrio* and non-*Vibrio* species.

A multisequence alignment file was generated using GTDB-Tk v0.2.2 (https://github.com/Ecogenomics/GTDBTk) with the following settings: '`gtdbtk classify_wf --genome_dir <gtdbtk.input> --out_dir <gtdbtk.output>`'. Sequences conserved between genomes were then removed using trimAl v1.4 ("trimal [trimAl]," 2011), with the following settings: '`trimal -in <gtdbtk.output> -out <trimal.output> -gt 0.9 -cons 60`'. A Newick file was then generated using IQ-tree v1.6.11 ("IQ-TREE: Efficient phylogenomic software by maximum likelihood"), where 1,000 bootstrapping iterations were performed using the following settings: '`iqtree -s <trimal.output> --bb 1000`'. To visualise phylogeny, the treefile produced from the previous command was uploaded to Interactive Tree of Life (iTOL) (Letunic).

2.4.9 Global Abundance

Global abundance of *V. parahaemolyticus* isolates EXE V18/004, V12/024, V05/313 and V05/027 was calculated using data published by (Biller *et al.*, 2018). Marine aquaculture favours coastal regions, where eutrophication causes excessive richness of nutrients and hence favours bacterial species such as *Vibrio* spp. (Cloern, 2001). Therefore, cruises with coastal data were chosen from the sample sites published, namely: GA02, GA03 and GA10. Within this, samples of depth more than 200 m were also removed, since *Vibrio parahaemolyticus* is a bacterium found in more shallow, coastal waters (Letchumanan *et al.*, 2015a). Contigs present within these samples were further filtered; those with length less than 2,000 bp were discarded.

Raw data was quality-checked for adapter removal, removal of optical duplicate reads before , bowtie 2 v2.3.4.3 (Langmead & Salzberg, 2012) was used to align the reads from metagenomic samples (Biller *et al.*, 2018) against the genomes from all four *V. parahaemolyticus* isolates . First an index was built, using the following settings: '`bowtie2-build -f <input.fastas> <index.file>`'. To standardise sequencing depth across samples, all metagenomic samples were randomly subsampled to 10 million reads using `seqtk` (https://github.com/lh3/seqtk). Next, each sequence was aligned, using the following settings: '`bowtie2 -x <index.file> -1 <subsample.forward.sequence> -2 <subsample.reverse.sequence> --threads 16 -S <output.sam>`. SAMtools v1.9 (Li *et al.*, 2009) was used, with the following settings, to store aligned files in a compact format:

'`samtools view -F 4 -bS -o <output.bam> --threads 16 <input.sam>`'

'`samtools sort --threads 16 -o <sorted output.bam> <input.bam>`'

'`samtools index <sorted input.bam>`'.

Finally, BamM v1.7.3 (http://ecogenomics.github.io/BamM/) was used to calculate mean coverage (excluding the top and bottom 10th percentile to reduce the influence of high or low coverage regions) for each input sequence, using the following settings: '`bamm parse -b <input.files.bam> -c <output.coverage.tsv> -m tpmean`'.

2.4.10 Screening Genome Sequences for Prophage

Genomes of *V. parahaemolyticus* isolates EXE V18/004, V12/024, V05/313 and V05/027 were screened for double-stranded DNA (dsDNA) bacteriophages and further, single-stranded DNA (ssDNA) Inoviridae, using VirSorter (Roux *et al.*, 2015) and Inovirus_detector (Roux *et al.*, 2019b), respectively.

2.5 Results and Discussion

2.5.1 *Vibrio parahaemolyticus* Whole Genome Sequences and Phylogeny

Genome annotation of hybrid assemblies (combined long and short read) generated 5, 2, 3 and 2 contigs, respectively, for *V. parahaemolyticus* strains EXE V18/004, V12/012, V05/313 and V05/027. All contigs were predicted to be circular by Unicycler and IMG. All strains were found to have two chromosomes (**Table 2**): one chromosome, with an average size of 3.3 Mbp and a smaller chromosome, with an average size of 1.8 Mbp. Assembled and annotated genomes are publicly available from JGI IMG/M (https://img.jgi.doe.gov/) using the following taxon identifiers (IDs): 2816332655 (*V. parahaemolyticus* EXE V18/004), 2816332656 (*V. parahaemolyticus* V12/024), 2816332657 (*V. parahaemolyticus* V05/313), and 2816332658 (*V. parahaemolyticus* V05/027) (Witherall *et al.*, 2019). Descriptive statistics for sequence runs and genome assembly are presented in **Table 2**.

Phylogenetic analysis was performed with 1,000 bootstrapping iterations to compare the genetic sequences of *V. parahaemolyticus* strains EXE V18/004, V12/024, V05/313 and V05/027 with the reference genomes listed previously (**2. 4. 8. Phylogenetic tree construction**). **Figure 3** confirms that *V. parahaemolyticus* strains EXE V18/004, V12/004, V05/313 and V05/027 are closely related to both one another and to the *V. parahaemolyticus* reference genome used. The phylogenetic tree in **Figure 3** places all *V. parahaemolyticus* species sequenced in a single clade, with both *V. parahaemolyticus* V05/027 and EXE V18/004 and the reference *V. parahaemolyticus* genome and *V. parahaemolyticus* V12/024 as being more closely related, as evidenced by shorter branch lengths.

2.5.2 Global Abundance

Global abundance for the following strains of *V. parahaemolyticus* was calculated using data provided by (Biller *et al.*, 2018): EXE V18/004, V12/024, V05/313 and V05/027. Abundance was also calculated for each of the reference genomes previously mentioned. Abundance for all isolates is presented in **Figures 4 - 6**,

Table 2: Chromosome length, sequence run statistics and assembly statistics for *Vibrio parahaemolyticus* strains EXE V18/004, V12/024, V05/313 and V05/027.

V. paraha-emolyticus strain	No. of contigs	Chromosome length (chromosome 1; chromosome 2 [bp])	No. of MinION reads	MinION median read length (bp)	Median short-read coverage (chromosome 1; chromosome 2 [x])	Median long-read coverage (chromosome 1; chromosome 2 [x])	G+C content (%)	No. of protein-coding genes
EXE V18/004	5	3,263,543; 1,747,363	241,527	1,943	38; 30	187; 151	45	4,524
V12/024	2	3,315,999; 1,877,872	18,595	17,487	27;22	61; 58	45	4,604
V05/313	3	3,319,614; 1,940,186	1,116,682	1,173	53; 42	784; 636	45	4,738
V05/027	2	3,438,892; 1,705,150	168,588	3,832	62; 51	135; 111	45	4,669

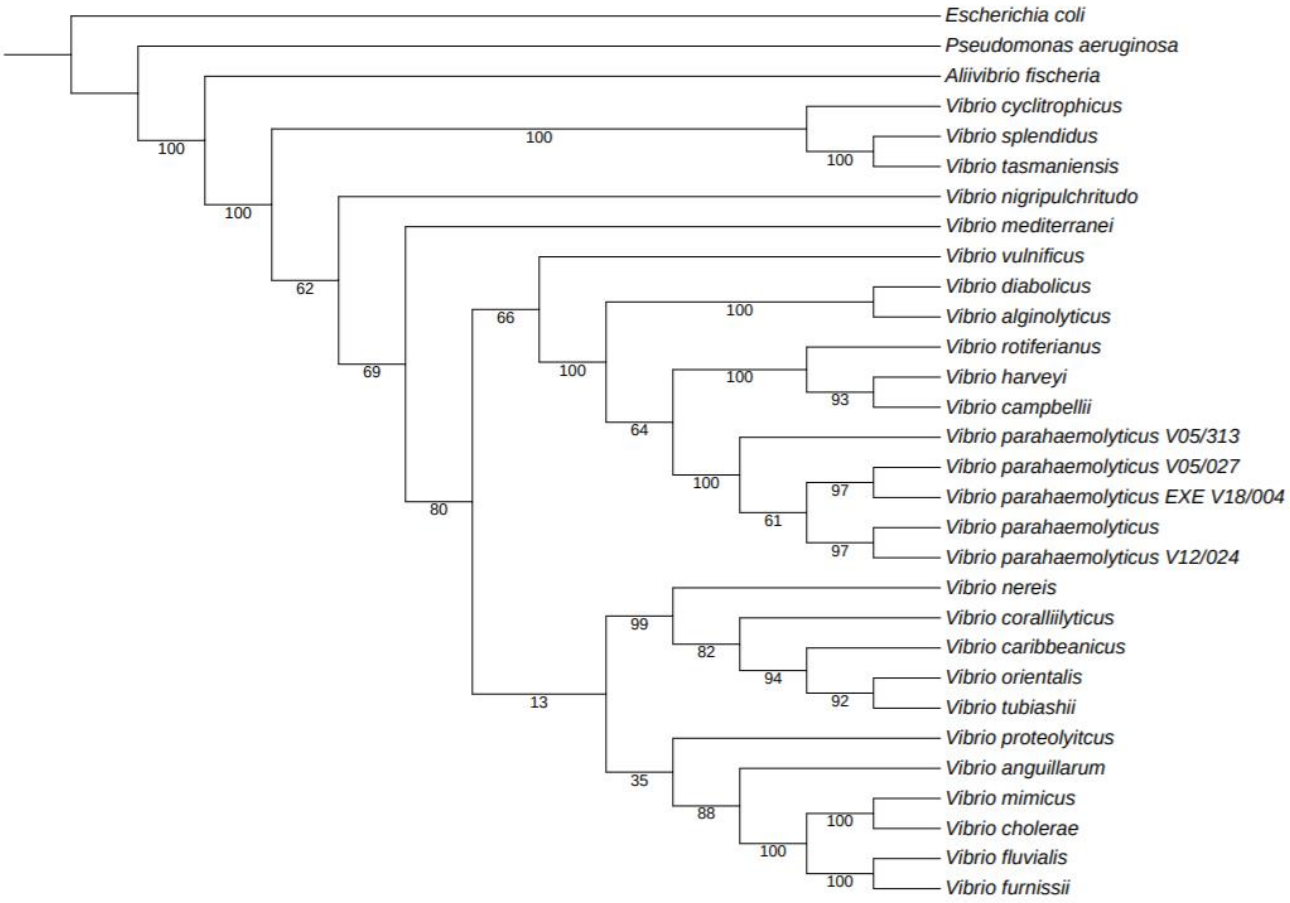

Figure 3: Rooted tree to show phylogeny of *Vibrio parahaemolyticus* strains EXE V18/004, V12/024, V05/313 and V05/027. Multiple sequence alignments were constructured using the Genome Taxonomy Database Toolkit (GTDB-Tk), which concatenates 120 phylogenetic bacterial marker, comprised of specific protein. Tree was organised using maximum-likelihood analysis and shows 1,000 bootstrap replicates.

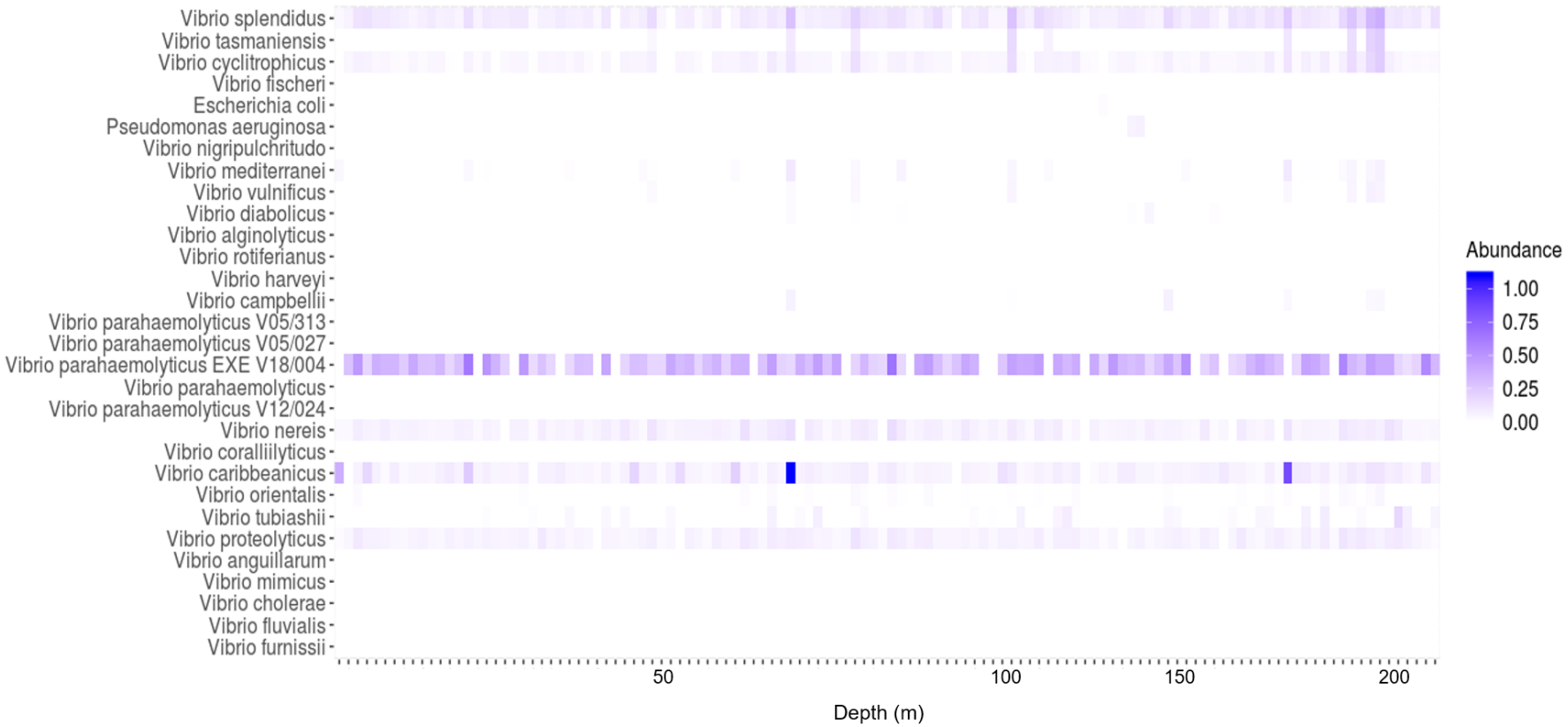

Figure 4: Heat map to depict global abundance for all isolates from samples sites studied in cruise GA02 (Biller *et al.*, 2018). Abundance was calculated bioinformatically using bow-tie2. Y-axis shows isolate strains analysed. X-axis shows samples sites from cruise GA02, in ascending order of depth (0 – 200 m). Higher abundance is demonstrated by blue colour and lower (or no) abundance is demonstrated by lack of colour.

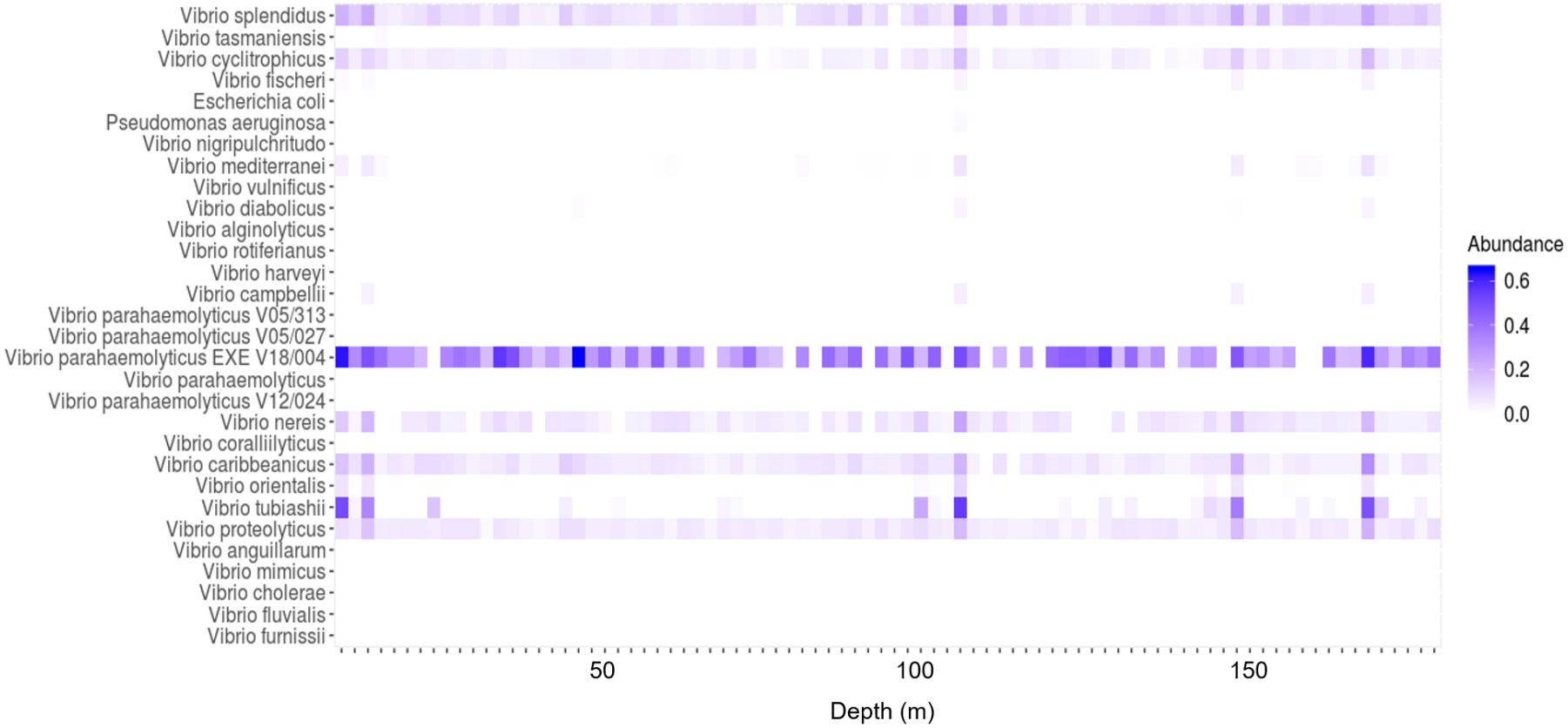

Figure 5: Heat map to depict global abundance for all isolates from samples sites studied in cruise GA03 (Biller *et al.*, 2018). Abundance was calculated bioinformatically using bow-tie2. Y-axis shows isolate strains analysed. X-axis shows samples sites from cruise GA03, in ascending order of depth (0 – 186 m). Higher abundance is demonstrated by blue colour and lower (or no) abundance is demonstrated by lack of colour.

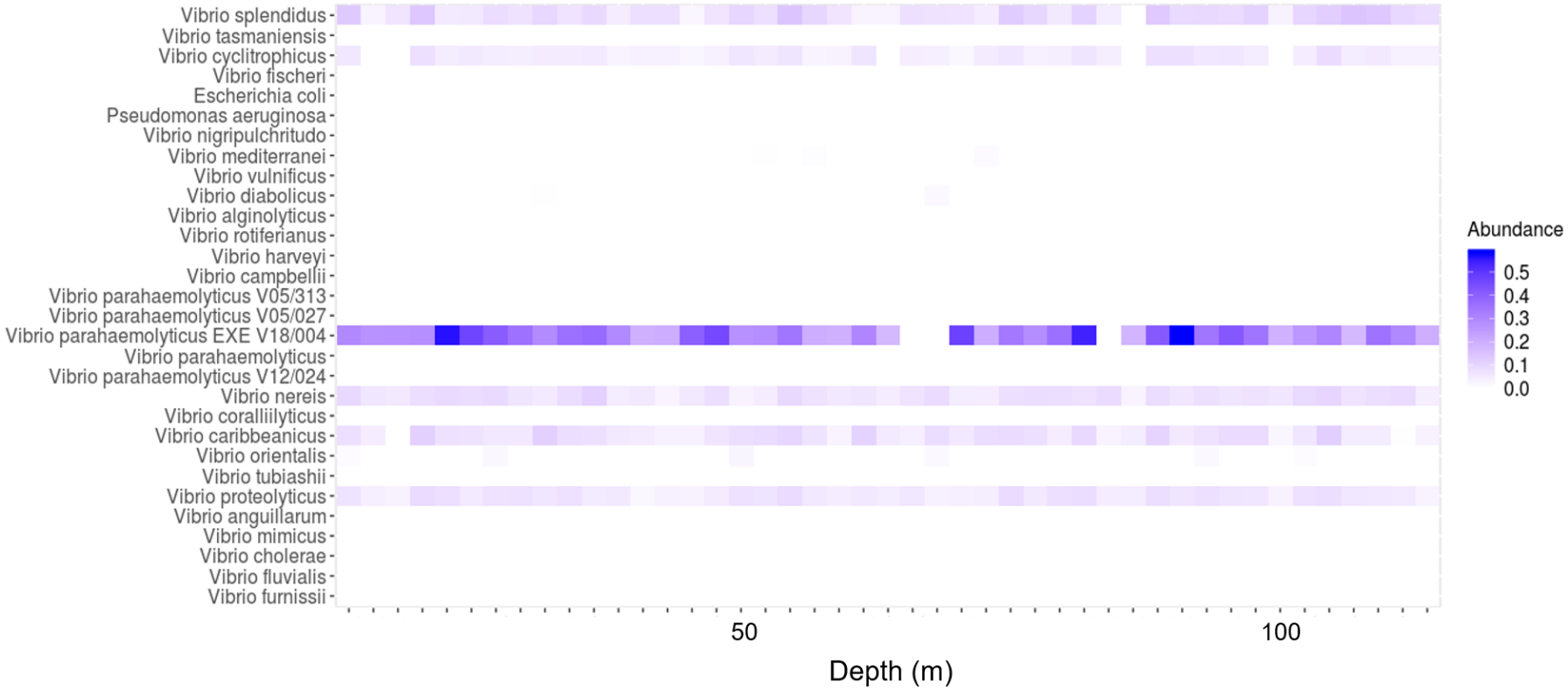

Figure 6: Heat map to depict global abundance for all isolates from samples sites studied in cruise GA10 (Biller *et al.*, 2018). Abundance was calculated bioinformatically using bow-tie2. Y-axis shows isolate strains analysed. X-axis shows samples sites from cruise GA10, in ascending order of depth (0 – 121 m). Higher abundance is demonstrated by blue colour and lower (or no) abundance is demonstrated by lack of colour.

with the x-axis of each graph ordered by ascending depth. There was little recruitment of reads to either reference strains or strains used in this study from the Biller dataset (**Figures 4 - 6**). V12/024, V05/313 and V05/027 showed no recruitment in any of the samples in any cruise, suggesting that these particular isolates are endemic to the UK waters from which they were isolated. On the contrary, *V. parahaemolyticus* EXE V18/004 was found to have relatively high abundance across all three cruises, with no correlation with depth.

V. parahaemolyticus is present in estuarine and coastal marine waters, globally in both temperate and tropical waters, with abundance varying according to various geographical and environmental factors (Karunasagar & Karunasagar, 2018). Factors that may favour the presence of *V. parahaemolyticus* include high zooplankton abundance (Venkateswaran *et al.*, 1989), above-average temperature (Martinez-Urtaza *et al.*, 2010, 2018; Kim *et al.*, 2012) and salinity (Deepanjali *et al.*, 2005; Johnson *et al.*, 2012), amongst others. Since *V. parahaemolyticus* is considered to have wide global abundance, the low levels observed here, using metagenomic data acquired from Biller *et al.* (2018) may be due to data being primarily collected from the open ocean. Whilst cruises selected for this research (GA02, GA03 and GA10) were done so due to their close proximity to coastal regions relative to other cruise data, none of the three consists of solely coastal data: GA02 collected data from the centre of the Atlantic Ocean; GA03 collected samples along a transect across the North Atlantic Ocean, from coast to coast and GA10 sampled in the South Atlantic Ocean, from the tip of South Africa, to the open ocean (**Figure 7**). Furthermore, the cruises selected in this study sampled sites solely from the Atlantic Ocean, limiting the scope of estimating global abundance. Whilst the data suggests that *V. parahaemolyticus* strains V12/024, V05/313 and V05/027 are endemic to UK waters, it is also entirely possible that these strains, whilst not abundant in the Atlantic Ocean, are present in other global waters. Whilst more research is evidently needed, using data collected from coastal waters across the globe, it is perhaps unlikely that strains of *V. parahaemolyticus* present in the UK, would be lacking in the Atlantic Ocean, but abundant further afield, considering tidal currents and the proximity of the waters (Cartwright David Edgar *et al.*, 1980).

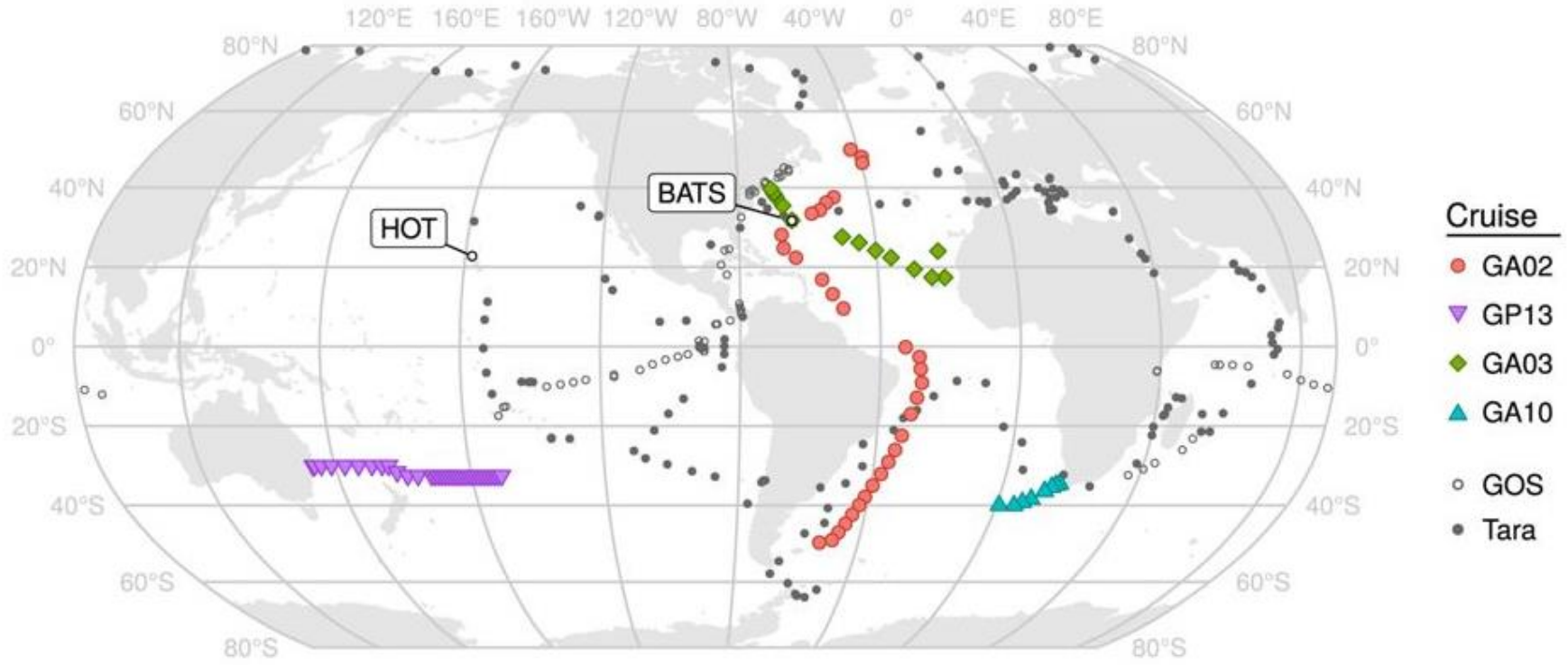

Figure 7: Schematic to show locations of sample sites for each GEOTRACE cruise where data was collected in Biller *et al.* (2018). Image adapted from Biller *et al.* (2018). Red circle shows cruise GA02, from the Northern Atlantic Ocean to the Southern Atlantic Ocean. Green diamond shows cruise GA03, from the North Western Atlantic Ocean to the North Eastern Atlantic Ocean. Blue triangle shows cruise GA10 in the Southern Atlantic Ocean from the tip of South Africa to the open ocean. Image also includes positions for the Bermuda-Atlantic Time Series (BATS) and Hawaii Ocean Time Series (HOT), as well as the Global Ocean Sampling expedition (GOS) and Tara Oceans datasets for context (Rusch *et al.*, 2007; Pesant *et al.*, 2015).

V. parahaemolyticus is bacterium with high genetic diversity (Han *et al.*, 2016) and is primarily classified by serotyping, determined by the specific combination of somatic or capsular antigens (Nair *et al.*, 2007). The most recent research into *V. parahaemolyticus* serotypes report a total of 84 distinct serotypes across pathogenic and environmental isolates (Li *et al.*, 2016). Therefore, in this study, a sequence similarity of 90 % was used when comparing each *V. parahaemolyticus* strain to the metagenomic data set, in order to ensure that it was possible to distinguish between distinct *V. parahaemolyticus* strains. The stark difference in abundance between *V. parahaemolyticus* EXE V18/004 and strains V12/024, V05/313 and V05/027 highlights the need to carry out abundance studies at the strain level; when talking about pathogenic bacteria, it is perhaps no longer relevant to consider the abundance of a species as a whole, but rather to investigate the abundance of bacterial strains.

Furthermore, it is important to note the impact that season and hence corresponding temperature or stratification of nutrients may have on global abundance of *V. parahaemolyticus*. Of the three GEOTRACE cruises analysed, two cruises, GA02 and GA03, sampled data long term, with samples spanning over 10 months and 14 months, respectively. The third cruise (GA10) sampled data over the course of two months, from October 2010 to December 2010, inclusive (Biller *et al.*, 2018). GEOTRACE cruise GA02 sampled water along a track from the North to the South Atlantic Ocean, from May 2010 to March 2011, hence data was primarily been collected during the summer months; due to seasonal change between the Northern and Southern Hemispheres; GEOTRACE cruise GA03 sampled water in the North Atlantic Ocean, from October 2010 to December 2011 and so samples were collected throughout all seasons; GEOTRACE cruise GA10 collected water samples from the Southern Atlantic ocean, from October 2010 to December 2010 and hence were collected during the summer months of the Southern Hemisphere. *V. parahaemolyticus* has been shown to have increased abundance during warmer summer months and decreased abundance over the winter (DePaola *et al.*, 2003; Martinez-Urtaza *et al.*, 2010). Whilst the majority of data collected during the GEOTRACE cruises analysed was collected throughout the summer period, only *V. parahaemolyticus* EXE V18/004 showed had any abundance across the three cruises. Correlations

in literature between temperature and *V. parahaemolyticus* abundance support the theory that strains V12/024, V05/313 and V05/027 are endemic to the UK.

With SST rising due to changes in climate, it is important to consider that the abundance of pathogenic marine bacteria such as *V. parahaemolyticus* is likely to increase in temperate regions in coming years. Such increases in abundance have the potential to facilitate the spread of pathogenic bacteria throughout global oceans, since increased temperatures impact all biogeochemical processes that occur within the ocean. For example, increased SST can result in earlier and larger planktonic blooms (Dale, Edwards & Reid, 2006) and it has been suggested that zooplankton may facilitate the global spread of pathogenic *V. parahaemolyticus*, since genetically similar populations of *V. parahaemolyticus* were found in zooplankton up to 1500 km apart (Martinez-Urtaza *et al.*, 2012). Therefore, impacts of rising SST on planktonic blooms have consequences not only on biomass consumption within food webs, but potentially on the dispersal on pathogenic marine bacteria.

2.5.3 *Inoviridae* are Present in *Vibrio parahaemolyticus*

In total, 10 dsDNA high quality (category 5) prophage and 5 Inoviruses were detected and manually curated across four *V. parahaemolyticus* strains EXE V18/004, V12/024, V05/313 and V05/027 (**Table 3**). All strains contained at least one dsDNA prophage and ssDNA *Inoviridae* were found in *V. parahaemolyticus* strains V12/024, V05/313 and V05/027, ranging in nucleotide lengths from 6,902 bp to 12,620 bp.

Marine bacteriophages are hugely abundant, contributing to, and controlling, vast communities of microorganisms in the ocean (Brussaard *et al.*, 2008). Prophages are a subset of bacteriophages which are genetically integrated into the genome of the bacterial host, typically long-term (Casjens, 2003). Prophages have the ability to continue viral assembly and produce phage progeny from the bacterial host (Canchaya *et al.*, 2003). The impact of prophage on the survival and success of a bacterial host has been discussed in detail: the presence of prophage can inhibit superinfection of the host bacterium (Abedon & Lejeune, 2007; Bondy-Denomy & Davidson, 2014); prophage can be responsible for the presence and

Table 3: Putative viral sequences identified in *Vibrio parahaemolyticus* strains EXE V18/004, V12/024, V05/313 AND V05/027.

V. parahaemolyticus strain (chromosome)	Viral type	Viral length (nucleotides)	Locus (bp)
EXE V18/004 (1)	dsDNA	80,691	1,128,757-1,209,448
V12/024 (1)	dsDNA	83,313	964,157-2,047,470
V12/024 (2)	dsDNA	179,156	648,466-827,622
V12/024 (1)	dsDNA	23,450	1,159,176-1,182,626
V12/024 (1)	ssDNA (Inovirus)	8,729	1,722,396-1,731,125
V12/024 (2)	ssDNA (Inovirus)	7,778	1,174,273-1,182,051
V05/313 (1)	dsDNA	93,767	1,307,712-1,401,479
V05/313 (2)	dsDNA	127,595	941,423-1,069,018
V05/313 (2)	dsDNA	18,876	1,302,491-1,321,367
V05/313 (1)	ssDNA (Inovirus)	6,902	1,634,040-1,640,941
V05/313 (2)	ssDNA (Inovirus)	12,620	1,304,662-1,317,281
V05/027 (1)	dsDNA	76,012	1,981,080-2,057,092
V05/027 (1)	dsDNA	128,907	1,438,793-1,567,700
V05/027 (1)	dsDNA	109,064	175,390-284,454
V05/027 (2)	ssDNA (Inovirus)	7,728	693,882-701,609

transfer of virulence traits between bacteria through horizontal gene transfer (Cheetham & Katz, 1995; Boyd & Brüssow, 2002; Boucher & Stokes, 2006; Abedon & Lejeune, 2007) and prophage can influence the evolution of bacterial species, as well as the emergence of distinct bacterial strains (Banks, Beres & Musser, 2002; Brüssow, Canchaya & Hardt, 2004; Fortier & Sekulovic, 2013).

In this instance, a total of fifteen prophages were found present across *V. parahaemolyticus* strains EXE V18/004, V12/024, V05/313 and V05/027. Five of these prophages were determined to be ssDNA *Inoviridae* and were found in *V. parahaemolyticus* strains V12/024, V05/313 and V05/027. Most species of *Vibrio* have at least one intact, or complete, prophage present in their genome genome and 1.2 % of prophages found in *Vibrio* spp. carry functional antibiotic resistance genes (Millard, 2019). Bioinformatic analysis of bacterial genomes can provide valuable insight into the presence of prophage and this is an important step in the development of bacteriophage therapy. Prophages have also been found to exist as plasmids in the lysogen of *V. parahaemolyticus*, for example temperate phage VP822, which has been found to encode transcriptional regulators for bacterial quorum sensing and therefore may hold some influence over host-associated bacterial traits (Lan *et al.*, 2009).

It has been proposed that prophages are common in marine bacteria since they improve the likelihood of host survival in unfavourable conditions (Warwick-Dugdale *et al.*, 2019a). For example, prophages may regulate metabolic activity, through the inhibition of unnecessary pathways, or by acting as gene transfer agents for horizontal gene transfer in marine bacteria (Paul, 2008). Although prophages may benefit the survival of a bacterial host, their presence may limit success of phage therapy.

Inoviridae have been shown to be responsible for phage conversion in *Vibrio* spp. and can directly impact on the virulence of the host (Faruque & Mekalanos, 2003). Bioinformatic analysis suggests that 45 % of *Vibrio* spp. have at least one intact prophage belonging to the *Inoviridae* family (Castillo *et al.*, 2018). The most well-documented example of *Inoviridae*-associated virulence in bacteria is in *Vibrio cholerae*, through the encoding of virulence toxins CTX and Zonula occludens toxin (Zot) (Waldor & Mekalanos, 1996). However, Zot-encoding prophages were

found in 78 % of clinically-isolated *V. parahaemolyticus*, suggesting that Inoviruses can be present in *Vibrio* spp. outside of *V. cholerae* (Castillo *et al.*, 2018). Furthermore, other virulence toxins have also been found to be encoded by prophage-like elements in *V. parahaemolyticus*, include RTX toxins, lipases and hemolysins (Castillo *et al.*, 2018). *Inoviridae* phage f237 has been found integrated in pandemic isolate *V. parahaemolyticus* O3:K6 (Nasu *et al.*, 2000). *Inoviridae* have been found to be widespread, not only in marine bacteria, but in nearly all ecosystems on Earth (Roux *et al.*, 2019a), supporting the symbiosis of *Inoviridae* and *Vibrio* spp. globally.

3 Vibriophage Isolation

3.1 Introduction

Despite the high estimates for bacteriophage populations, there are fewer than 15,000 complete phage nucleotide sequences listed by NCBI Virus (as of January 2020). Although it should be noted that, this number is somewhat higher than figures published within the last five years, suggesting that interest in bacteriophages is rapidly increasing (Keen, 2015). This renewed interest in bacteriophage research and their potential use as therapeutic agents in the last sixty years may be influenced by both the rising global antibiotic resistance epidemic, and improved methods of detection and sequencing (Gregory *et al.*, 2019; Warwick-Dugdale *et al.*, 2019b; Trubl *et al.*, 2019). As previously mentioned, there are record high numbers of multidrug resistant bacteria, hence the search for alternative treatments to bacterial infection is now more important than ever. Bacteriophage therapy provides one such solution to this problem, yet the lack of research in this field means the phage therapy is far behind, compared to other, more extensively researched alternatives such as new antibiotic compounds or probiotics.

Whilst there is record of success using bacteriophage therapy in aquaculture and other industries, the relatively narrow host-ranges of phages tends to limit their success as therapeutic agents without the constant isolation of new organisms to meet emerging threats. Current culture-based isolation methods tend to rely on the use of agar overlay assays, whereby molten ‘overlay’ agar is used to entrap viral particles on bacterial host lawn, limiting the ability of bacteriophages to diffuse and hence lytic infection will result in visible plaques in the agar. This method has been successfully employed in the isolation of vibriophages (Matsuzaki *et al.*, 1992; Yu *et al.*, 2013; Silva *et al.*, 2014; Kokkari *et al.*, 2018). Recently, a novel agar overlay assay has been described, whereby a number of optimised techniques allow for increased efficiency and throughput in bacteriophage isolation (Kauffman & Polz, 2018).

Phage specificity is perhaps one of the largest benefits, yet also one of the largest challenges in bacteriophage therapy. Not only are bacteriophages natural

predators of bacteria and ubiquitous in nature, they are also both self-limiting and self-replicating in their host cell (Carvalho *et al.*, 2010). This means that bacteriophages have more specific action on the target bacteria than broad-spectrum antibiotics (Madhusudana Rao & Lalitha, 2015). However, limited range in target hosts of bacteriophages also means it can be challenging to isolate novel viruses and that successful elimination of a bacterial pathogen often relies on the combination of multiple bacteriophages applied simultaneously - such mixtures are often termed 'phage cocktails' (Nilsson, 2014). Futhermore, the presence of prophage may prevent superinfection of bacteria, thus hindering bacteriophage isolation, when using these host bacteria (Abedon & Lejeune, 2007; Bondy-Denomy & Davidson, 2014). Bacerial hosts may be 'cured' of prophage or temperate phage, via a process referred to as prophage induction, whereby integrated viruses are expelled from the bacterium in which they are found. Prophage induction can be carried out through the application of mitomycin C (Cavin *et al.*, 1991; Lan *et al.*, 2009), through selection for thermo-inducible mutants or exposure to UV light (Gasson & Davies, 1980; Shimizu-Kadota & Sakurai, 1982). In all, high-throughput isolation of bacteriophages and subsequent evaluation of host-range, whilst challenging, is perhaps the most important step in creating successful phage therapies that are able to efficiently eliminate bacterial infection.

3.2 Chapter Aims

This chapter first set out to use the previously sequenced *V. parahaemolyticus* stains to isolate novel vibriophages (**Figure 8**). Such phages will be specific to these host strains. The next step was to encapsulate these phages for future experiments to treat *V. parahaemolyticus* infection of *C. gigas* oysters. If bacteriophage therapy is going to become a commercially viable alternative to antibiotic treatment, it is crucial to isolate an abundance of novel phages.

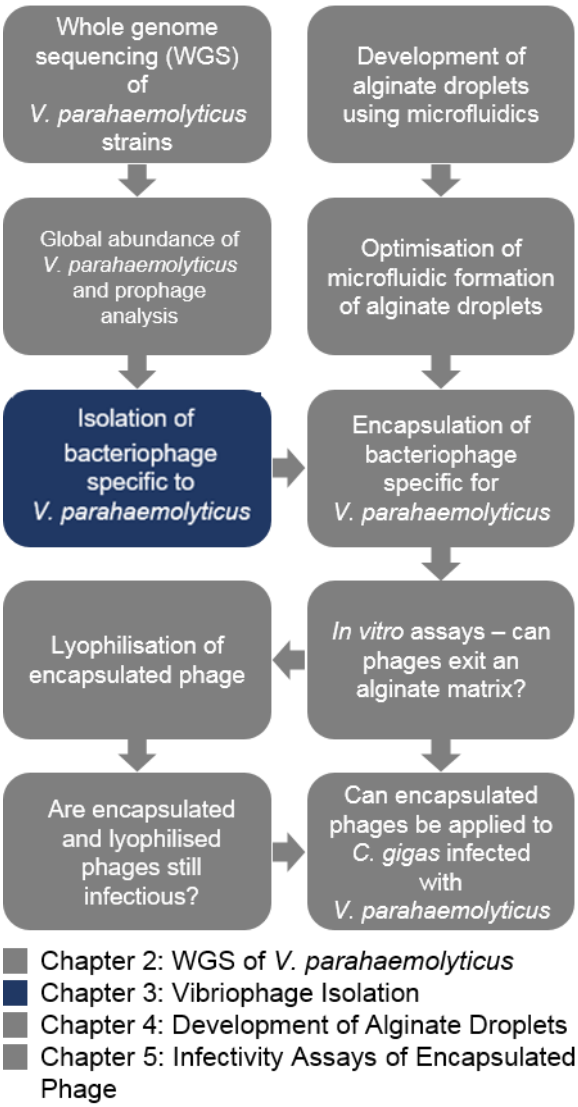

Figure 8: Schematic representation of experimental workflow in Chapter 3. Steps relevant only to Chapter 3 have been highlighted.

3.3 Materials and Methods

3.3.1 Bacterial and Viral Strains

V. parahaemolyticus strains EXE V18/004, V12/024, V05/313 and V05/027 were acquired as previously described in **2. 4. 1. Bacterial strains**. *Vibrio parahaemolyticus* strain NCIMB 1902 was kindly provided by the Millard Lab (University of Leicester), as were both vibriophages sm030 and sm031. *Vibrio* sp. bacteriophage ATCC 11985-B1 was purchased from the American Type Culture Collection (ATCC).

3.3.2 Preparation of 0.5 % Marine Agar

400 mL of seawater was filtered using a 0.22 µm pore size PVDF Durapore® membrane (Millex). To this, was added the following: 2 g bacto-peptone (Oxoid); 0.4 g yeast extract (Oxoid); 2 g No. 2 Agar Bacteriological (Lab M), before autoclaving for 15 minutes at 121°C.

3.3.3 Preparation of 3 % NaCl 1.2 % Nutrient Agar

To 400 mL of deionised (DI) H_2O (Milliq) was added the following: 3.2 g Nutrient Broth (Oxoid); 12 g NaCl (Thermo Fisher Scientific), 4.8 g No. 2 Agar Bacteriological (Lab M), before autoclaving for 15 minutes at 121°C.

3.3.4 Preparation of 3 % NaCl 0.5 % Nutrient Agar

To 400 mL of DI H_2O was added the following: 3.2 g Nutrient Broth (Oxoid); 12 g NaCl (Thermo Fisher Scientific), 2 g No. 2 Agar Bacteriological (Lab M), before autoclaving for 15 minutes at 121°C.

3.3.5 Preparation of 3 % NaCl Nutrient Broth (NB)

To 400 mL of DI H_2O was added the following: 3.2 g NB (Oxoid); 12 g NaCl (Thermo Fisher Scientific), before autoclaving for 15 minutes at 121°C.

3.3.6 Preparation of Bacterial Cultures

Initial streak plates for *V. parahaemolyticus* NCIMB 1902 were provided on marine agar, by the Millard Lab (University of Leicester). From these, single colonies of each strain were picked and re-plated on marine agar (*see* **2. 4. 2.**). *V. parahaemolyticus* strains EXE V18/004, V12/024, V05/313 and V05/027 were re-streaked as previously described in **2. 4. 4.**

For all strains, overnight *V. parahaemolyticus* cultures were prepared by picking a single colony of *V. parahaemolyticus* from a streak plate (prepared on marine agar) and growing it in 10 mL marine broth, in a shaking incubator at 220 rpm, 37 °C for 18h. Overnight *V. parahaemolyticus* cultures had a cell density of approximately 10^9 cells mL^{-1}.

3.3.7 Flow Cytometry for High-throughput Isolation of Vibriophage

Flow cytometry was used to screen for positive infection of cultures using an in-house protocol (Buchholz *et al.*, *in prep*) (**Figure 9**). Briefly, sea water samples collected from the Western English Channel (WEC) were sequentially filtered through a series of membranes (GF/D, 0.22 µm pore size and 0.1 µm Nuclepore), to remove the majority of non-viral-like particles. Viral particles within the filtrate were concentrated 50-fold using tangential flow filtration with a 30 kDa cutoff. Using a 96-well plate, a series of exponentially growing cultures were set up for each strain of *V. parahaemolyticus* and excluding controls, 10 % (v/v) viral concentrate was added. Cultures were then incubated overnight, at first at 37 °C (non-shaking). Different treatment groups included: (i) medium only control; (ii) *V. parahaemolyticus* and medium control; (iii) *V. parahaemolyticus* culture and 0.01 um filtered phage sample; (iv) *V. parahaemolyticus* culture and 0.02 um filtered phage sample. However, this resulted in the development of condensation on the lid of the plate and therefore, resulted in cross-contamination between wells and treatments. Following this, cultures were set up again in the same manner, but incubated overnight at 20 °C, which significantly reduced condensation build-up on the lid of the plate. Plates were then diluted 100-fold in 1 X PBS (Sigma-Aldrich) and stained for 1 h, using SYBR Green (Themo Fisher). A flow cytometer (BD Accuri C6 Plus) was used to measure cell counts, which were visualised on a C6 using side-scatter and green fluorescence from a blue

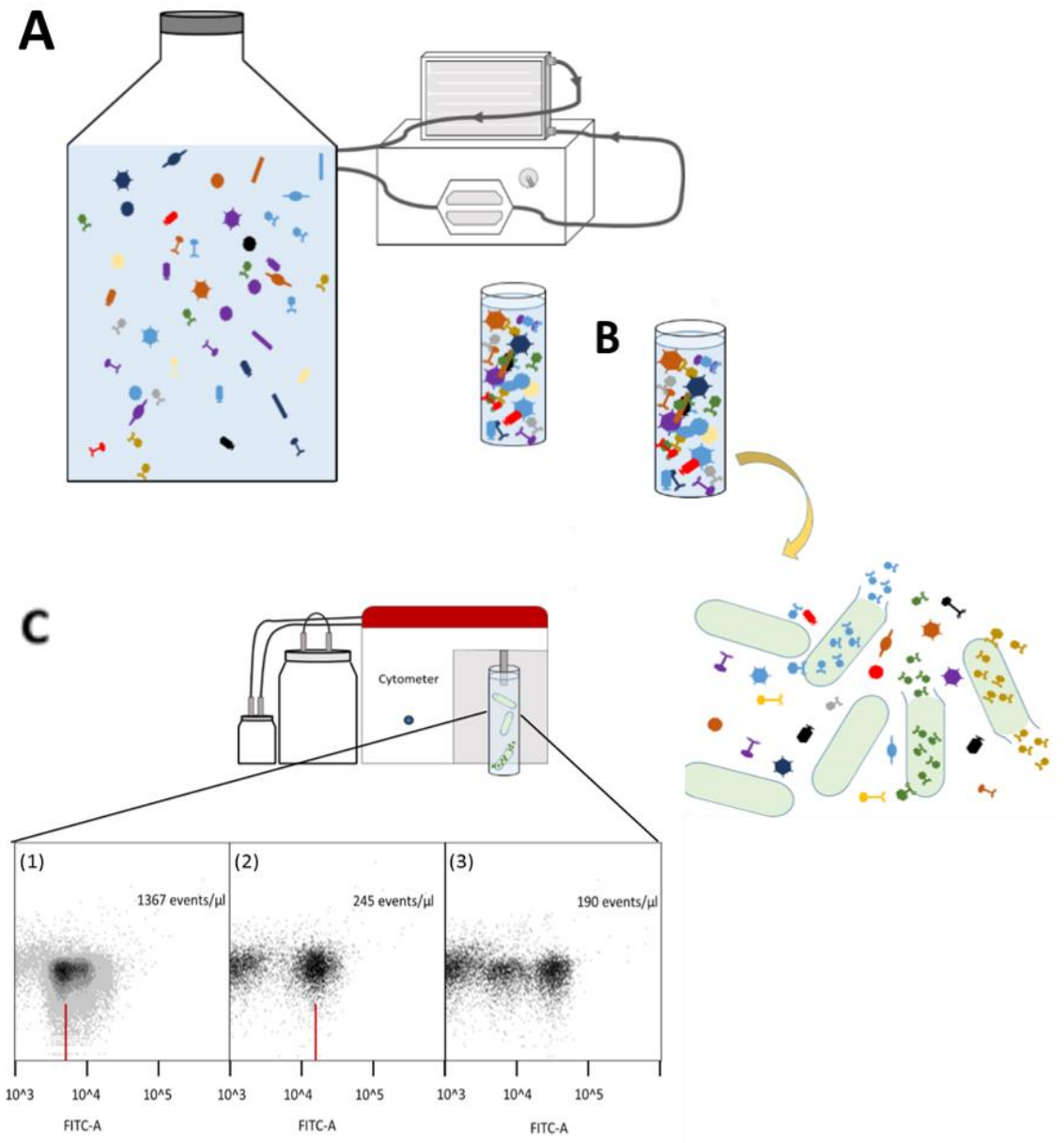

Figure 9: Schematic representing workflow for high-throughput bacteriophage isolation using flow cytometry. Figure adapted from Buchholz (2019). **(A)** Sea water samples were sequentially filtered through a series of membranes (GF/D, 0.22 µm pore size and 0.1 µm Nucleopore) to remove non-viral-like particles. Viral particles were then concentrated 50-fold using tangential flow filtration with a 30 kDa cut-off. **(B)** 10 % (v/v) viral concentrate was added to exponentially growing cultures for each strain of *Vibrio parahaemolyticus* (EXE V18/004, V12/004, V05/313, V05/027 and EXE V13/004). Cultures were then incubated overnight at 20 °C (non-shaking). **(C)** Cultures were then diluted 100-fold in 1 X PBS and stained for 1 h using SYBR Green. A flow cytometer was then used to measure cell counts, which were visualised on a BD Accuri C6 Plus, using side-scatter and green fluorescence from a blue laser. Positive infected was defined as a reduction in cell density of an order of magnitude relative to uninfected controls. **(C1)** shows an uninfected control culture of SAR11 strain HTCC 1062, whilst **(C2)** and **(C3)** show infected cultures of the same strain.

laser. Positive infection was defined as a reduction in cell density of an order of magnitude, relative to uninfected controls (Zhao *et al.*, 2013).

3.3.8 Vibriophage Enrichment

Adding cultures of host bacterial strains to a viral sample, or vice-versa, can increase the abundance of low-concentration viruses that infect the host, prior to viral isolation (Suttle, 2007). 10 % (v/v) viral sample from filtered sea water (**3. 3. 7 Flow cytometry for high-throughput isolation of vibriophage**) was added to exponentially growing *V. parahaemolyticus* cultures for each of the following strains: EXE V18/004, V12/024, V05/313 and V05/027. Following incubation overnight (37 °C, 220 rpm), each culture was filtered through a 0.22 µm pore size PVDF membrane, to remove cellular debris.

Water samples were also collected from the River Dart (Devon, UK) downstream of a local oyster farm (50.389 °N, 3.580 °E). These water samples were filtered through a series of membranes (GF/D, 0.22 µm pore size), after which, overnight *V. parahaemolyticus* cultures and the nutrients for MB were added, before overnight incubation at 37 °C, 220 rpm. Cultures were filtered through a 0.22 µm pore size PVDF membrane, to remove bacterial cellular debris.

3.3.9 Plaque Assay

Plaque assays were carried out for each *V. parahaemolyticus* host strain: EXE V18/004, V12/024, V05/313 and V05/027, following a previously described method (Kauffman & Polz, 2018). Briefly, 100 uL of overnight *V. parahaemolyticus* culture was pipetted directly onto pre-warmed (37 °C) 1.2 % marine agar. Following this, 100 uL of enriched viral sample (**3. 3. 8. Vibriophage enrichment**) was pipetted directly into the host droplet. Different to the method published by Kauffman and Polz (2018), 3 mL of molten overlay 0.5 % marine agar (50 °C) was pipetted onto the bottom 1.2 % marine agar. The petri dish was swirled briefly to mix the bacteria, viral sample and overlay agar. After a 30 min cooling period, or once the overlay agar had set, the plate was incubated at 37 °C for 24 h.

3.3.10 Spot Plaque Assay

1 mL of overnight *V. parahaemolyticus* culture was added to 3 mL molten overlay 0.5 % marine agar (50 °C). After brief mixing by vortexing, the bacterial host/agar overlay mixture was aseptically poured onto pre-warmed (37 °C) 1.2 % marine agar. After a 30 min cooling period, 5 µL aliquots of serially diluted (down to 10^{-5}) enriched viral sample (**3. 3. 8. Vibriophage enrichment**) were pipetted directly onto the 0.5 % agar overlay. After another 30 min cooling period, the plate was incubated at 37 °C for 24 h.

For spot assays involving the infection of *V. parahaemolyticus* NCIMB 1902 by sm030 and sm031, the above method was used, apart from the following exception: plates were incubated at 28 °C for 24 h.

Where lysis was evident, areas of agar were picked using 1 mL plastic pipettes (Sigma-Aldrich), dissolved in 1 mL MB and left overnight at 4 °C. This mixture was vortexed for 10 s and used in a serial dilution (down to 10^{-5}) for subsequent spot assays.

3.4 Results and Discussion

3.4.1 Flow Cytometry for High-throughput Isolation of Vibriophage

Cell counts were measured using a flow cytometer, with the expectation that infected cultures would show decreased cell counts relative to control treatments, without phages. Unfortunately, despite diluting the cultures 100-fold prior to counting the cells, 'events μL^{-1}' (used as a proxy for cells μL^{-1}) was considered too high: even medium-only control wells showed as many as 7,605 events μL^{-1} (**Figure 10**). This was considered higher than the maximum limits for the flow cytometer and hence, the experiment was stopped, and only plaque assays were used in an attempt to isolate vibriophages specific to *V. parahaemolyticus*.

In recent years, the use of flow cytometry has been optimised for the enumeration of viruses and viral-like particles (Marie *et al.*, 1999; Brussaard, 2009; Brown *et al.*, 2015; Carlson-Jones *et al.*, 2016). Flow cytometry has also been

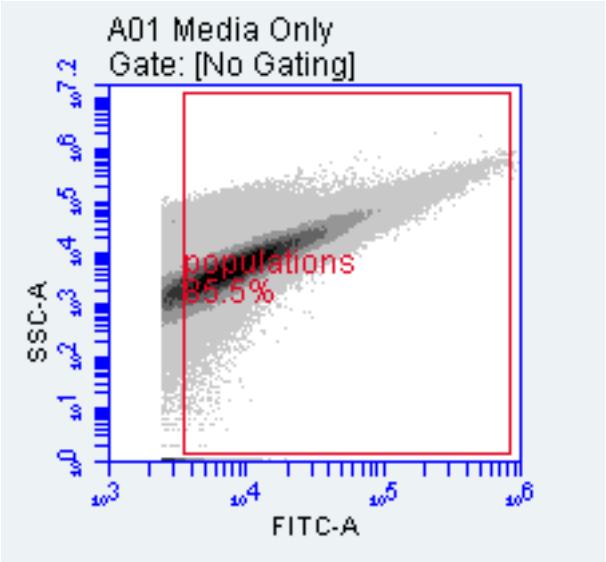

Plot 3: A01 Media Only	Count	Events / µL	% of This Plot	% of All	Mean FITC-A	CV FITC-A
All	266,171	7605	100.00%	100.00%	17,615.52	201.90%

Figure 10: Cytogram image showing 'Medium Only' control group in high-throughput isolation of vibriophages and accompanying descriptive statistics. Figure shows a cell count of 7,605 event µL $^{-1}$ and a highly dense cytogram, where no population should be present.

used to detect bacteriophage-infected *Lactococcus lactis* cells, in order to improve the likelihood of early intervention during the process of dairy fermentation (Michelsen *et al.*, 2007). Therefore, if we are able to use flow cytometry for the detection of cellular changes caused by bacteriophage infection, it is feasible that flow cytometry could be used for the high-throughput isolation of bacteriophages, by monitoring cell counts of 'infected' cultures. Whilst this method has been used successfully in the isolation of abundant SAR11 pelagiphage (Buchholz, 2019), in this instance it was not possible to detect bacteriophages specific to *V. parahaemolyticus* strains EXE V18/004, V12/024, V05/313, V05/027 and EXE V13/004.

One possible explanation for the high levels of background noise observed in this experiment may be due to the staining of nucleic acids present in the yeast extract within the medium used. On reflection, if this is the case, it may be that replicating this experiment with more diluted samples, or adjusted medium, may prevent the background noise from exceeding machine limits for detection.

3.4.2 Plaque and Spot Assays for Isolation of Vibriophage

Following the enrichment of viral samples from the WEC, plaque assays were carried out (Kauffman & Polz, 2018) on all strains of *V. parahaemolyticus* (EXE V18/004, V12/024, V05/313, V05/027 and EXE V13/004), whereby zones of no growth, or 'plaques' would suggest the presence of phage. Initial plaque assays showed no lysis, hence spot plaque assays were then used, under the hypothesis that concentrated applications of viral sample may increase the likelihood of infection. However, these again showed no plaque formation.

Water samples were collected from the River Dart (UK), downstream of a local oyster farm (50.389 °N, 3.580 °E). Here, it was hypothesised that water downstream of concentrated *C. gigas* populations would be more likely to contain *V. parahaemolyticus* and therefore, have an increased chance of containing bacteriophages that would be able to infect the strains of *V. parahaemolyticus* used in this experiment. These water samples were further enriched for all strains of *V. parahaemolyticus* (EXE V18/004, V12/024, V05/313, V05/027 and EXE V13/004) and then used again in plaque assays (Kauffman & Polz, 2018)

and spot plaque assays. Multiple assays were carried out, but all assays showed no plaque formation.

The method followed for the isolation of vibriophages in this thesis follows those successfully used in the literature. Vibriophages have been successfully isolated from random water samples throughout the world: in Shanghai, China, 34 phages specific to *V. parahaemolyticus* were isolated from surface water samples (Yin *et al.*, 2019); phage qdvp001 was isolated from effluent in Qingdao, China (Wang *et al.*, 2016); lytic phage VP06 of *V. parahaemolyticus* was isolated from seawater, sediment and homogenised oyster and clam tissue in Taiwan (Wong *et al.*, 2018); five bacteriophages specific to *V. parahaemolyticus* strain MTCC-451 were isolated from water and sediment samples of shrimp ponds in South East India (Alagappan *et al.*, 2010) and in Japan, vibriophages have been isolated from marine water samples as early as the late 20th century (Koga, Toyoshima & Kawata, 1982; Matsuzaki *et al.*, 1992). Whilst there are plenty of examples of the isolation of vibriophages in the literature, it would appear reported methods for doing so do not capture the difficulty of phage isolation. Similar difficulties in isolating vibriophages for particular host strains have been observed by other groups (Millard, *pers comms.*). In this case, agar overlay methods of seawater samples should be sufficient for the isolation of vibriophages, but it may be that a major sampling campaign to maximise the diversity of water samples used for isolation is required to improve chances. Such a campaign was beyond the time constraints of this project.

Furthermore, at least four of the five *V. parahaemolyticus* strains used as hosts during bacteriophage isolation (EXE V18/004, V12/024, V05/313 and V05/027) were found to have at least one prophage, or prophage-like element present during whole genome sequencing (see **2. 5. 3. *Inoviridae* are present in *Vibrio parahaemolyticus***). Whilst sequencing was beneficial for the rapid identification of the presence of prophage in each host strain, it was not possible to evaluate whether each prophage sequence was active or ancestral to the strain. For this reason, prophage induction was not pursued, since it was considered to be too high-risk and time-consuming for the project at hand. As well as the presence of prophages, bacteria have a number of defence mechanisms to prevent infection by phages. These include: (i) the modification of surface receptors to prevent

phage adsorption. For example, *Staphylococcus aureus* strain Cowan I produces a cell-wall anchored protein A, which binds to immunoglobulin G and masks phage receptors, or the use of lipoproteins in *E. coli* to mask the outer-membrane protein OmpA, another phage receptor (Nordström and Forsgren, 1974; Riede and Eschbach, 1986). Phage adsorption can also be prevented through bacterial production of inhibitors that competitively bind to phage receptors, such as the inhibition of FhuA in *E. coli* (an iron-siderophore transporter, which also acts as a receptor for coliphages such as T1 and T5) through competitive binding of the antimicrobial peptide microcin J25 (Destoumieux-Garzón *et al.*, 2005); (ii) superinfection exclusion (Sie) proteins are membrane anchored and block viral DNA from entering host cells, therefore preventing further infection of similar phages. For example the Sp system of phage T4 blocks peptidoglycan degradation during subsequent phage entry and therefore prevents phage DNA from passing the peptidoglycan layer of the cell wall of *E. coli* (Lu and Henning, 1994); (iii) restriction modification systems, which cleave viral DNA once it has entered the host cell (Meselson, Yuan and Heywood, 1972; Pingoud *et al.*, 2005).

Host-range is another factor that may impact the successful isolation of vibriophages and varies greatly between phages. On one hand, one of the first isolated vibriophages (bacteriophage KVP40) exhibits broad host-range, with the capability to infect at least eight distinct *Vibrio* species and one *Photobacterium* sp. (Matsuzaki *et al.*, 1992). In this case, broad host-range in KVP40 is facilitated by recognition of an outer-membrane protein (OmpK) common to *Vibrio* spp. (Inoue, Matsuzaki & Tanaka, 1995). Contrary to this, of the three phages isolated and tested for host-range by Yin *et al.* (2019), host-specificity ranged from 15 % to 51 % against tested *V. parahaemolyticus* strains (Yin *et al.*, 2019). Hence, host-specificity varies between distinct bacteriophages and may contribute to challenges during vibriophage isolation.

Vibrio spp. are renowned for rapid growth (Yoon *et al.*, 2008) and *V. parahaemolyticus* is no exception to this, with cultures reaching stationary phase within 8 h (Wong & Wang, 2004). On the other hand, vibriophages have been found to have much slower growth of up to 1-2 weeks, are often tailless and can be killed by chloroform, which is regularly used in bacteriophage isolation methods (Polz, 2019) (although not in this study). In combination, these factors

suggest that the isolation of vibriophages is more varied and challenging than initially thought. In the case of this experiment, agar overlay assays were incubated overnight and therefore, if vibriophages can take up to 2 weeks to lyse bacteria and form plaques, it is possible that plates were not incubated for long enough and that bacteriophages were isolated, but unable to grow and complete replication.

3.4.3 Vibriophages sm030 and sm031

Due to time constraints and the lack of success in isolation of vibriophages from environmental samples, vibriophages sm030 and sm031 were provided by the Millard Lab (University of Leicester). Whilst waiting for the delivery of *V. parahaemolyticus* NCIMB 1902, plaque and spot assays were carried out as above, with all environmental strains of *V. parahaemolyticus*: EXE V18/004, V12/024, V05/313, V05/027 and EXE V13/004. All assays with environmental strains of *V. parahaemolyticus* and vibriophages sm030 and sm031 showed no signs of lysis.

Spot assays were carried out, using vibriophages sm030 and sm031 to infect *V. parahaemolyticus* NCIMB 1902. After incubation at 28 °C, lysis was clearly visible by both sm030 and sm031, down to dilutions of at least 10^{-4} in all assays and as much as 10^{-5} in some assays (**Figure 11**).

Firstly, it is interesting to consider the results of this section in tandem with the earlier and failed attempts to isolate vibriophages. It may be that if earlier assays were carried out at 28 °C, bacteriophage isolation would have been more successful. Worthy of note is that the majority of reported vibriophage isolations in the literature are carried out at 37 °C, hence why assays in **3. 3. 2. Plaque and spot assays for isolation of vibriophage** followed as such (Alagappan *et al.*, 2010; Wang *et al.*, 2016; Wong *et al.*, 2018; Yin *et al.*, 2019). However, correspondence with Dr Andrew Millard, regarding the isolation of vibriophages sm030 and sm031, as well as consequent plaque formation suggested that 28 °C was a more optimal temperature. It is recommended that in future endeavours to isolate vibriophages, a range of temperatures is considered, between ambient water temperatures and 37 °C.

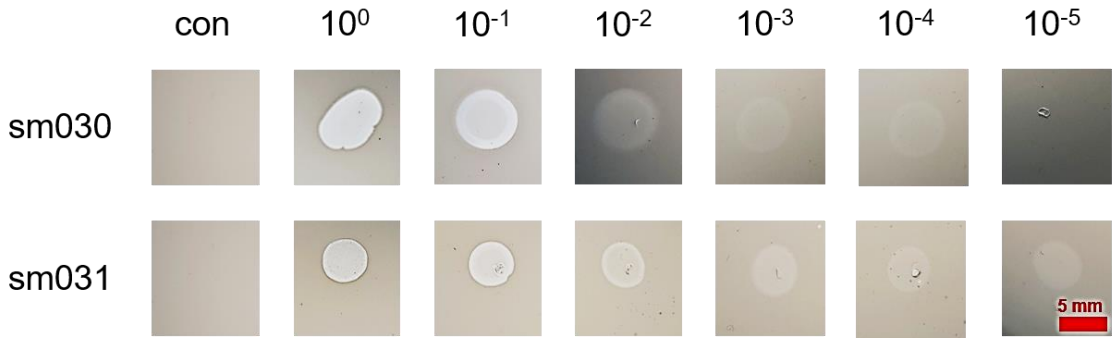

Figure 11: Spot plaque assays of vibriophages sm030 and sm031 on *Vibrio parahaemolyticus* NCIMB 1902 host lawns after overnight incubation at 28 °C. 'con' column shows control groups with 0.02 µm filtered viral sample. Subsequent columns show serially diluted viral samples 10^0 – 10^{-5}. Scale bar measures 5 mm.

3.4.4 *Vibrio* sp. Bacteriophage ATCC 11985-B1

Vibrio sp. bacteriophage ATCC 11985-B1 was also purchased, in an attempt to find a vibriophage that could infect *V. parahaemolyticus* strains EXE V18/004, V12/024, V05/313, V05/027 and EXE V13/004. Plaque and spot assays were carried out as described above, with plates incubated at 37 °C for 24 h, as recommended by ATCC. Turbid plaques were visible for *V. parahaemolyticus* strains EXE V18/004 and V12/024, with undiluted inoculum (**Figure 12**), but not in sequential serial dilutions in spot assays. Turbid plaques have been long-been associated with temperate phage and there are many examples of such in various *Vibrio* spp. including *V. cholerae*, *V. harveyi* and *V. parahaemolyticus* (Scott, 1974; Taniguchi *et al.*, 1984; Ehara *et al.*, 1997; Khemayan *et al.*, 2006; Shivu *et al.*, 2007).

It should be noted that in some cases, faint and turbid plaques could be visible on medium-only control assays, although this phenotype was not consistent between replicates. It is therefore not clear whether the occasional occurrence of plaques on medium-only control assays was due to contamination or a compound in the medium negatively impacting the growth of *V. parahaemolyticus* and further, it is not certain whether the plaques observed with bacteriophage 11985-B1 were associated with infection. Since MB was used in all assays and MB is widely considered a successful growth medium for *V. parahaemolyticus* and other *Vibrio* spp. (Dawson, Humphrey & Marshall, 1981; Sugano *et al.*, 1993; Kawagishi *et al.*, 1996), it is unlikely that any ingredient in MB would have the ability to cause plaque formation, or cell lysis, during spot assays.

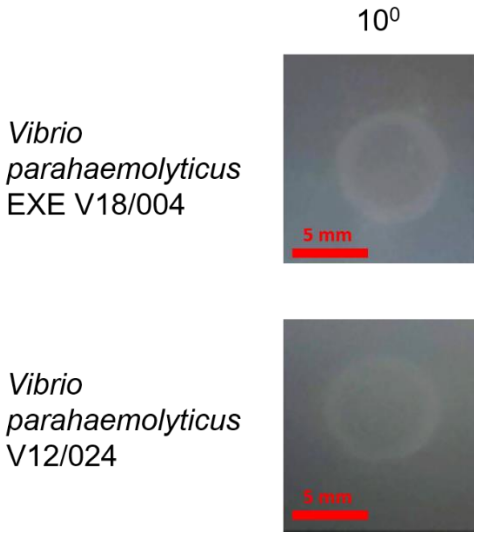

Figure 12: Turbid plaques are present in undiluted viral inoculum containing bacteriophage ATCC 11985-B1 on host strains *Vibrio parahaemolyticus* EXE V18/004 and *V. parahaemolyticus* V12/024. Scale bar measures 5 mm. Turbid plaques were not present in subsequent serial dilutions in either host strain.

4 Development of Alginate Droplets

4.1 Introduction

Sodium alginate is a naturally occurring polymer derived from brown algae (King, 1983) and has been researched extensively over the years for use in a range of biotechnological and pharmaceutical research areas (Lee & Mooney, 2012). Alginate is favoured for a number of reasons, including low toxicity and biocompatibility, ease of gelation, through cationic cross-linking (Wee & Gombotz, 1998). Whilst alginate droplets have been used in research for years, to encapsulate cells or in drug delivery (Lee & Mooney, 2012), traditional methods for the production of alginate droplets tend to result in large variation in size and morphology of droplets, with poor reproducibility (Colom *et al.*, 2017; Li *et al.*, 2018). More recently, 'droplet microfluidics' has emerged as a field, using principles of physics with minute microfluidic devices in an attempt to combat these problems (Kaminski, Scheler & Garstecki, 2016).

Since microfluidics first emerged as a field of research, approximately thirty years ago, interest has only continued to increase (Whitesides, 2006). The high-throughput nature of this field means that a number of these experiments can be performed in a fraction of the time, such as screening for disease biomarkers, biological assays, single-cell analysis and screening bacterial populations for the presence of persisters and viable but non-culturable cells (Joensson & Andersson Svahn, 2012; Guo *et al.*, 2012; Bamford *et al.*, 2017; Kaushik, Hsieh & Wang, 2018). Droplet microfluidics is based on the controlled emulsification of aqueous and oil phases to create droplets, inside of microfluidics devices, at rates as high as 20,000 s^{-1} (Teh *et al.*, 2008). Traditionally, droplet microfluidics use devices manufactured from polydimethylsiloxane (PDMS), a widely-used silicon polymer (Eddings, Johnson & Gale, 2008). However, the negatives of using this material far outweigh the benefits: whilst PDMS arguably provides more control over microfluidic chip design, it is single-use, has high autofluorescence and restricted compatibility with many chemicals (Lee, Park & Whitesides, 2003; Gervais *et al.*, 2006; Chen *et al.*, 2008). Conversely, if properly cared for, glass microfluidic devices can be re-used repeatedly, have decreased autofluorescence, are more stable under increased pressure and have improved

optical characteristics during analysis (Tonin, Descharmes & Houdré, 2016). Despite this, to date there is no published description of sodium alginate production in a glass microfluidic device.

Oysters are size-selective filter feeders, therefore control of microparticle size is important when designing droplets for use in phage therapy of oysters (Barille *et al.*, 1997). Hence, using a microfluidic system in the formation of alginate droplets for phage encapsulation in a crucial step in optimising their production and delivery through the high-throughput formation of monodisperse droplets.

4.2 Chapter Aims

The main aim of this chapter was to develop and optimise a protocol for the microfluidic synthesis of monodisperse sodium alginate droplets, for the purpose of encapsulating bacteriophages, using a glass microfluidic chip (**Figure 13**). In order to do so, the following steps are necessary: (1) optimising sodium alginate concentration to be used within a microfluidic device; (2) optimising $CaCl_2$ concentration to be used for droplet collection; (3) optimising surfactant concentration to be used during synthesis; (4) optimising the flow rate at which droplets are synthesised. All of the aforementioned optimisations, to improve droplet stability, must be completed before bacteriophages are able to be encapsulated in the alginate microcapsules.

4.3 Materials and Methods

4.3.1 Preparation of Low-salt Lysogeny Broth (LB)

To 400 mL of DI H_2O was added the following: 10 g Miller's LB Browth (Melford); 0.2 g NaCl (Thermo Fisher Scientific), before autoclaving for 15 minutes at 121 °C.

4.3.2 Preparation of Low-salt LB Agar

To 400 mL of DI H_2O was added the following: 10 g Miller's LB Browth (Melford); 0.2 g NaCl (Thermo Fisher Scientific); 4 g No. 2 Agar Bacteriological (Lab M), before autoclaving for 15 minutes at 121°C.

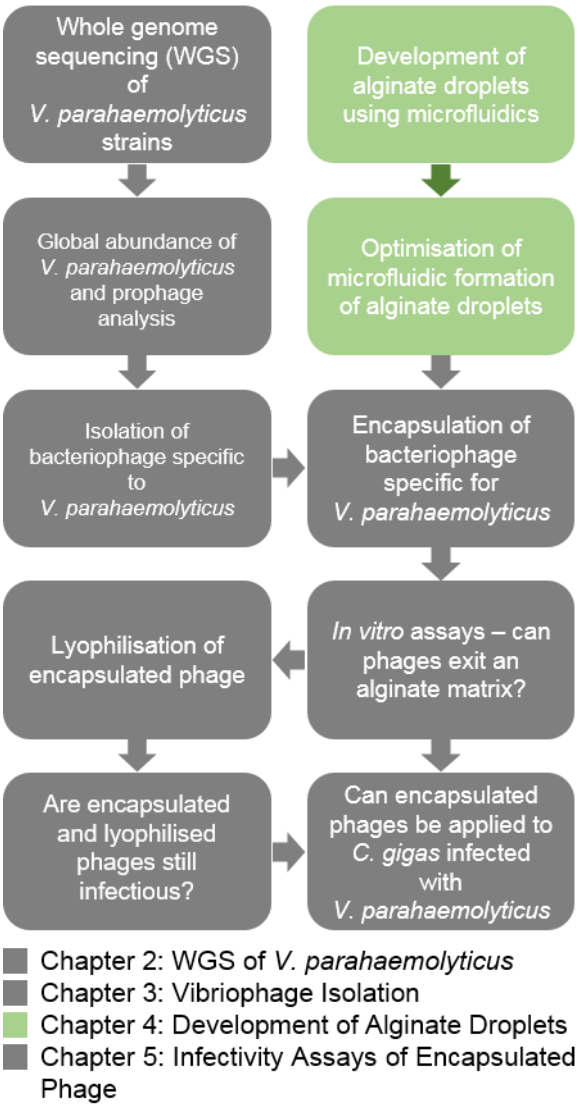

Figure 13: Schematic representation of experimental workflow in Chapter 4. Steps relevant only to Chapter 4 have been highlighted.

4.3.3 Preparation of Bacterial Cultures

A reporter strain of *Escherichia coli ompC*-GFP was obtained from the Pagliara Lab (University of Exeter). Overnight *E. coli* cultures were prepared by picking a single colony of *E. coli* from a streak plate (prepared on LB agar) and growing it in 100 mL LB, in a shaking incubator at 220 rpm, 37 °C for 18h. Overnight *E. coli* cultures had a cell density of approximately 10^9 cells mL^{-1}.

4.3.4 Materials and Reagents Used in Droplet Microfluidics

Sodium alginate, calcium chloride ($CaCl_2$), mineral oil and phosphate-buffered saline 1 X (PBS) were purchased from Sigma-Aldrich. HFE-7500 3M Novec Engineered Fluid was purchased from Fluorochem Ltd. 008-Fluorosurfactant was purchased from RAN biotechnologies. All solutions were filtered through a 0.22 µm pore size PVDF membrane before use in the microfluidic device. A Large Droplet Junction Chip (part number 3200512) was purchased from the Dolomite Centre Ltd, with the following properties: glass chip material; X-junction and T-junctions; 100 µm channel depth; fluorophilic inner channel coating (**Figure 14**). FEP tubing, with dimensions 1/16 in x 0.25 mm (part number 3200063) was also purchased from the Dolomite Centre Ltd. 1 mL plastic syringes were purchased from BD. A Low Pressure Syringe Pump neMESYS 290N (Cetoni), controlled by QmixElements software was used to control flow rate during all microfluidic experiments in this thesis, unless otherwise stated.

4.3.5 Imaging Microfluidic Droplets

To image droplet synthesis, the microfluidic chip was mounted onto an inverted microscope (IX73, Olympus). Images were collected using a 10x objective (Olympus), sCMOS camera (Zyla, Andor) and Andor SOLIS software. After collection, a volume of 15 µL of droplets were added to a Kova Glasstic Slide (Thermo Fisher) and imaged in the same way.

4.3.6 Microfluidic Synthesis of Water-in-oil (W-O) PBS Droplets

A carrier oil phase consisting of 008-Fluorosurfactant in HFE-7500 3M Novec Engineered Fluid, to a final concentration of 4 % w/w, was pre-mixed. 400 µL of

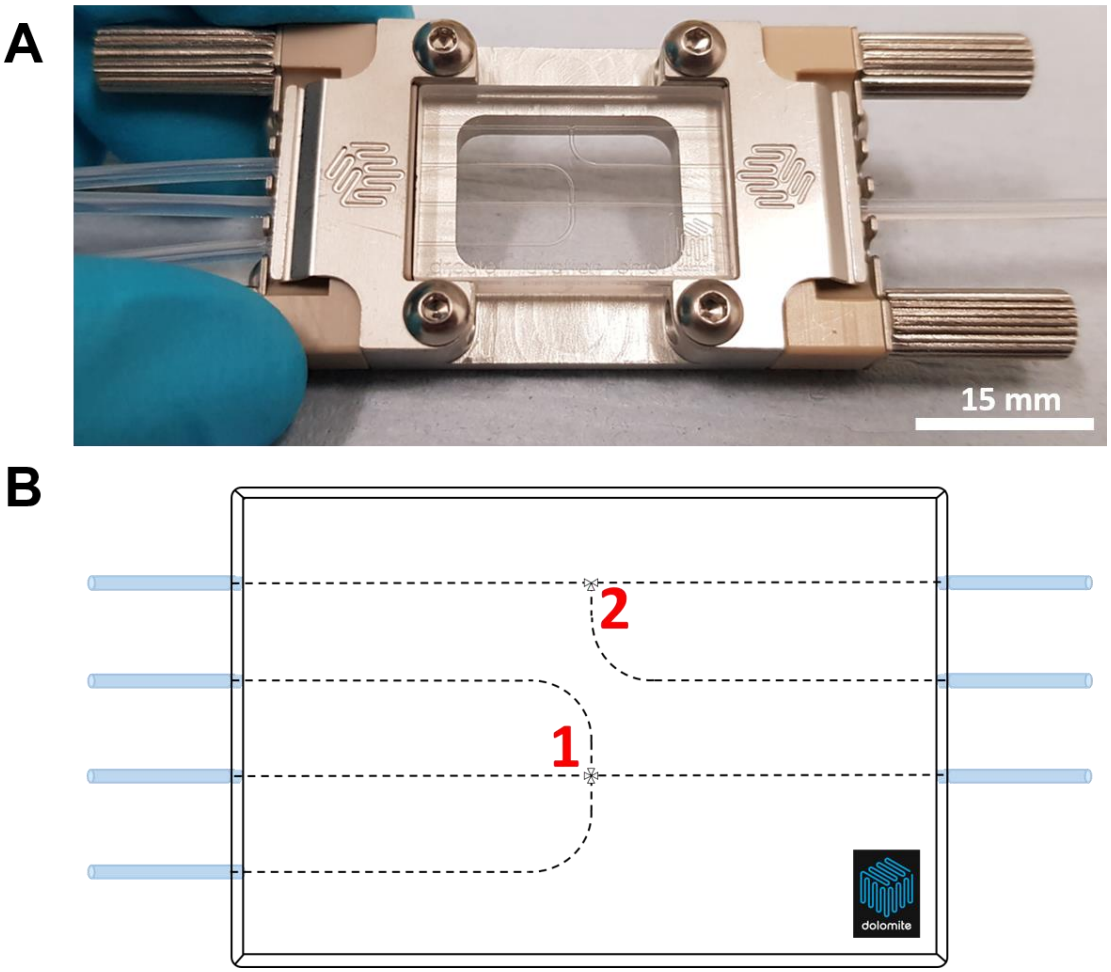

Figure 14: Photograph and schematic depicting the glass microfluidic chip used in all microfluidic experiments. (A) Photograph showing glass chip connected to tubing. Scale bar measures 15 mm. **(B) Schematic representation of droplet chip purchased from Dolomite. (B1)** shows X-junction and **(B2)** shows T-junction used to synthesise monodisperse alginate droplets.

this carrier oil phase was put into a 1 mL syringe and connected to the X-junction of the chip through the tubing, ensuring that all interfaces were water-to-water, without the introduction of any air bubbles. Since the X-junction has two input carrier oil channels, this was repeated for the second channel. For the aqueous phase, 400 µL of PBS was put into another 1 mL syringe and connected to the inner input channel of the X-junction.

The flow rate was maintained at 200 µL h^{-1} individually for each channel. An equilibration phase is required, using this flow rate, to remove all air from the microfluidic device. Following this, with the flow rate remaining at 200 µL h^{-1} for each channel, W-O PBS droplets were collected in 20 µL mineral oil, for a total time of 10 min. Droplets were imaged as described in **4. 3. 5. Imaging microfluidic droplets**.

4.3.7 Preliminary Sodium Alginate Concentration Tests

Aqueous sodium alginate at three different concentrations was made using DI H_2O: 0.5 % (w/w), 1 % (w/w) and 2 % (w/w). Each was mixed using a magnetic stirrer for 2 h. 400 µL of each was put into a 1 mL syringe and connected to a 10 cm length of tubing, then pushed through by hand.

4.3.8 Initial Microfluidic Synthesis of W-O Alginate Droplets

Aqueous $CaCl_2$ (2 % w/w) solution was made using DI H_2O and stirred briefly. Aqueous sodium alginate (1 % w/w) was made using DI H_2O and mixed using a magnetic stirrer for 2 h. For the aqueous phase, 400 µL aqueous sodium alginate was put into a 1 mL syringe and connected to the inner input channel of the X-junction, through tubing, ensuring that all interfaces were water-to-water, without the introduction of any air bubbles. A carrier oil phase consisting of 008-Fluorosurfactant in HFE-7500 3M Novec Engineered Fluid, to a final concentration of 4 % w/w, was premixed. 400 µL of this carrier oil phase was put into a 1 mL syringe, again ensuring no air bubbles entered the system. Since the X-junction has two input carrier oil channels, this was repeated for the second channel (**Figure 15**).

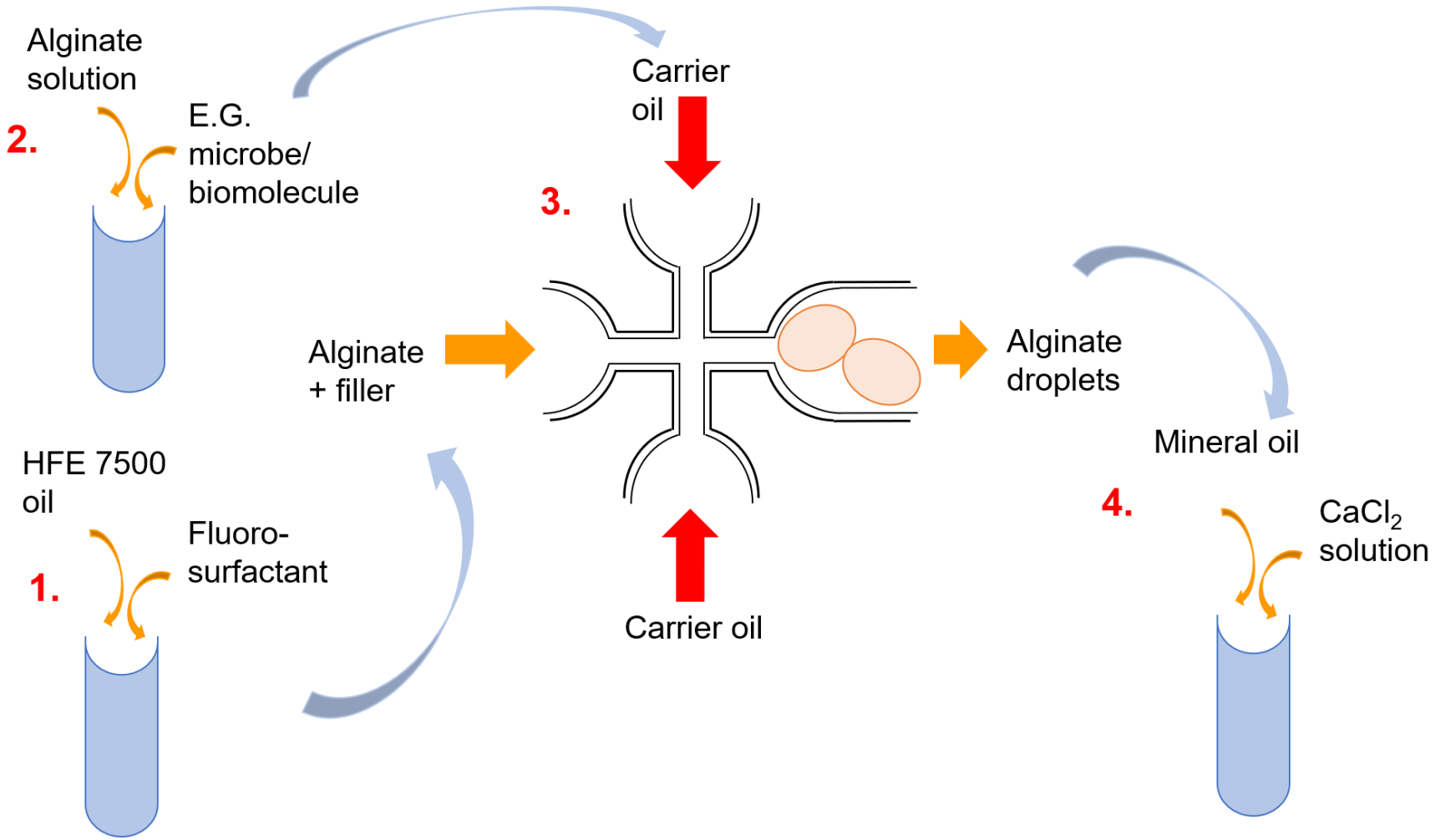

Figure 15: Schematic representing methodological workflow for the microfluidic synthesis of monodisperse alginate microcapsules. (1) Aqueous sodium alginate (1 % w/w) is filtered (0.22 µm pore size) and pre-mixed with the 'filler' substance, e.g. bacterial cells or bacteriophages. **(2)** HFE 7500 oil is mixed with 008-fluorosurfactant (4 % w/w) to form the carrier oil phase. **(3)** Alginate is passed through an inner channel at a flow rate of 100 µL h^{-1}, whilst two outer channels pass through a carrier oil phase at a flow rate of 200 µL h^{-1}. **(4)** Alginate droplets (with 'filler' encapsulated) are passed through an output channel and immediately collected in a 50:50 mixture of aqueous $CaCl_2$ solution (2 % w/w).

An initial flow rate of 400 µL h^{-1} was necessary to input the sodium alginate through the chip junction, into the outlet channel and equilibration was carried out at a flow rate of 400 µL h^{-1} for each channel. Following this, the flow rate was altered to 200 µL h^{-1} for the carrier oil phase and 100 µL h^{-1} for the aqueous phase. Sodium alginate droplets were collected in 100 uL $CaCl_2$ (2 % w/w). Droplets were imaged as described in **4. 3. 5. Imaging microfluidic droplets**.

4.3.9 Optimisation of Surfactant Concentration

To differentiate between sodium alginate droplets and air bubbles when imaging the droplets (**Figure 16**), 45 mL overnight culture of *E. coli* was transferred to a Falcon tube and centrifuged (4000 x g, 20 °C, 5 min). After removing the supernatant, the bacterial pellet was resuspended in 45 mL PBS. 1 mL of this suspension was added to 9 mL aqueous sodium alginate. Fluorescence seen in images could therefore be attributed to sodium alginate droplets and not to air bubbles. This method was used in all experiments where differentiation between alginate droplets and air bubbles was necessary.

For the aqueous phase, 400 µL of this sodium alginate and *E. coli* mixture was put into a 1 mL syringe and connected to the upper channel of the T-junction, without the introduction of air. For the carrier phase, 008-Fluorosurfactant in HFE-7500 3M Novec Engineered Fluid was premixed to two concentrations: 2 % (w/w) and 4 % (w/w) and 400 µL of this phase was put into a 1 mL syringe and connected to the T-junction, again through tubing and without introducing air bubbles. Droplets were synthesised using a carrier oil phase of either 2 % (w/w) or 4 % (w/w). An initial flow rate of 400 µL h^{-1} was used to equilibrate the synthesis of sodium alginate droplets. Following this, the flow rate was altered to 200 µL h^{-1} for the carrier oil phase and 100 µL h^{-1} for the aqueous phase. Sodium alginate droplets were collected in 100 uL $CaCl_2$ (2 % w/w). Droplets were imaged as described in **4. 2. 5. Imaging microfluidic droplets**.

4.3.10 Optimisation of Droplet Collection

1 mL of an *E. coli* in PBS suspension (see **4. 3. 9. Optimisation of surfactant concentration**) was added to 9 mL aqueous sodium alginate. Fluorescence

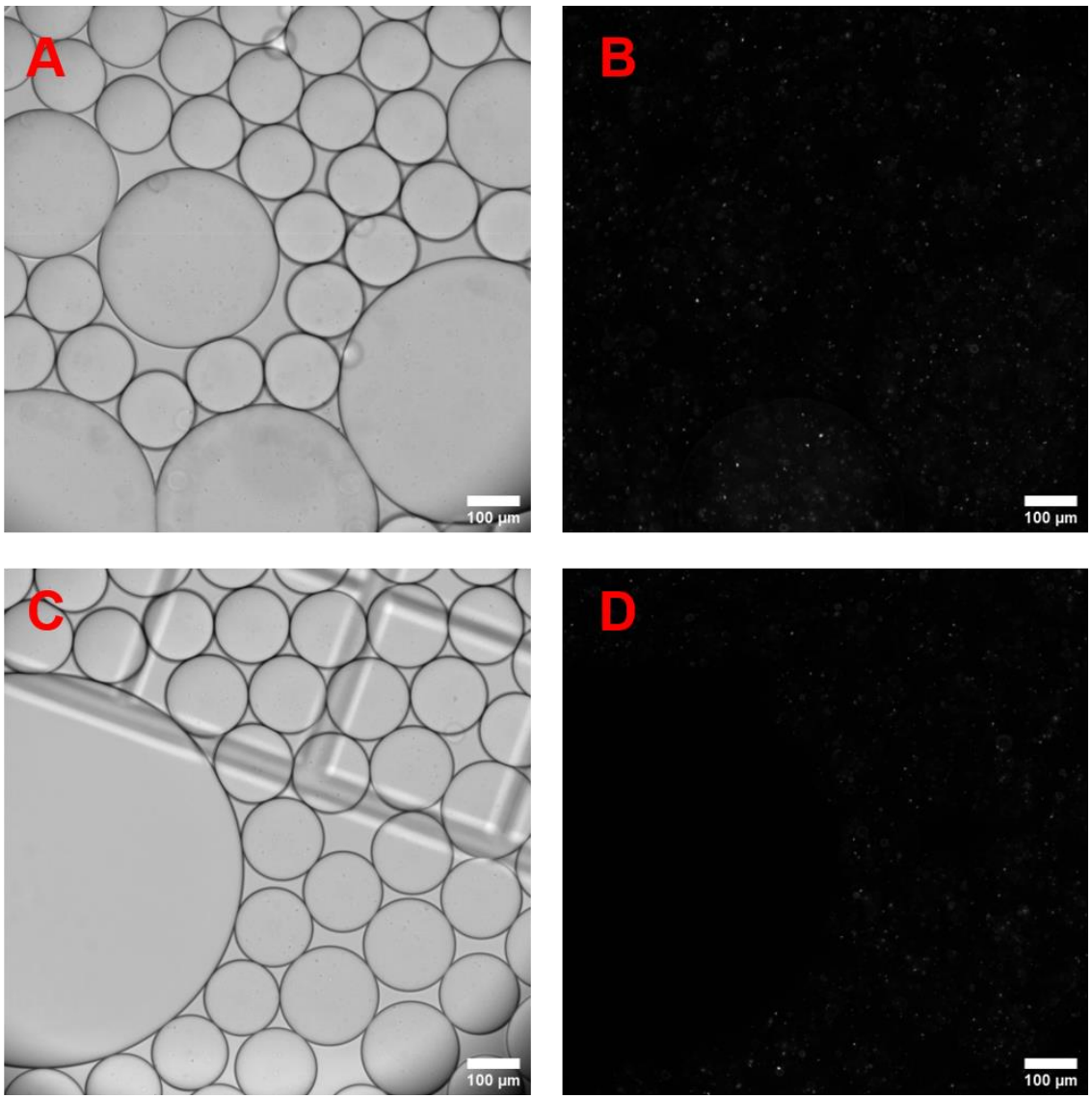

Figure 16: Microscope images to show how fluorescent *Escherichia coli* cultures can be used to differentiate between alginate droplets and air bubbles. (A) and **(C)** show bright-field images (10x objective, LED = 0.8, exposure = 0.001) of droplets of various sizes. **(B)** and **(D)** show fluorescent GFP images (10x objective, exposure = 0.8). Areas of fluorescence show encapsulated *E. coli* cells, whereas areas lacking in fluorescence show empty air bubbles. Scale bar measures 100 µm.

seen in images could therefore be attributed to sodium alginate droplets and not to air bubbles.

400 µL of an aqueous phase, consisting of a mixture of sodium alginate and *E. coli* and a carrier oil phase, consisting of premixed 008-Fluorosurfactant in HFE-7500 3M Novec Engineered Fluid 4 % (w/w) were put into separate 1 mL syringes, as described above. Both were connected to the microfluidic device, without the introduction of air. Four conditions of collection medium were used: (a) mineral oil; (b) $CaCl_2$ 2 % (w/w); (c) 50:50 mineral oil:$CaCl_2$ 2 % (w/w) and (d) $CaCl_2$ 2 % (w/w) transferred to PBS. Droplets were collected in a total of 100 µL medium, for each condition. For collection in condition (d), after an 8 min gelling time, sodium alginate droplets were transferred to 500 µL PBS.

Droplets were produced using a flow rate of 200 µL h^{-1} and 100 µL h^{-1}, respectively for the carrier oil phase and aqueous phase. Droplets were collected for 8 min and left to gel for 8 min, before being imaged at t = 0 h, 1 h and 24 h. Droplets were imaged as described in **4. 3. 5. Imaging microfluidic droplets**.

4.4 Results and Discussion

4.4.1 Preliminary Sodium Alginate Concentration Tests

Each concentration of sodium alginate (0.5 %, 1 % and 2 % w/w) was pushed manually through a 10 cm length of tubing. 0.5 % (w/w) sodium alginate was easily pushed through the tubing and showed no sign of resistance; 1 % (w/w) sodium alginate showed more viscosity than 0.5 % w/w, but was still pushed through the tube, with no-to-little sign of resistance; 2 % (w/w) sodium alginate was more viscous still, and demonstrated resistance when being pushed through the tubing. For this reason, 1 % (w/w) was chosen to be the standard concentration of aqueous sodium alginate to be used in all future experiments, since it provided a balance between viscosity and resistance, in order to form droplets that would not damage the microfluidic in anyway, but also remain stable post-formation.

4.4.2 Initial Microfluidic Synthesis of W-O Alginate Droplets

The first attempt at forming sodium alginate droplets used a rate of 200 μL h^{-1}, following the flow rate used in the formation of W-O PBS droplets. However, this was not fast enough to initialise the flow of sodium alginate through the cross-junction of the microfluidic chip and so this rate was increased to 400 μL h^{-1} across all channels. After the alginate was moving visibly with ease across the junction of the chip, the flow rate was equilibrated to 200 μL h^{-1} for the carrier oil phase and 100 μL h^{-1} for the aqueous phase. From this point, W-O sodium alginate droplets were formed using these flow rates and all droplets were collected in aqueous $CaCl_2$ at a flow rate of 100 μL h^{-1} (**Figure 17**).

In recent years, droplet microfluidics has been used more and more frequently for the encapsulation of living cells in therapeutics research and the pharmaceutical industry (Utech *et al.*, 2015). Alginate, derived from brown algae, is often the material of choice for encapsulation of living cells, due to its high biocompatibility (Ertesvåg & Valla, 1998). In comparison to traditional methods for the synthesis of alginate droplets, not only does microfluidics allow a high degree of control over the shape and size of alginate gels, but also provides more control over the consistency of droplets, resulting in those which are more monodisperse (Tan & Takeuchi, 2007; Martinez *et al.*, 2012; Utech *et al.*, 2015). Whilst methods for the fabrication of alginate droplets differ based on a number of protocol variations, including (i) microfluidic device, (ii) surfactant composition, (iii) collection method and (iv) collection medium, protocol generally includes the emulsification of an aqueous alginate phase in a carrier oil phase, then either flowed through or collected in an aqueous calcium phase, to facilitate cross-linking of the alginate gel (Huang, Lai & Lin, 2006; Chen *et al.*, 2013; Håti *et al.*, 2016; Zilionis *et al.*, 2017; Liu, Tottori & Nisisako, 2018).

4.4.3 Optimisation of Surfactant Concentration

Sodium alginate droplets were made using two different concentrations of 008-Fluorosurfactant in HFE-7500 Engineered Fluid: 2 % (w/w) and 4 % (w/w) and collected at a flow rate of 100 μL h^{-1}. Droplets were then imaged immediately after

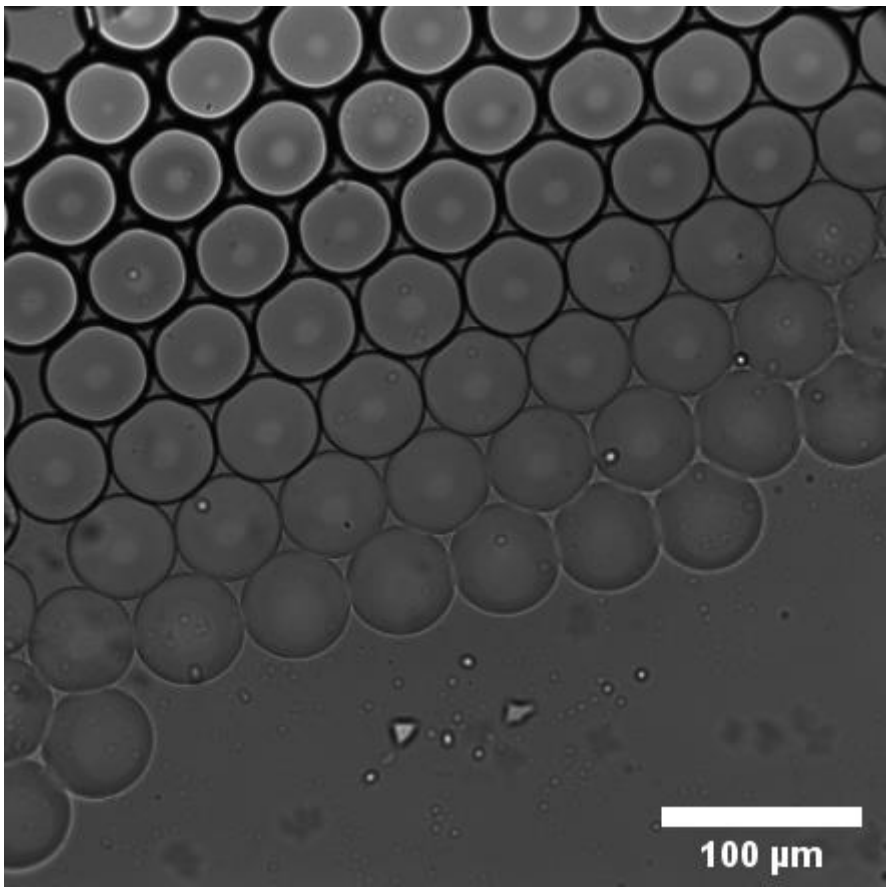

Figure 17: Microscope image to show initial synthesis of alginate droplets collected in $CaCl_2$ with an average diameter of 53 µm. Bright-field image (10x objective, LED = 0.8, exposure = 0.001).

production (**Figure 18**) and droplet diameter was measured using ImageJ (Schneider, Rasband & Eliceiri, 2012). Droplets made with a surfactant concentration of 2 % (w/w) visibly diminished in size during imaging and overall, had an increased range in droplet diameter (29.6 - 115.2 μm) compared to droplets made with a surfactant concentration of 4 % (w/w) (120.2 - 136.3 μm). In general, droplets produced with a surfactant concentration of 4 % (w/w) were more monodisperse and had increased stability over time, compared to those made with a concentration of 2 % (w/w).

Surfactant is added during droplet formation in microfluidic devices in order to stabilise droplets post-production and prevent their coalescence (Kovalchuka *et al.*, 2018). In essence, surfactant molecules are comprised of a hydrophobic tail and a hydrophilic head which are attracted to the carrier oil phase and aqueous inner phase, respectively, providing more stability and preventing segregation of the 'oil' and water' phases during droplet formation (Baret, 2012). Dolomite Centre Ltd suggest low volumes of surfactant to be used, between 1 - 5 % (v/v), in order to provide sufficient stabilisation (*Droplet Chips User Guide*). Literature is consistent within this range of surfactant (**Table 4**).

Furthermore, surfactant concentration has been found to impact wetting properties of inner channel walls in microfluidic devices, whereby surfactant concentrations of 0.0001 % - 2 % (w/w) have been used to observe the changing interactions between oil-in-water and water-in-oil emulsions within the same microfluidic device (Xu *et al.*, 2006). Whilst such research provides evidence for the role of surfactant in the control of droplet formation, the same paper suggests that droplet diameter is independent of surfactant concentration and hence, contradicts the results presented in this thesis (Xu *et al.*, 2006). It is possible that despite the different concentrations used in this experiment (2 % w/w and 4 % w/w) did not alter initial droplet size, but rather the stability of the droplet, or in other words, a reduced surfactant concentration may cause droplet shrinkage. Therefore, more research is required in order to confirm the influence of surfactant concentration of droplet size. Despite this, it can definitely be concluded that the addition of surfactant is essential for the long-term stability of emulsions and for the prevention of coalescence post-formation of droplets.

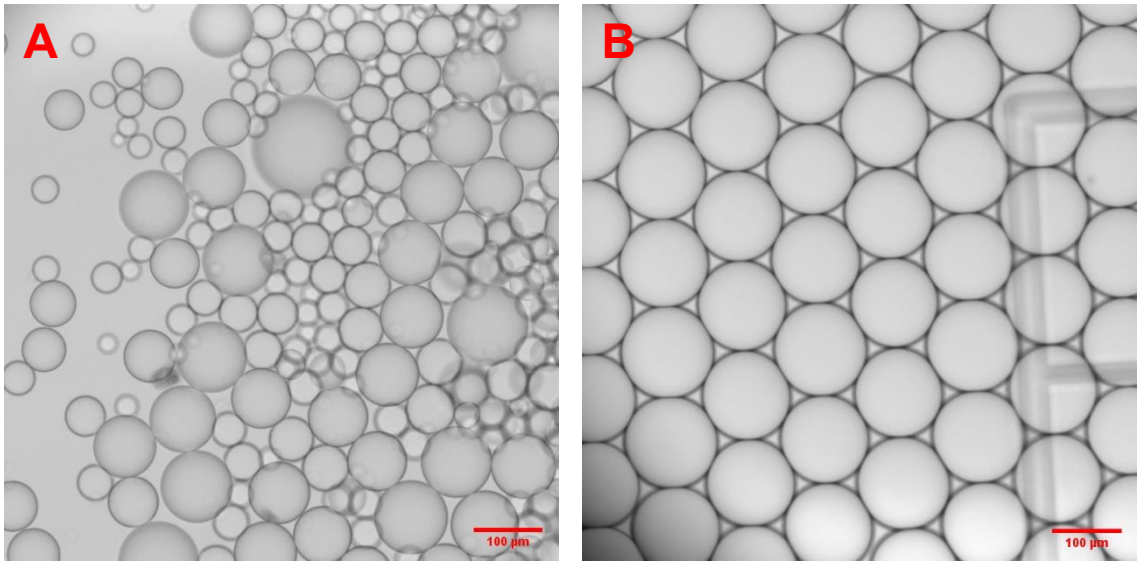

Figure 18: Brightfield (10X objective, LED = 0.8, exposure = 0.001) images showing sodium alginate droplets made with a surfactant concentration of (A) 2 % (w/w) and (B) 4 % (w/w). Droplets made with a surfactant concentration were more monodisperse and stable over time. **(A)** Droplets made using a surfactant concentration of 2 % (w/w) shrank over time compared to droplets in **(B)** made with a surfactant concentration of 4 % (w/w). Scale bar measures 100 µm.

Table 4: Table to show records of surfactant type and concentration used in published literature.

Surfactant type	Surfactant concentration	Reference
Span-80	5 % (w/w)	Chen *et al.* (2013)
Span-80	1 % (w/w)	Zilinois *et al.* (2017)
Fluorinated	2 % (w/w)	Håti *et al.* (2016)
70 % Span-20 and 30 % Span-80 mixture	2 % (w/w)	Conchouso *et al.* (2014)

4.4.4 Optimisation of Droplet Collection

Sodium alginate droplets were made using a flow rate of 100 µL h^{-1} and collected in one of the following four collection media: (a) mineral oil; (b) $CaCl_2$ 2 % (w/w); (c) 50:50 mineral oil to $CaCl_2$ 2 % (w/w) and (d) $CaCl_2$ 2 % (w/w) transferred to PBS. Droplets were collected in a total of 100 µL medium, for each condition. For collection in condition (d), after an 8 min gelling time, sodium alginate droplets were transferred to 500 µL PBS. Images were taken at *t* = 0, 1 and 24 h post-collection.

For all time points, droplets collected in a 50:50 mixture of 2 % (w/w) aqueous $CaCl_2$ and mineral oil were the most monodisperse in size, with a range of droplet diameter of 118 – 327 µm over 24 h (**Figure 19 E-F, M-N and U-V**). Whilst droplets collected in either mineral oil, or 2 % (w/w) aqueous $CaCl_2$ showed some monodisperse droplets at all time points, diameter ranged in 83 – 588 µm and 102 – 549 µm, for mineral oil and $CaCl_2$, respectively (**Figure 19 A-D, I-L and Q-T**). Fluorescent images show abnormally large droplets, relative to the flow rate used, in those collected in mineral oil (**Figure 19 B and J**), as well as abnormal droplet shape and merging in those collected in $CaCl_2$ only (**Figure 19L**). These differences had been overlooked in earlier experiments, thus emphasising the importance of further developing a system for differentiating between droplets, liquid and air bubbles, for analysis. For example, bright-field images taken at *t* = 0 h of droplets collected in 2 % (w/w) aqueous $CaCl_2$, before being transferred to PBS, appear to show that some are abnormally large in size (**Figure 19G**), however, corresponding fluorescent images reveal that these larger droplets are actually likely to be liquid or air bubbles (**Figure 19H**). Despite this, images taken at *t* = 1 h, show larger droplets, likely caused by the merging of smaller monodisperse droplets, have developed and this is confirmed by fluorescent images (**Figure 19 O and P**). For these conditions, it was therefore concluded that a 50:50 mixture of mixture of 2 % (w/w) aqueous $CaCl_2$ and mineral oil was the preferred collection method for sodium alginate droplets.

Research differs in gel-crosslinking and collection protocols. Alginate hydrogels can be cross-linked in-chip, either (i) through the use of calcium disodium ethylenediamine tetraacetate (CaEDTA), whereby an alginate solution containing

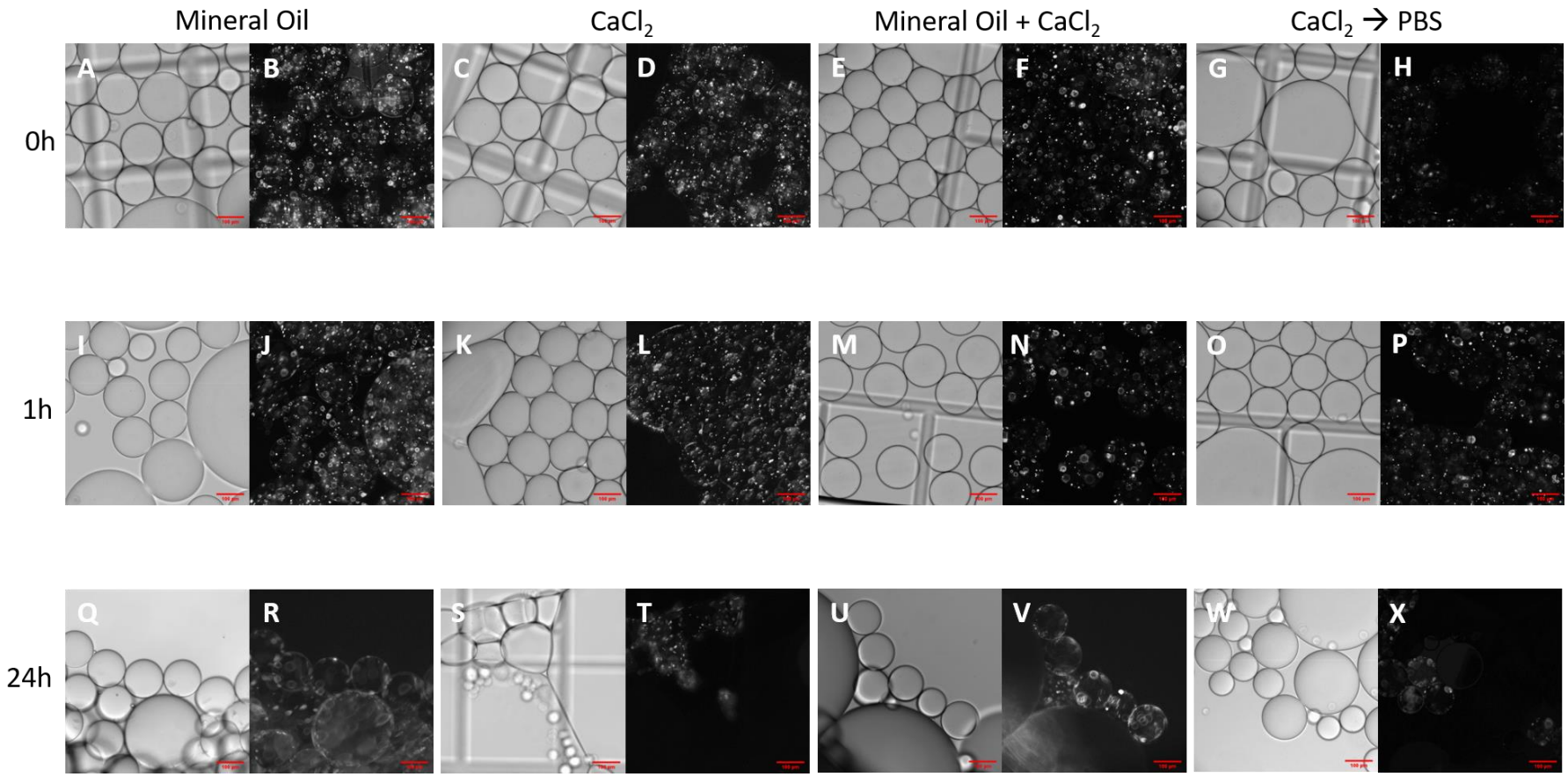

Figure 19: Brightfield (10x objective, LED = 0.8, exposure = 0.001) and fluorescent images (10x objective, GFP, exposure = 0.8) taken at *t* = 0 h, 1 h and 24 h, showing alginate droplets collected in four types of collection medium: (1) mineral oil (A-B, I-J and Q-R), (2) 2 % (w/w) $CaCl_2$ solution (C-D, K-L and S-T), (3) a 50:50 mixture of mineral oil and 2 % (w/w) $CaCl_2$ solution (E-F, M-N and U-V) and (4) 2 % (w/w) $CaCl_2$ solution transferred to 1 X PBS (G-H, O-P and W-X). GFP *Escherichia coli* was used to differentiate between alginate droplets and air bubbles, therefore alginate droplets are evident through fluorescence in GFP images. Scale bar measures 100 µm.

gelling ions is mixed with a second solution containing exchange ions, causing the gelling ion (e.g. Ca^{2+}) to be displaced by the exchange ion (e.g. Zn^{2+}) and therefore, able to form crosslinks between alginate molecules (Håti *et al.*, 2016) or (ii) through chip-design, in that a first flow-focusing channel will result in the formation of sodium alginate droplets and then afterwards, further along the channel, a second input will surround these droplets with Ca^{2+} ions, before the droplets coalesce (Liao *et al.*, 2018). If alginate droplets are not cross-linked whilst inside the microfluidic device, then in order to prevent coalescence, they must be collected directly into a medium containing Ca^{2+} ions (Chen *et al.*, 2013). In cases of external ion cross-linking, no previous study has reported the requirement of additional compounds (such as the mineral oil required here) to stabilise the droplets.

It is possible that in this case, droplet instability in this study can be attributed to excessive temperatures during formation, since increased temperature impact on the stability of droplet shape and size (Serp *et al.*, 2002). During this project, experiments were performed at room temperature, which was in the range of 24 - 25 °C. Correspondence with Professor Mike Allen suggested that a temperature of 4 - 5 °C would increase droplet stability and reduce the need for additional mineral oil during collection. Initial results of experiments performed at 4 °C (**Figure 20**) are promising and suggest improved droplet stability upon collection in $CaCl_2$ without any mixing with mineral oil, but more research is required to optimise this. The presence of mineral oil during collection is a potential issue as it might interfere with subsequent uses for the alginate microcapsules, for example, when administering encapsulated phage during bacteriophage therapy. Future experiments were conducted without the presence of mineral oil, where droplets were instead collected in aqueous $CaCl_2$ solution (2 % w/w), on ice with a temperature of 4 °C. However, it should be noted that this experiment suggests the presence of mineral oil during collection of alginate droplets may improve droplet stability at increased temperatures.

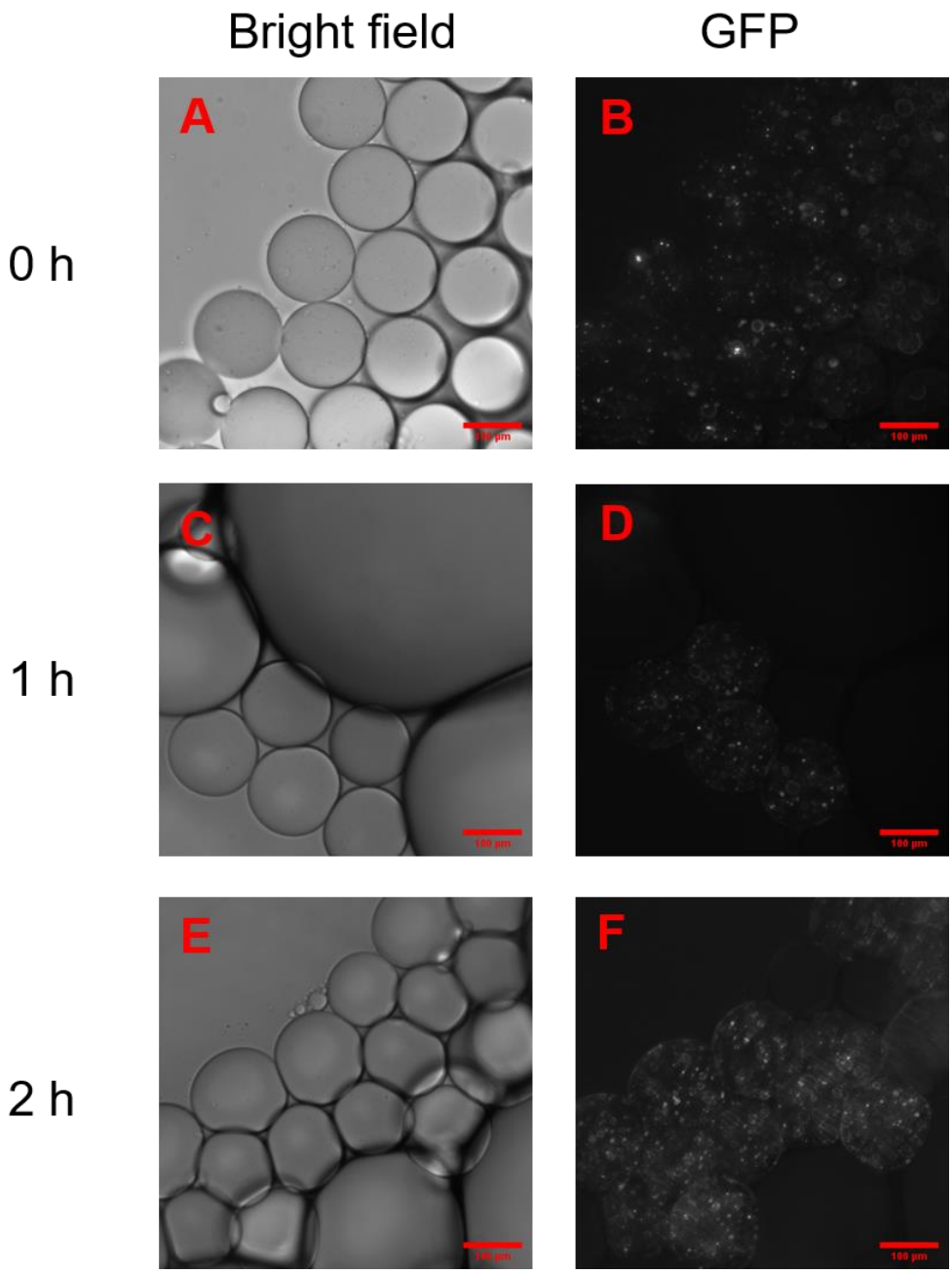

Figure 20: Brightfield (10x objective, LED = 0.8, exposure = 0.001) and fluorescent (GFP, 10x objective, exposure = 0.8) images to show alginate droplets collected at 4 °C at *t* = 0 h, 1 h and 2 h post-collection. Fluorescence is designated by encapsulated GFP-expressing *Escherichia coli*. **(A-B)** show droplets collected at *t* = 0 h post-collection. **(C-D)** sow droplets collected at *t* = 1 h post-collection. **(E-F)** show droplets collected at *t* = 2 h post-collection. Scale bars measure 100 µm.

5 Infectivity Assays of Encapsulated Phage

5.1 Introduction

For decades, *E. coli* and bacteriophage T4 have been used as a model system for host-phage interactions (Lenski, 1988). Often, this system is our first port of call when developing new protocols, since the bacterial host and viral predators are best understood. The field of droplet microfluidics is relatively and thus, limited research has been conducted into the encapsulation of bacteriophages. T4 phage has been encapsulated in chitosan-modified alginate droplets and mannitol-modified alginate droplets (Moghtader, Eğri & Piskin, 2017; Śliwka *et al.*, 2019). The antibiotic resistance crisis highlights the need for more research for new therapeutics, to which phage therapy poses a promising solution. Whilst the effects of lyophilisation have been studied on T4 bacteriophages since the late 20th century (Shapira & Kohn, 1974), little, if any, research has been conducted on the effects of lyophilisation of T4 phage post-encapsulation. However, one paper has suggested encapsulated and lyophilised phage may be suitable for the treatment of lung infections (Puapermpoonsiri, Spencer & van der Walle, 2009).

If research into T4 encapsulation is scarce, evidence for the encapsulation of vibriophages is even more so. Various papers have assessed the use of direct applications of vibriophages in the treatment of *V. parahaemolyticus*, both in oysters and in the treatment of AHPND (Jun *et al.*, 2016; Plaza *et al.*, 2018; Yin *et al.*, 2019; Richards *et al.*, 2019). Research into bacteriophage encapsulation, including the efficacy of infections and the stability of encapsulated phage during storage, is crucial in order to further progress in this field. Encapsulation has multiple potential benefits: (i) concentrated delivery of bacteriophages directly to the site of infection, whereby alginate droplets can be essentially flooded with phage and therefore deliver a higher volume of phage per unit area than free phage; (ii) alginate, or otherwise protective compounds, can provide a protective layer between phage and the harsh environment surrounding them (Abdelsattar *et al.*, 2019); (iii) high-throughput production of alginate droplets compared to traditional methods means that personalised bacteriophage cocktails can be concocted and produced at a rapid rate for the treatment of bacterial infections

and (iv) exploitation of the filter-feeding mechanism for deriving nutrition used by oysters, ensuring phages are delivered only to organisms mature enough to filter particles of a particular size.

Therefore, research into the efficacy of encapsulated bacteriophages during infection, as well as the viability and longevity of such droplets is crucial. Furthermore, we must research the use of techniques such as and similar to lyophilisation in order to assess whether they are a hindrance or can provide benefit to the development of these therapeutic tools.

5.2 Chapter Aims

This chapter set out to apply the protocol developed in **Chapter 4 Development of Alginate Droplets** to encapsulate bacteriophages (**Figure 21**). This will involve an assessment of (1) whether phages are able to exit alginate matrices and (2) whether encapsulated bacteriophages can be applied to liquid bacterial cultures and remain infective post-lyophilisation. The work was first carried out in a model system (*E. coli* host and bacteriophage T4) and secondly, in a host-virus system relevant to vibriosis in *C. gigas* oysters: vibriophages sm030 and sm031 were used to infect host strain *V. parahaemolyticus* NCIMB 1902. These steps are crucial pre-cursors for the application of encapsulated bacteriophages to infected organisms.

5.3 Materials and Methods

5.3.1 Bacterial Strains

A reporter strain of *Escherichia coli omp*C-GFP was obtained from the Pagliara Lab (University of Exeter), together with a working stock of bacteriophage T4 (~ 1×10^8 PFU mL^{-1}). *Vibrio parahaemolyticus* strain NCIMB 1902 and vibriophage sm030 and sm031 were acquired as previously described in **3. 3. 1. Bacterial and viral strains**.

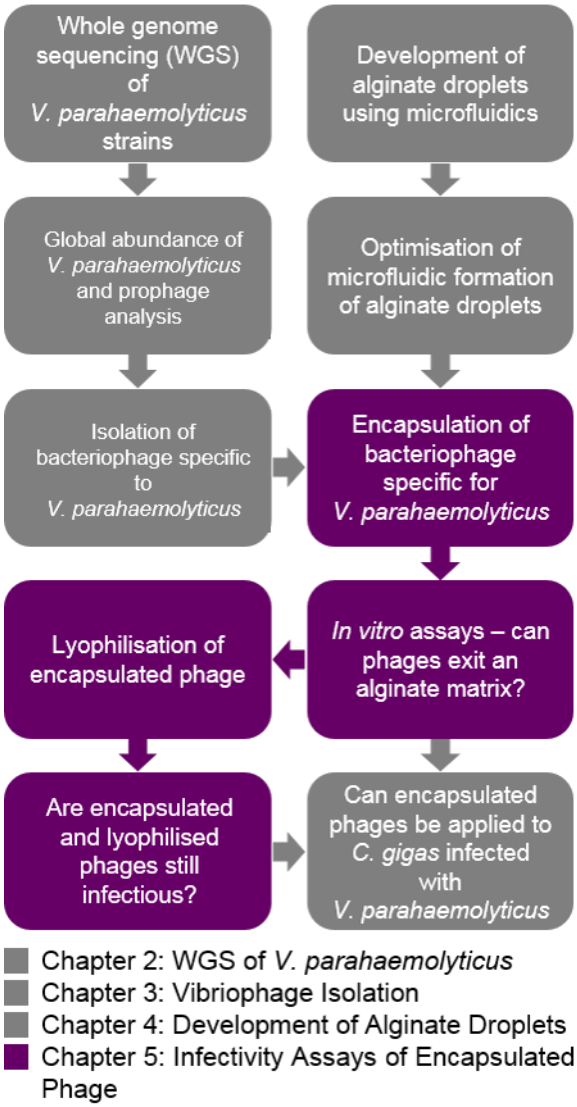

Figure 21: Schematic representation of experimental workflow in Chapter 5. Steps relevant only to Chapter 5 have been highlighted.

5.3.2 Preparation of Media and Reagents

See **2. 4. 3. Preparation of Marine Broth (MB)** and **4. 3. 1. Preparation of low-salt lysogeny broth (LB)**, respectively, for the preparation of MB and low-salt LB. Aqueous sodium alginate 1 % (w/w) and $CaCl_2$ 2 % (w/w) were prepared as described in **4. 3. 8. Initial microfluidic synthesis of sodium alginate droplets**. Carrier oil phase of 008-Fluorosurfactant in HFE-7500 3M Novec Engineered Fluid 4 % (w/w) was prepared as described in **4. 3. 8. Initial microfluidic synthesis of sodium alginate droplets**.

5.3.3 Preparation of Bacterial Cultures

Overnight *E. coli* cultures were prepared by picking a single colony of *E. coli* from a streak plate (prepared on low-salt LB agar) and growing it in 10 mL low-salt LB, in a shaking incubator at 220 rpm, 37 °C for 18h. Overnight *E. coli* cultures had a cell density of approximately 10^9 cells mL^{-1}.

V. parahaemolyticus cultures were prepared by picking a single colony from a streak plate (prepared on marine agar) and growing it in 10 mL marine broth, in a shaking incubator at 220 rpm, 37 °C for 18h. *V. parahaemolyticus* cultures had a cell density of approximately 10^9 cells mL^{-1}.

5.3.4 High-throughput Analysis of Bacteriophage T4 Infection After Gelling in Alginate

A 96 well plate was used for the high-throughput analysis to assess whether bacteriophage T4 were able to diffuse out of an alginate matrix. Five conditions were used on the plate: **(a)** a control with sodium alginate and only LB; **(b)** a control with sodium alginate and *E. coli* but no T4; **(c)** sodium alginate with T4 and *E. coli*; **(d)** a control with LB only and **(e)** a control with *E. coli* and T4 phage. For each condition containing alginate, 50 µL of alginate was added to each well, followed by either 50 µL LB for conditions **(a)** and **(b)**, or 50 µL T4 phage stock for condition **(c)**. 50 µL $CaCl_2$ solution was then added to each well, before a 10 min gelling time, after which, 150 µL LB was added to wells in condition **(a)**, whilst 150 µL overnight *E. coli* culture was added to wells in conditions **(b)** and **(c)**. 300 µL LB was added to all wells in condition **(d)**. For condition **(e)**, 50 µL T4 phage

stock was added to each well, before 250 µL overnight *E. coli* culture was added. For each well, cell density was measured using OD 600 nm, every 10 min for 24 h using a Multiskan GO microspectrophotometer (Thermo Fisher), with plate settings shaking (low) and incubated at 37 °C.

5.3.5 High-throughput Analysis of Vibriophages sm030 and sm031 Infection After Gelling in Alginate

A 96 well plate was used for the high-throughput analysis of whether vibriophages sm030 and sm031 are able to exit alginate matrices. Eight conditions were used on the plate: **(a)** a control with sodium alginate and only MB; **(b)** a control with sodium alginate and *V. parahaemolyticus* but no vibriophages; **(c)** sodium alginate with sm030 and *V. parahaemolyticus*; **(d)** sodium alginate with sm031 and *V. parahaemolyticus;* **(e)** a control with MB only; **(f)** a control with only *V. parahaemolyticus* and MB; **(g)** a control with *V. parahaemolyticus* and sm030 and **(h)** a control with *V. parahaemolyticus* and sm031. For each condition containing alginate, 50 µL of alginate was added to each well, followed by either 25 µL MB for conditions **(a)** and **(b)**, 25 µL vibriophage sm030 stock for condition **(c)**, or 25 µL vibriophage sm031 stock for condition **(d)**. 25 µL $CaCl_2$ solution was then added to each well, before a 10 min gelling time, after which, 100 µL MB was added to wells in condition **(a)**, whilst 100 µL overnight *V. parahaemolyticus* culture was added to wells in conditions **(b)**, **(c)** and **(d)**. 200 µL MB was added to all wells in condition **(e)**. For condition **(f)**, 25 µL MB was added to each well, before 175 µL overnight *V. parahaemolyticus* culture. For conditions **(g)** and **(h)** 25 µL sm030 and sm031 phage stock were added respectively, to each well, before 175 µL overnight *V. parahaemolyticus* culture was added.

Cell density for each well was measured using OD 600 nm, every 10 minutes for 24 h using a Multiskan GO microspectrophotometer (Thermo Fisher), with plate settings shaking (low) and incubated at 37 °C.

Since the soft body tissue temperature of oysters reflects that of the surrounding seawater (Chinnadurai *et al.*, 2013), a second experiment was carried out to investigate whether vibriophages are able to exit alginate matrices at 15 °C. The exact experimental as above was followed, with the following exceptions: the

plate was incubated at 15 °C, and optical density readings were taken every 10 min for 7 h.

5.3.6 Encapsulating Bacteriophage in Alginate Droplets

In order to encapsulate bacteriophage (T4, sm030 or sm031), 500 µL viral stock was added to 1.5 mL aqueous 1 % (w/w) sodium alginate, which had been filtered using a 0.22 µm pore size PVDF membrane, before vigorous vortexing. 400 µL of this mixture was used as the aqueous phase, alongside 400 µL of 008-Fluorosurfactant in HFE-7500 3M Novec Engineered Fluid 4 % (w/w) as the carrier oil phase. Each syringe, containing 400 µL, was connecting to the droplet junction chip (T-junction), through tubing, ensuring no air entered the system. After equilibration at 400 µL h^{-1} for each channel, flow rate was set to 200 µL h^{-1} for the carrier oil phase, and 100 µL h^{-1} for the aqueous phase. Droplets were collected on ice, into 100 µL 2 % (w/w) aqueous $CaCl_2$ for 10 min.

5.3.7 Lyophilisation of Bacteriophage Encapsulated in Alginate Droplets

Droplets with encapsulated bacteriophages, as described in **5. 3. 6. Encapsulating bacteriophage in sodium alginate droplets** were frozen for 1 h at -80 °C, before lyophilisation for 2 h at -110 °C using a 4 L ScanVac CoolSafe freeze dryer (Labogene). After lyophilisation, droplets were stored at 4 °C before use in further experiments.

5.3.8 Viability of Lyophilised Bacteriophage Encapsulated in Alginate Droplets

Lyophilised sodium alginate droplets, with encapsulated bacteriophages (T4, sm030 or sm031), were hydrated using 500 µL of either low-salt LB (T4) or MB (sm030 and sm031). Immediately, 300 µL were removed and added to 300 µL of the appropriate medium. This was then filtered through a 0.22 µm pore size PVDF membrane and used as viral sample in spot plaque assays, following the method previously described in **3. 3. 10. Spot plaque assay**.

The remaining 200 µL of hydrated sodium alginate droplets was added to 20 mL exponential *E. coli* (T4 phage) and *V. parahaemolyticus* (sm030 and sm031

phage) cultures. Control cultures without any phage and with un-encapsulated, un-lyophilised phage were also set up for both *E. coli* and *V. parahaemolyticus*. For *E. coli* cultures only, cell density (OD 600 nm) readings were recorded every hour for t = 0 h to t = 7 h, using an Ultrospec 100 *pro* spectrophotometer (Amersham Biosciences). For both *E. coli* and *V. parahaemolyticus*, cultures were incubated overnight (37 °C, 220 rpm), following which each culture was centrifuged (4000 x g, 20 °C, 15 min) and filtered through a 0.22 µm pore size PVDF membrane, to remove bacterial cells. The filtrate was used as viral sample, and following serial dilution (down to 10^{-5}), was used in spot plaque assays as a control to confirm infectivity, following the method previously described in **3. 3. 10. Spot plaque assay**.

5.3.9 Imaging Hydrated-lyophilised Alginate Droplets

T4 bacteriophage was encapsulated and lyophilised as seen in **5. 3. 6. Encapsulating bacteriophage in sodium alginate droplets** and **5. 3. 7. Lyophilisation of bacteriophage encapsulated in sodium alginate droplets**. Following this, the sodium alginate droplets were hydrated using 500 µL low-salt LB. 100 µL of this was then pipetted into one well of a 96 well plate, and imaged on an inverted microscope (IX73, Olympus), using a 10x objective (Olympus), sCMOS camera (Zyla, Andor) and Andor SOLIS software.

5.4 Results and Discussion

5.4.1 High-throughput Analysis of Bacteriophage T4 Infection After Gelling in Alginate

Bacteriophage T4 was trapped in sodium alginate gels across a 96 well plate, with the following treatments: **(a)** a control with sodium alginate and only LB; **(b)** a control with sodium alginate and *E. coli* but no T4; **(c)** sodium alginate with T4 and *E. coli*; **(d)** a control with LB only and **(e)** a control with *E. coli* and T4 phage. Although cell density (OD 600 nm) was measured every 10 min for 24 h, contamination occurred at t = 4 h and therefore, data recorded after this point was discounted. Data was corrected against the 'blank' control groups: **(a)** and **(d),** and mean growth curves were modelled using the ggplot2 '`geom_smooth`' function, showing standard error to a confidence interval of 95 % (**Figure 22**).

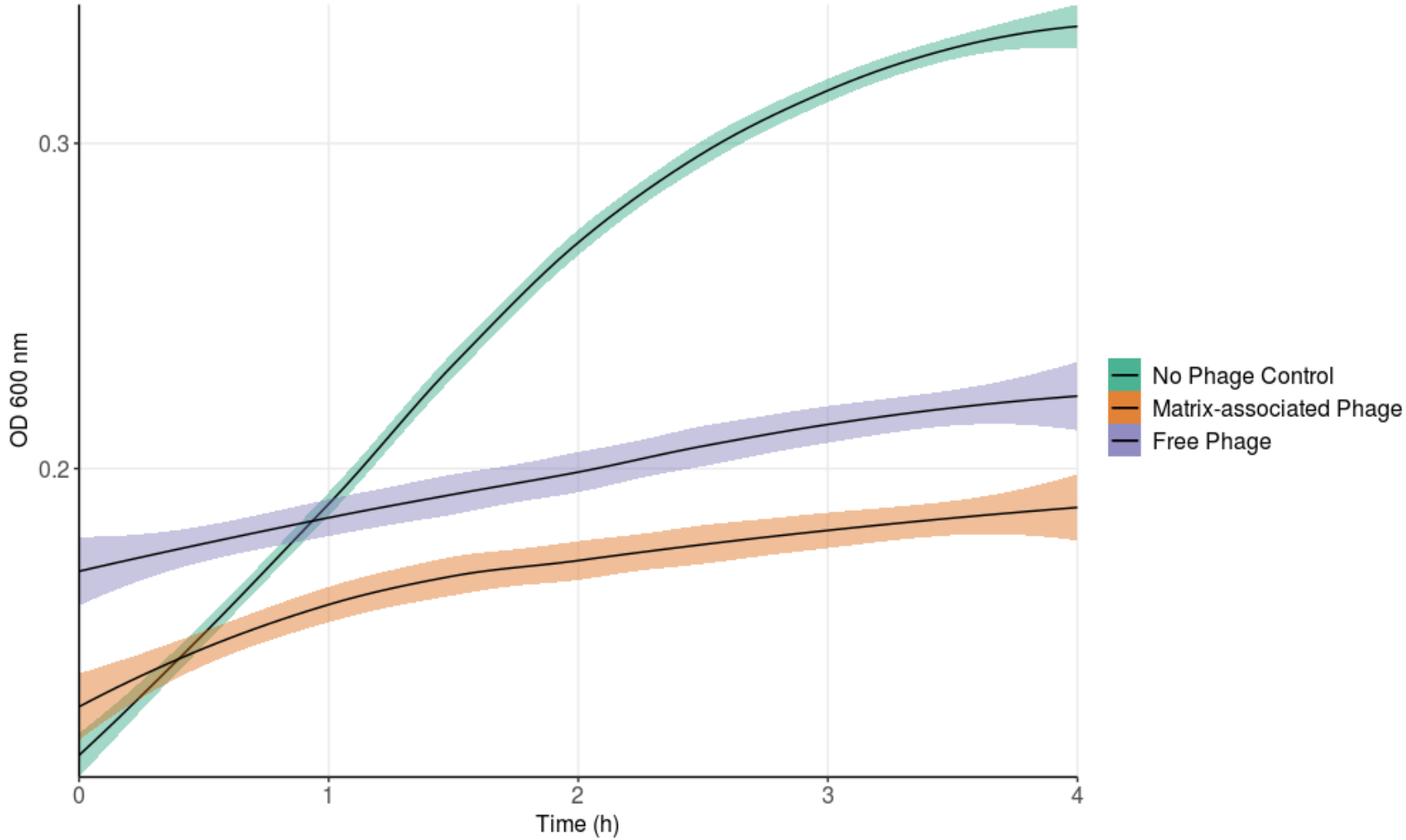

Figure 22: Smoothed conditional mean growth curves of *Escherichia coli* cultures infected with no phage (green), matrix-associated T4 bacteriophage (orange) and free T4 bacteriophage (purple). Matrix-associated phage were trapped in a sodium alginate matrix. Data presented shows cell density (OD 600 nm), measured every 10 min for 4 h at 37 °C. Confidence interval (green, orange or purple fill) is 95 %. Growth of *E. coli* is significantly reduced by addition of matrix-associated phage, compared to free phage and no phage controls.

Figure 22 shows exponential growth of the 'no phage control' group (uninfected *E. coli* cells on sodium alginate) from t = 0 h to t = 4 h, with an average optical density of 0.356 at t = 4 h. The 'free phage' group (*E. coli* cells infected with untrapped T4 phage) show visibly reduced growth compared to uninfected cells, with an average OD 600 nm of 0.226 at t = 4 h. The 'matrix-associated phage' group (phage entrapped in an alginate matrix) shows the most reduced cell growth compared to both groups, with an average OD 600 nm of 0.198 at t = 4 h.

Additionally, data wer also modelled using the ggplot2 '`geom_line`' function, to illustrate variance between replicates (**Figure 23**). Both **Figure 22** and **Figure 23** combine replicates from two separate experiments, carried out under exactly the same conditions but at different times. **Figure 23** clearly demonstrates two distinct populations in the 'free phage' treatment group, indicative of two replicated experiments. Of interest here, is the lack of such a distinction in either of the other two treatment groups: whilst there is significant variance observed in both 'no phage control' and 'matrix-associated phage', there are no distinct populations observable in either group. In fact, there are similar levels of variance apparent in both 'no phage control' and 'matrix-associated phage', yet there is a significant lack of variance within each of the individual populations observed in 'free phage', despite the clear difference in optical density between the two populations.

Despite the variance present between replicates and the presence of two distinct 'free phage' populations, **Figure 23** shows replicates from 'matrix-associated phage' to have the lowest out of the three treatments groups and replicates from the 'no phage control' group to have the highest optical densities, respectively. Whilst there is some overlap between replicated from 'free phage' and 'matrix-associated phage', both groups have significantly lower optical densities, when compared to the control group (**Figure 22**). Therefore, not only are bacteriophages able to exit alginate matrices, but it would appear that phages entrapped in an alginate matrix are more infective to exponential *E. coli* cultures than free-swimming phages.

Initial research into the efficacy of using phages to treat bacterial infection proved promising, but has also found that bacteriophages are generally less

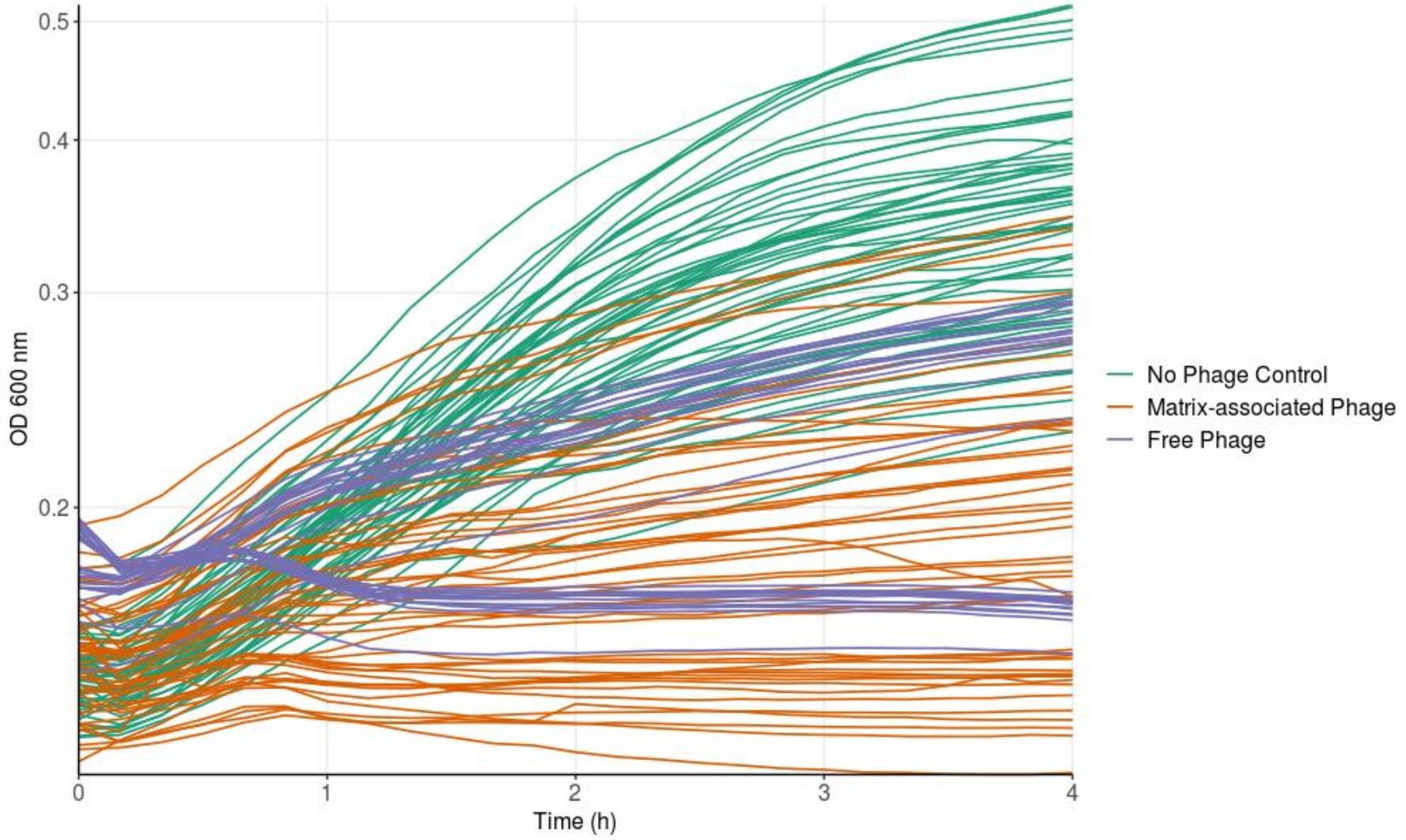

Figure 23: Growth curves of individual replicates of *Escherichia coli* cultures infected with no phage (green), matrix-associated T4 bacteriophage (orange) and free T4 bacteriophage (purple). Matrix-associated phage were trapped in a sodium alginate matrix. Data presented shows cell density (OD 600 nm), measured every 10 min for 4 h at 37 °C.

stable in solution with reductions in phage number during the various stages of processing and storage required (Malik *et al.*, 2017). Encapsulation of phages in alginate droplets has the potential to improve this, contributing to the long-term success of phage therapy. Multiple papers have suggested that encapsulation of phages increases stability, even under conditions of stress (Moghtader, Eğri and Piskin, 2017; Ramirez *et al.*, 2018). Moreover, the same research suggests that modifying the outside of the alginate droplets, for example with chitosan (Moghtader, Eğri & Piskin, 2017; Abdelsattar *et al.*, 2019) or mannitol (Śliwka *et al.*, 2019), can further improve stability. Encapsulated phage, as the above results and literature suggest, may give a more sustained infection, with higher efficacy than phage in solution.

In mucosal layers it has been suggested that phages may employ a 'subdiffusive' approach in order to improve efficacy of host infection, whereby random trapping of phages in mucosal layers results in increased infection of neighbouring bacteria (Barr *et al.*, 2015). A potential theory here, to explain increased bacterial killing by encapsulated phages, is that encapsulated phages may act in a similar way, with their heads embedded in the alginate matrix and tails extended from the surface of the droplet. In order to assess this, transmission electron microscopy could elucidate the position of encapsulated. More research is necessary in order to determine whether bacteriophages are evenly dispersed through the droplets in which they are encapsulated, or whether they embed in the surface of the alginate gel. Additionally, atomic force microscopy could be applied to provide a detailed insight into the droplet surface and if phage embedding is the case, illustrate this clearly.

5.4.2 High-throughput Analysis of Vibriophage sm030 and sm031 Infection After Gelling in Alginate

Vibriophages sm030 and sm031 were trapped in sodium alginate gels across a 96 well plate, with the following treatments: **(a)** a control with sodium alginate and only MB; **(b)** a control with sodium alginate and *V. parahaemolyticus* but no vibriophage; **(c)** sodium alginate with sm030 and *V. parahaemolyticus*; **(d)** sodium alginate with sm031 and *V. parahaemolyticus;* **(e)** a control with MB only; **(f)** a control with only *V. parahaemolyticus* and MB; **(g)** a control with

V. parahaemolyticus and sm030 and **(h)** a control with *V. parahaemolyticus* and sm031. Although cell density (OD 600 nm) was measured every 10 min for 24 h, contamination occurred at t = 7 h and therefore, data recorded after this point was discounted. Data was corrected against the 'blank' control groups: **(a)** and **(e),** and growth curves were modelled using the ggplot2 '`geom_smooth`' function, showing standard error to a confidence interval of 95 % (**Figure 24**).

Similar to the results observed with bacteriophage T4 and *E. coli* (**Figure 22**), **Figure 24** shows clear distinction in cell growth of *V. parahaemolyticus* at 37 °C between treatment groups: **(b)** 'no phage control (alginate)' and **(f)** 'no phage control (no alginate)' had the highest OD 600 nm readings, whilst **(g)** 'free sm030 phage' and **(h)** 'free sm031 phage' were reduced and **(c)** 'matrix-associated sm030 phage' and **(d)** 'matrix-associated sm031 phage' even more so. At t = 7 h, groups **(b)**, **(f)**, **(c)** and **(d)** had average optical densities of 0.427, 0.434, 0.259 and 0.236, respectively. Average optical density could not be calculated in this way for groups **(g)** and **(h)**, since group **(g)** had only one replicate and **(h)** only two, after removal of abnormal or contaminated wells. Nonetheless, at t = 7 h, the replicate in group **(g)** had an optical density of 0.335 and the two replicates in group **(h)** had optical densities of 0.298 and 0.370.

To illustrate this, variance was plotted using ggplot2, with the function '`geom_line`' (**Figure 25**). Due to time constraints, more replicates were unable to be carried out, following the discovery of contaminated wells. However, **Figure 25** shows clear distinction between pairs of treatment groups. Whilst more replicates need to be carried out for groups **(g)** and **(h)** - the 'free phage' control groups - 'matrix-associated phage' groups **(c)** and **(d)** overall, exhibit the lowest optical density.

Furthermore, a decrease in optical density was apparent in the majority of conditions, including controls: for treatment groups **(b)** and **(f)** this occurred between t = 4 h and t = 5 h; for group **(g)** this occurred at approximately t = 6 h

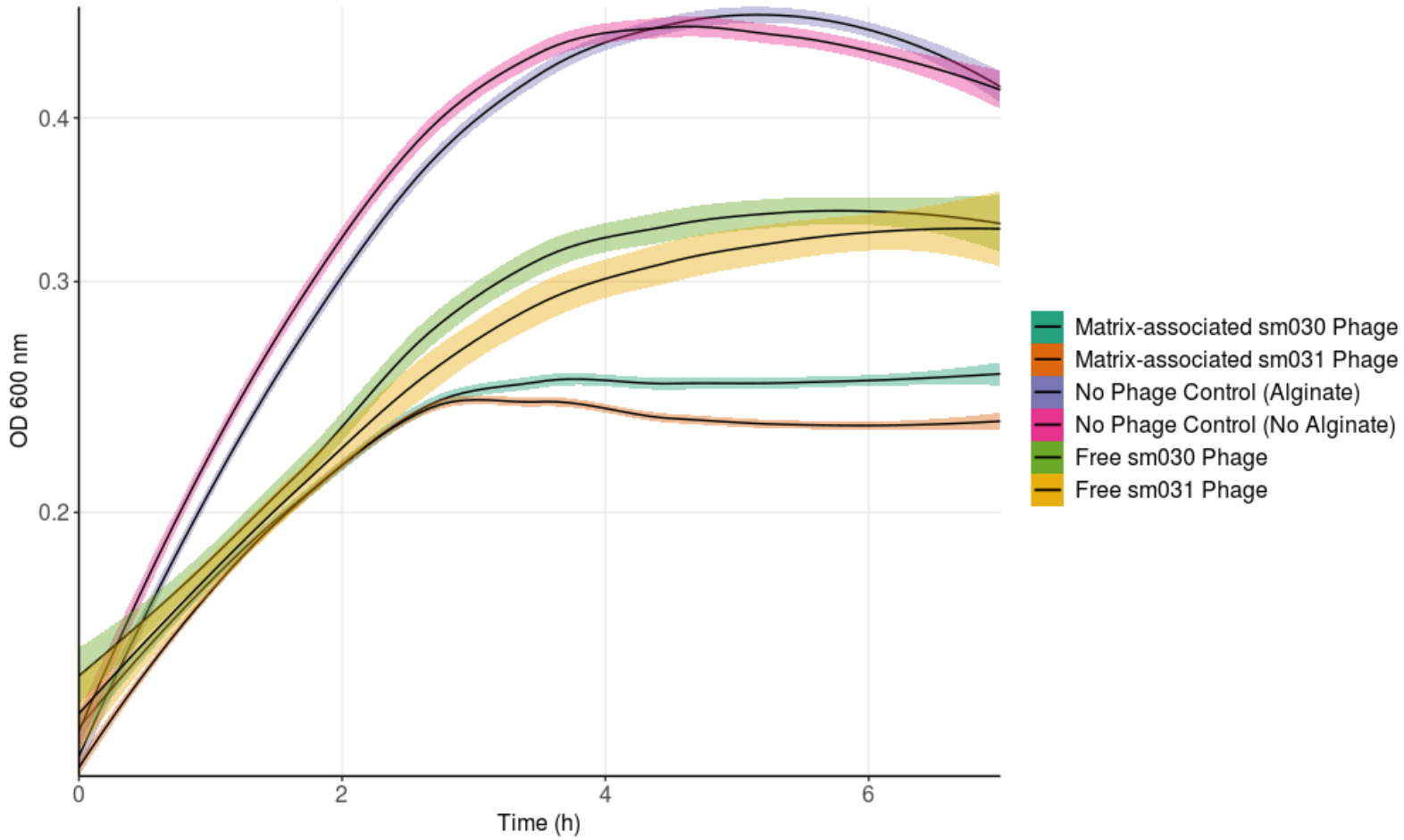

Figure 24: Smoothed conditional mean growth curves of *Vibrio parahaemolyticus* cultures infected with no phage but matrix-associated (purple), no phage with no alginate matrix (pink), matrix-associated sm030 bacteriophage (dark green), matrix-associated sm031 bacteriophage (orange), free sm030 bacteriophage (light green) and free sm031 bacteriophage (yellow). Matrix-associated controls and phages were trapped in a sodium alginate matrix. Data presented shows cell density (OD 600 nm), measured every 10 min for 7 h at 37 °C. Confidence interval (purple, pink, dark green, orange, light green or yellow fill) is 95 %. Growth of *V. parahaemolyticus* is significantly reduced by addition of matrix-associated phage, compared to free phage and no phage controls.

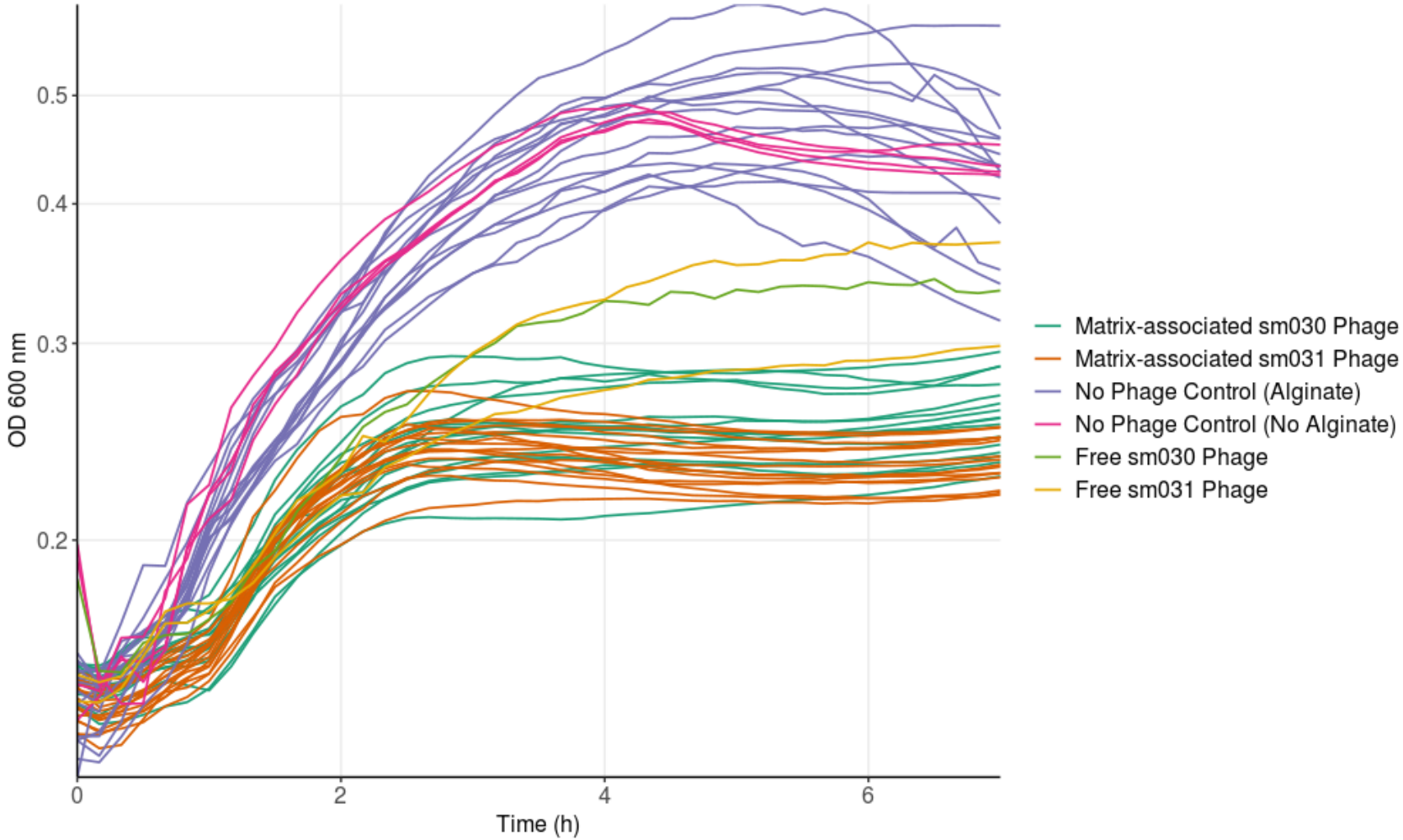

Figure 25: Growth curves of individual replicates of *Vibrio parahaemolyticus* cultures infected with no phage but matrix-associated (purple), no phage with no alginate matrix (pink), matrix-associated sm030 bacteriophage (dark green), matrix-associated sm031 bacteriophage (orange), free sm030 bacteriophage (light green) and free sm031 bacteriophage (yellow). Matrix-associated controls and phages were trapped in a sodium alginate matrix. Data presented shows cell density (OD 600 nm), measured every 10 min for 7 h at 37 °C.

and for groups **(c)** and **(d)** this happened between *t* = 3 h and *t* = 4 h. Although, it should be noted that in both groups **(c)** and **(d)**, optical density appears to increase again at *t* = 7 h. It is possible that contamination did not occur at equal times across all treatments, and hence this may be the cause for the observed increase in optical density.

Despite this, for *V. parahaemolyticus* cultures grown at 37 °C, results support those seen in **5. 4. 1. High-throughput analysis of bacteriophage T4 infection after gelling in alginate**, in that bacteriophages trapped in sodium alginate reduced bacterial cell growth more than free-swimming bacteriophages, compared to control groups.

For *V. parahaemolyticus*, this assay was also carried out at 15 °C. This was because alginate matrices are less stable with increased temperatures (Andresen & Smidsørod, 1977) and therefore, this may explain the success of previous encapsulated treatments. If this is the case and temperature does have such an impact on the stability of encapsulated phage, a temperature of 15 °C is more relevant to *C. gigas* aquaculture, when the internal temperature of oysters is likely to reflect that of the surrounding seawater (Chinnadurai *et al.*, 2013) and hence oysters must be treated at the appropriate temperature. Experimental set up was exactly the same as described above, except for the following changes: the plate was incubated at 15 °C and optical density was measured every 10 min for 7 h. The same treatment groups were used as above, with data corrected against the 'blank' control groups **(a)** and **(e)** and modelled as described above.

Figure 26 shows results divergent from those previously seen, where the average optical density measured at *t* = 7 h for each group was as follows: 0.277 for group **(b)**; 0.165 and 0.176 for groups **(g)** and **(h)**, respectively and 0.175 and 0.173 for groups **(c)** and **(d)**, respectively. An average optical density was not able to be calculated for group **(f)**, since there were only two replicates in this treatment group after removing contaminated wells. However, these two replicates had optical densities of 0.549 and 0.587.

A reduction of bacterial density was observed in the presence of both free and encapsulated phage controls; there is reduced optical density in **(g)**, **(h)**, **(c)** and

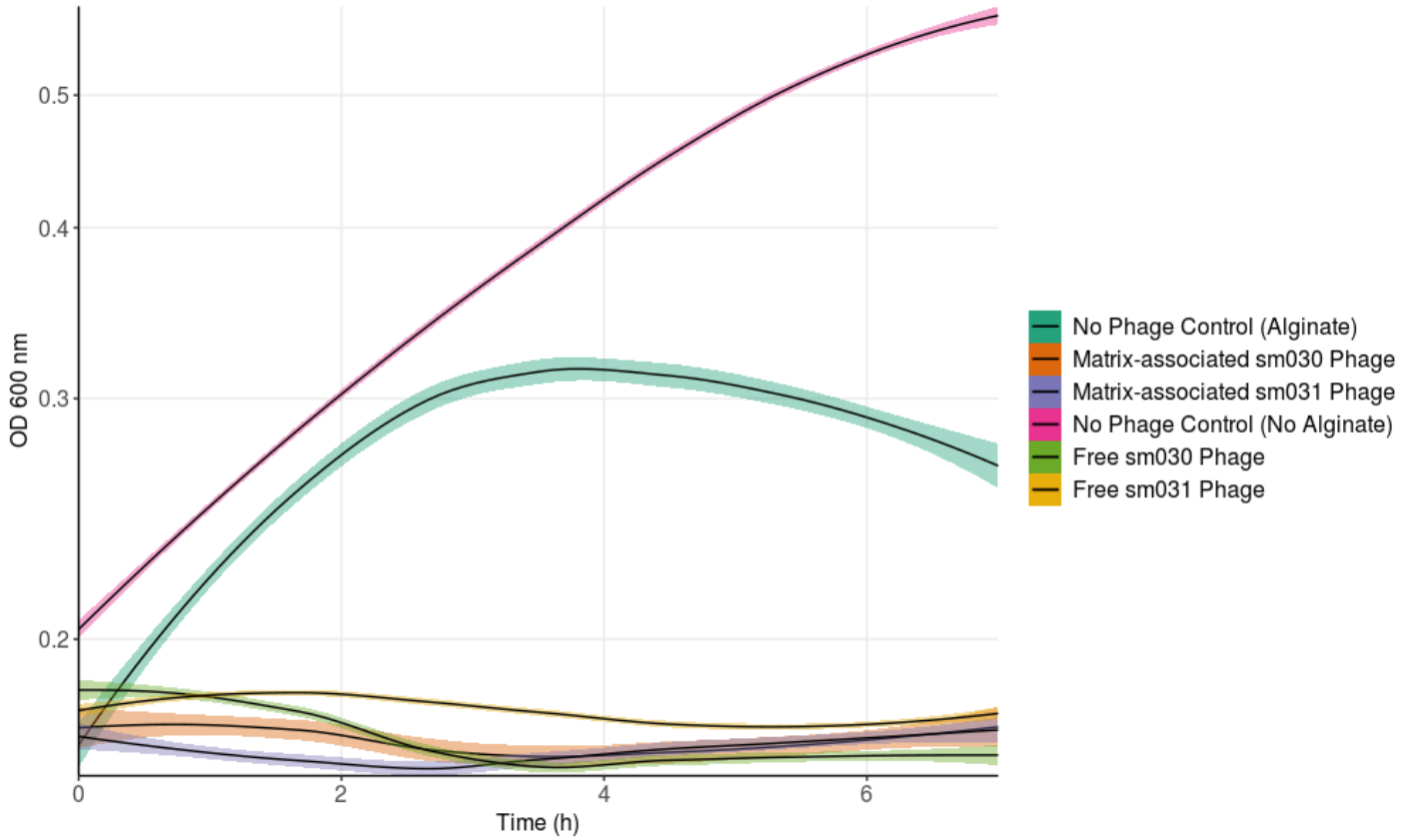

Figure 26: Smoothed conditional mean growth curves of *Vibrio parahaemolyticus* cultures infected with no phage but matrix-associated (dark green), matrix-associated sm030 bacteriophage (orange), matrix-associated sm031 bacteriophage (purple), no phage with no alginate matrix (pink), free sm030 bacteriophage (light green) and free sm031 bacteriophage (yellow). Matrix-associated controls and phages were trapped in a sodium alginate matrix. Data presented shows cell density (OD 600 nm), measured every 10 min for 7 h at 15 °C. Confidence interval (dark green, orange, purple, pink, light green or yellow fill) is 95 %.

(d) when compared to control groups **(b)** and **(f)** (**Figure 26**). In fact, across all four conditions with bacteriophages present, there was little difference in optical density at t = 7 h, suggesting that infectivity of vibriophages is not negatively impacted when trapped inside sodium alginate gels, at 15 °C. Furthermore, differentiation between density at t = 7 h seems more likely attributed to the bacteriophages used to infect *V. parahaemolyticus*, as opposed to whether or not it was encapsulated in sodium alginate: both groups with encapsulated phage **(c)** and **(d)** had very similar OD 600 nm at t = 7 h; 'free sm031 phage' **(h)** had a measured optical density slightly higher than that of the encapsulated groups and 'free sm030pPhage' **(g)** had an optical density slightly lower than all others. Despite this, all four conditions with bacteriophages had significantly lower optical density than either of the control groups with no bacteriophages.

Again, variance was plotted using ggplot2, with the function '`geom_line`' (**Figure 27**). Overall, replicates from groups **(d)**, **(f)**, **(g)** and **(h)** show little variance between replicates and whilst group **(b)** 'no phage control (alginate)' varies in optical density significantly between replicates, group **(c)** 'matrix-associated sm030 phage' largely exhibits low variance, with the exception of two replicates.

Overall, encapsulation in an alginate matrix did not negatively impact the infectivity of three separate bacteriophages: bacteriophage T4, vibriophage sm030 and vibriophage sm031. In fact, at 37 °C, infectivity seems to be increased (evidenced by decreased optical density of cultures), when compared to uninfected cultures or cultures infected by un-encapsulated bacteriophages. Even at 15 °C, infectivity of encapsulated vibriophages was very similar to un-encapsulated phage. Whilst variance is clearly apparent within the treatment groups, across all three experiments, this is to be expected in biological experiments and is indicative of scenarios that are likely to occur in real-life applications of bacteriophage therapy. These results provide promising insight into the use of encapsulated bacteriophages in the treatment of bacterial infections.

Here, it has been shown in a model system (*E. coli* and bacteriophage T4), as well as a system relevant to aquaculture (*V. parahaemolyticus* and vibriophages

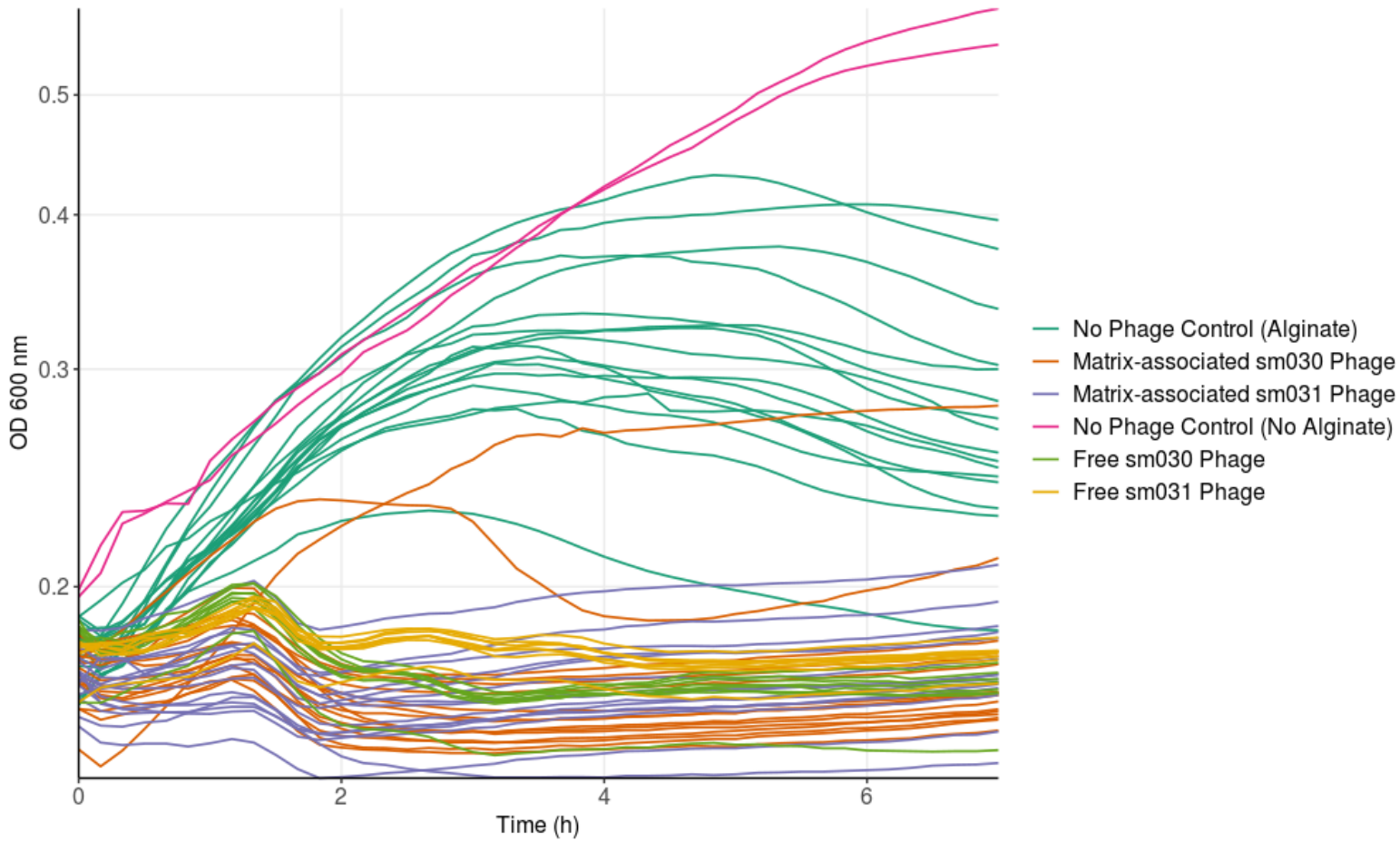

Figure 27: Growth curves of individual replicates of *Vibrio parahaemolyticus* cultures infected with no phage but matrix-associated (dark green), matrix-associated sm030 bacteriophage (orange), matrix-associated sm031 bacteriophage (purple), no phage with no alginate matrix (pink), free sm030 bacteriophage (light green) and free sm031 bacteriophage (yellow). Matrix-associated controls and phages were trapped in a sodium alginate matrix. Data presented shows cell density (OD 600 nm), measured every 10 min for 7 h at 15 °C.

sm030 and sm031) that encapsulation of bacteriophages reduces cell density and therefore, has increased infectivity relative to un-encapsulated phage. As mentioned in the previous section (**5. 4. 1. High-throughput analysis of bacteriophage T4 infection after gelling in alginate**), improved phage stability and infectivity has been shown in T4 infection of *E. coli*. Whilst there is less research reporting on the encapsulation of vibriophages, methylcellulose films containing phage encapsulated in sodium alginate have proven to inactivate *V. parahaemolyticus* ATCC 17802, a human pathogen (Kalkan, 2018). Furthermore, the results presented here for bacteriophage T4 and vibriophages are similar to those presented for *Salmonella* phage Felix O1, which suggest that encapsulation improves phage stability and provides protection en-route to infection sites (Ma *et al.*, 2008; Tang *et al.*, 2013) and those presented for the treatment of *Staphylococcus aureus* (Ma *et al.*, 2012).

The variance observed in **Figures 25** and **27** are indicative of real-life scenarios involving bacteriophage infection; as always, treatment involving biological entities is likely to vary between treatments. This emphasises the requirement for more research in this area, so more specific and personalised therapeutic plans can be devised. Moreover, this requires the constant isolation of novel bacteriophages and improved delivery methods. All experiments were incubated at the designated temperatures (37 °C or 15 °C) in a closed environment, therefore it is unlikely that the variance seen in **Figures 25** and **27** are due to differences in temperature across the plates. It is possible that more variance in mixing efficiency between replicate wells could account for this variance, since clonal cultures and identical medium were used in all experiments. Nonetheless, this is a relatively novel area of research and results presented here suggest that matrix-associated phages are still infective to bacterial hosts. This is an important first step in developing bacteriophage therapies.

5.4.3 Viability of Encapsulated and Lyophilised Bacteriophage T4

Bacteriophage T4 were microfluidically encapsulated in sodium alginate and then lyophilised for 2 h. Droplets were imaged post-rehydration (**Figure 28**). Spot plaque assays were carried out using an aliquot of the rehydrated droplets, immediately after rehydration. Results from these spot plaque assays showed no

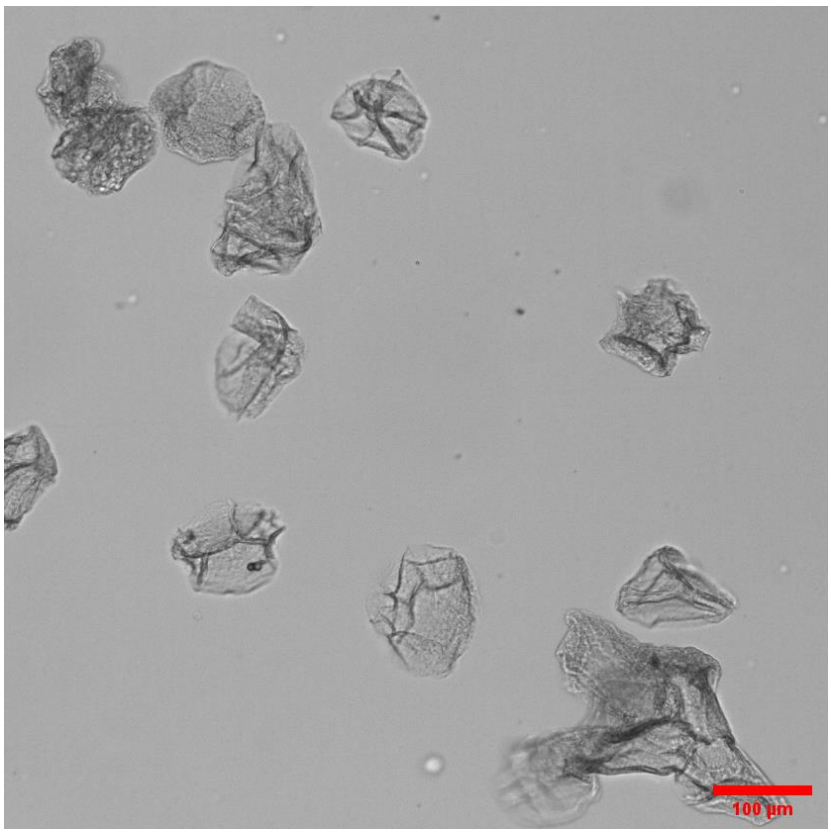

Figure 28: Brightfield image (10x objective, LED = 0.8, exposure = 0.001) of re-hydrated alginate microcapsules containing bacteriophage T4. Prior to re-hydration, alginate droplets containing phage T4 had been lyophilised for 2 h at -110 °C. Scale bar measures 100 µm.

evidence of lysis, after overnight incubation at 37 °C. The remaining aliquot of rehydrated-lyophilised droplets was added to an exponentially growing culture of *E. coli*. Hence, treatment groups were as follows: 'no phage control', 'un-encapsulated phage (not lyophilised, **NL**)' and 'encapsulated phage (lyophilised, **L**)'. For each treatment group, optical density readings were measured every hour from t = 0 h and t = 7 h (**Figure 29**). Addition of encapsulated phage did not impact host growth in contrast to the free phage treatment and followed a similar growth curve to the 'no phage control' group (**Figure 29**). However, as a result of low droplet volume (200 µL) and time constraints, only one repeat was able to be carried out for this experiment. This must be taken into consideration when analysing **Figure 29**, as consequently, it is not possible to carry out sufficient statistical analysis between the treatment groups.

At t = 7h, all cultures were incubated overnight at 37 °C and subsequently filtered through a 0.2 µm membrane, in order to remove bacterial debris. The resultant filtrates were used as viral samples in spot plaque assays. Assays carried out using the filtrate from both 'un-encapsulated phage (**NL**)' and 'encapsulated phage (**L**)' showed clear plaques at all dilutions (**Figure 30**), providing strong evidence for the presence of lytic phage in the 'encapsulated phage (**L**)' treatment group, despite the results evidenced in **Figure 29**.

This result, in tandem with the lack of lysis seen in plaque assays carried out with sample taken immediately after rehydration, supports that the bacteriophages were encapsulated in sodium alginate and not present in the medium surrounding the droplets. Whilst this demonstrates the promising uses of bacteriophage encapsulation, **Figure 29** suggests that the mechanism for rehydrating lyophilised and encapsulated bacteriophages requires further optimisation.

Bacteriophages have been lyophilised for decades, for the purposes of research and to improve stability during transport (Williams & Fraser, 1953; Steele, Davies & Greaves, 1969; Jończyk *et al.*, 2011). Although it should be noted that the process of lyophilisation was thought of as somewhat damaging to the physical structure of the phage - for example lyophilisation of bacteriophage T4 has been demonstrated to damage the head proteins so severely that the phage DNA is

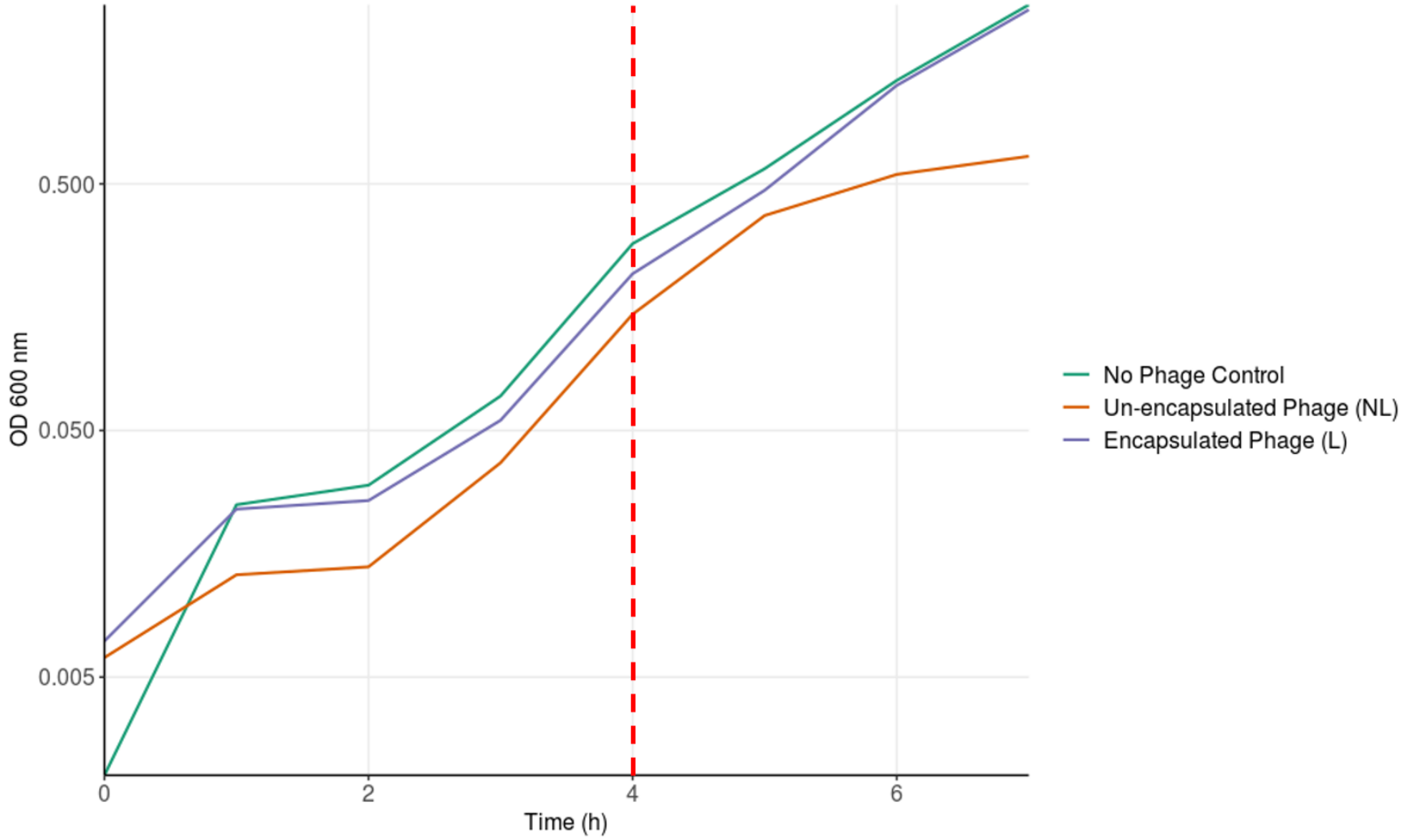

Figure 29: Growth curves of *Escherichia coli* cultures infected with no phage (green), un-encapsulated and un-lyophilised (NL) phage (orange) and encapsulated and lyophilised (L) phage (purple). Encapsulated and lyophilised phage were microfluidically encapsulated in sodium alginate droplets, before lyophilisation for 2 h at -110 °C. Cell density (OD 600 nm) measurements were taken every 1 h for 7 h. Phage treatments were added to each culture at *t* = 4 h (red dotted line).

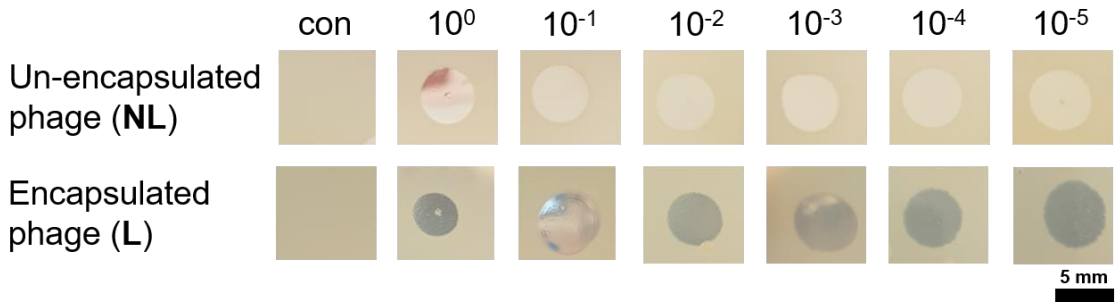

Figure 30: Spot plaque assays carried out using filtrate (0.2 µm) from two cultures of *Escherichia coli* infected with (1) un-encapsulated and un-lyophilised (NL) bacteriophage T4 and (2) encapsulated and lyophilised (L) bacteriophage T4. Encapsulated T4 were microfluidically encapsulated in sodium alginate, before being added to an exponentially growing *E. coli* culture. Spot plaque assays were carried out using a serial dilution of filtrate from concentrations 10^0 to 10^{-5}. Scale bar measures 5 mm.

lost (Shapira & Kohn, 1974). Despite this, advances in technology throughout the years have led to the established use of lyophilisation for bacteriophage storage (Puapermpoonsiri, Ford & van der Walle, 2010). Whilst this is promising for the commercial use of bacteriophage therapy, it should be noted that responses to lyophilisation are phage-dependent and stability during storage can differ significantly (Skaradzińska *et al.*, 2018).

In the case of lyophilised T4 phage that has been encapsulated, it may be that the alginate matrix provides a protective coating for the bacteriophages, preventing the loss of DNA and protein degradation. Phages have been encapsulated in modified alginate spheres and subsequently used to reduce populations of enteric *E. coli* in bovine animals, where un-encapsulated phage did not survive (Dini *et al.*, 2012). More recently, this has been demonstrated within simulated gastrointestinal environments, through the use of alginate modified with mannitol (Śliwka *et al.*, 2019). Bacteriophage T4 first encapsulated in biodegradable poly(DL-lactic-co-glycolic acid) and later lyophilised, show resilience to stress and have the potential to be inhaled in the treatment of human lung infections (Puapermpoonsiri, Spencer & van der Walle, 2009). Similar results to those presented here have been found in *Salmonella* phage Felix O1 (Vinner & Malik, 2018).

It is important to note that release of bacteriophages in culture, as presented here, may have been impacted by temperature, since increased temperatures reduce the stability of alginate gels (Andresen & Smidsørod, 1977). Experiments here were carried out at 37 °C and whilst this may have contributed to the release of phage from the alginate droplets, these results are supported by those mentioned in the aforementioned studies. Of issue is the relevance of this to an aquaculture setting; temperatures are very unlikely to reach 37 °C, even internally in treated aquatic animals, such as *C. gigas*. It is for this reason that the bacteriophage gelling experiment was repeated with *V. parahaemolyticus*, not only at 37 °C but also at 15 °C - a temperature more relevant to the temperature of aquaculture farms in the UK.

5.4.4 Viability of Encapsulated and Lyophilised Vibriophages sm030 and sm031

Vibriophages sm030 and sm031 were microfluidically encapsulated in sodium alginate and subsequently lyophilised for 2 h. Spot plaque assays were carried out using aliquots of the rehydrated droplets containing either vibriophage sm030 or vibriophage sm031, immediately after rehydration. Results from these spot plaque assays showed no evidence of lysis, after overnight incubation at 28 °C. The remaining aliquots of droplets containing either phage sm030 or phage sm031 were added to exponentially growing cultures of *V. parahaemolyticus* and incubated overnight at 37 °C. Cultures were then filtered through a 0.22 µm pore size PVDF membrane and the subsequent filtrates used again in spot plaque assays. These plaque assays showed evidence of lytic phage visible down to dilutions of 10^{-4} for both phage sm030 and phage sm031 (data not shown in text).

Due to time constraints, replicates were not able to be carried out and so evidently, more research is needed to confirm these findings. However, the results of spot plaque assays carried out provide some evidence that (i) bacteriophages can be successfully trapped and encapsulated in sodium alginate; (ii) that such droplets are able to be lyophilised and (iii) that after a sufficient rehydration period - albeit more research is required to investigate the details of this further - bacteriophages are still viable and are able to cause the successful lysis of bacteria.

Results presented here demonstrate that at in culture, at 37 °C, encapsulated and lyophilised vibriophages behave in a similar way as exhibited by T4 bacteriophage. Furthermore, these findings are supported in the literature and in other species of phage (see **5. 4. 3. Viability of encapsulated and lyophilised bacteriophage T4**). The use of bacteriophage ATCC-11985 and host strain *Vibrio* spp. 11985 as a proxy for the treatment of *V. parahaemolyticus* in fish aquaculture has been reported. Here, a proof of concept experiment demonstrated that the ingestion of vibriophage 11985-coated fish feed reduced *Vibrio* spp. populations (Huang & Nitin, 2019). This has also been suggested to be useful in the treatment of bacterial infections on the surface of fruit and vegetables (Oliveira *et al.*, 2014; Vonasek *et al.*, 2018).

Whilst evidence is lacking for the success of encapsulated vibriophages, various papers have assessed the use of bacteriophages in the treatment of aquatic *V. parahaemolyticus* infections: Zhang *et al.* (2018) found bacteriophages applied directly to the surface of oyster meat reduced *V. parahaemolyticus* populations by up to 99 % (Zhang *et al.*, 2018); similar results were seen previously, during depuration of oysters, whereby a 2-fold log decrease in CFU g^{-1} was observed after bacteriophage application for 36 h (Rong *et al.*, 2014); again, similar results were presented by Jun *et al.* (2014), whereby a decrease in *V. parahaemolyticus* growth from 1.44 x 10^6 CFU ml^{-1} to 1.94 CFU ml^{-1} was reported (Jun *et al.*, 2014a); Yin *et al.* (2019) presented promising reports of bacteriophage activity against *V. parahaemolyticus* biofilms (Yin *et al.*, 2019). Encapsulation of bacteriophages requires far more research but seems a promising approach to the treatment of bacterial infection in an aquaculture setting.

6 Conclusions

Through this project, good progress has been made in developing a protocol for the high-throughput synthesis of monodisperse alginate droplets, using microfluidics. These droplets can be used in the encapsulation of bacteriophages and reduce populations of a crucial pathogenic bacterium, *V. parahaemolyticus*, even after lyophilisation. Lyophilisation could therefore improve the commercial viability of encapsulated bacteriophages, for use in bacteriophage therapy.

In the first instance, the whole genome sequencing of four environmental *V. parahaemolyticus* strains has been undertaken and the sequences analysed in the context of their phylogenetic relationships with other *Vibrio* strains and global abundance data. Furthermore, monodisperse sodium alginate microcapsules have been produced, for the first time, using a glass microfluidic device. These droplets were used to successfully encapsulate and retain three distinct bacteriophages (T4, sm030 and sm031) and have been shown to be effective against *E. coli* (T4) and *V. parahaemolyticus* (sm030 and sm031) bacterial infections. Preliminary results suggest it is possible to lyophilise bacteriophages which have been encapsulated in sodium alginate and that these phages remain infective post-rehydration. However, more research is required to optimise this process and determine exactly how the phages may be affected by lyophilisation within alginate droplets. It has been established that the isolation of vibriophages is more difficult than perhaps is suggested in currently published literature. This may be due to a number of factors, including: (i) presence of prophage in the bacterial genomes (Bondy-Denomy & Davidson, 2014); (ii) narrow host-range of vibriophages (Yin *et al.*, 2019); (iii) vibriophages may replicate and grow much more slowly when compared to the rapid growth of *V. parahaemolyticus* bacteria (Polz, 2019); (iv) too high temperature (37 °C) used to incubate plaque assays, since it has been suggested that optimal temperature for vibriophage growth is 28 °C (correspondence from Dr Andrew Millard, 2019). Whilst it should be noted that other papers have successfully isolated vibriophages incubated at 37 °C (Alagappan *et al.*, 2010; Wang *et al.*, 2016; Wong *et al.*, 2018; Yin *et al.*, 2019), it is certainly possible that the temperature at which isolation is carried out may impact on phage replication.

Initially, this project aimed to develop a bacteriophage cocktail comprised of appropriate, isolated vibriophages for use in the treatment of *V. parahaemolyticus* infection of *C. gigas* oysters. Unfortunately, the extended timeframe required to successfully cultivate either novel or known vibriophages prevented such application. Therefore, this project has demonstrated that the development of bacteriophage therapy for use in shellfish aquaculture requires more research in order to be successful. However, good steps forwards in the processes require to do so have been made, notably in the development of droplet microfluidics to produce monodisperse sodium alginate microcapsules, the size of which can be determined through the control of the aqueous and carrier phase flow rates (Abkarian, 2005; Loizou, Wong & Hewakandamby, 2018). This, in particular, is a promising piece of technology for the design of alginate droplets for use in shellfish aquaculture, since bivalves such as *C. gigas* oysters are size-selective filter feeders (Barille *et al.*, 1997). Therefore, controlling droplet size in this manner, to be suitable for filtration by oysters or other filter-feeding bivalves, is an invaluable tool for developing phage therapy with strong efficacy. It is also possible that other organisms, microalgae for example, can be encapsulated in alginate droplets, alongside bacteriophages, to increase preferred uptake by *C. gigas*, or other similar species (Pales Espinosa, Barillé & Allam, 2007). Moreover, the results demonstrated by the lyophilisation of alginate-encapsulated bacteriophages are promising for the improved long-term viability and transportation of bacteriophage cocktails. Research suggests that lyophilised phage can be stable for as long as 24 months and that encapsulated phages retain high viability when stored at 4 °C (Łobocka, Głowacka & Golec, 2018; González-Menéndez *et al.*, 2018). Therefore, it is likely that a combination of these methods (encapsulation in alginate and lyophilisation) may further improve long-term phage viability during storage and shipping across the world. Improvement of these methodologies is imperative for the development of stable commercial phage therapies that also have high efficacy.

Global abundance data presented in this thesis suggests that distribution of *V. parahaemolyticus* strains across the globe is potentially strain-specific. When this is considered with the apparent narrow host-range of *Vibrio* spp. bacteriophages, it is possible that the isolation of new viruses for use in

bacteriophage therapy against *V. parahaemolyticus* will be challenging. However, it should be considered that the metagenomic data used in this thesis was predominantly collected in the open ocean, whilst *V. parahaemolyticus* is most commonly found in coastal, shallow waters (Letchumanan *et al.*, 2015b). Hence, more research into the global abundance of *V. parahaemolyticus*, and its specific bacteriophages, as well as the abundance of other important pathogenic bacteria, is of key importance in the search for alternatives to antibiotic pharmaceuticals. Whilst this requires considerable further research and sampling of waters across the globe, on local, national and international scales, there are already some reported metagenomics datasets for marine species (Pesant *et al.*, 2015; Biller *et al.*, 2018). Metagenomic analyses are growing exponentially in number and quality and this is something which is only predicted to improve further in future years (National Research Council (US) Committee on Metagenomics: Challenges & Applications, 2007).

To conclude, this project has completed preliminary research into the feasibility of using encapsulated bacteriophages to treat *V. parahaemolyticus* infection of *C. gigas* oysters in aquaculture. What this thesis has predominantly highlighted is that initial results are promising, but more research is necessary into understanding how to improve these therapies and how best to develop specific treatments for bacterial disease. Despite the challenges presented, for example the lack of isolation of vibriophages, this project still goes some way in demonstrating the narrow host-range of viruses specific to *V. parahaemolyticus* strains. Four novel environmental strains of *V. parahaemolyticus* have been fully sequenced (Witherall *et al.*, 2019) and three distinct bacteriophages have been successfully encapsulated in sodium alginate microcapsules for the first time in a glass microfluidic device. It has also been demonstrated that this phages remain infective following encapsulation and lyophilisation in a host-virus model system (*E. coli* and T4) as well as in host-virus system more specific to *C. gigas* aquaculture (*V. parahaemolyticus* and sm030/sm031). Therefore, whilst this thesis concludes that bacteriophage therapies into the treatment of *V. parahaemolyticus* infections of *C. gigas* oysters are not yet at a level where they are commercially viable, it is possible that with more research such therapies may be used.

Bibliography

Abdelsattar AS, Abdelrahman F, Dawoud A, Connerton IF, El-Shibiny A. 2019. Encapsulation of *E. coli* Phage ZCEC5 in Chitosan-Alginate Beads as a Delivery System in Phage Therapy. *AMB Express* 9:87.

Abedon ST, Lejeune JT. 2007. Why Bacteriophage Encode Exotoxins and other Virulence Factors. *Evolutionary bioinformatics online* 1:97–110.

Abedon ST, Thomas-Abedon C. 2010. Phage Therapy Pharmacology. *Current pharmaceutical biotechnology* 11:28–47.

Abkarian MFM. 2005. Microfluidic Flow Focusing: Drop Size and Scaling in Pressure versus Flow-Rate-Driven Pumping. *Electrophoresis* 26:3716–3724.

Agarwal R, Johnson CT, Imhoff BR, Donlan RM, McCarty NA, García AJ. 2018. Inhaled Bacteriophage-Loaded Polymeric Microparticles Ameliorate Acute Lung Infections. *Nature Biomedical Engineering* 2:841–849.

Ahmed HA, El Bayomi RM, Hussein MA, Khedr MHE, Abo Remela EM, El-Ashram AMM. 2018. Molecular Characterization, Antibiotic Resistance Pattern and Biofilm Formation of *Vibrio parahaemolyticus* and *V. cholerae* Isolated from Crustaceans and Humans. *International journal of food microbiology* 274:31–37.

Alagappan KM, Deivasigamani B, Somasundaram ST, Kumaran S. 2010. Occurrence of *Vibrio parahaemolyticus* and its Specific Phages from Shrimp Ponds in East Coast of India. *Current microbiology* 61:235–240.

Andresen I-L, Smidsørod O. 1977. Temperature Dependence of the Elastic Properties of Alginate Gels. *Carbohydrate research* 58:271–279.

Angulo C, Loera-Muro A, Trujillo E, Luna-González A. 2018. Control of AHPND by Phages: A Promising Biotechnological Approach. *Reviews in Aquaculture* 51:135.

Ashrafudoulla M, Mizan MFR, Park H-D, Byun K-H, Lee N, Park SH, Ha S-D. 2019. Genetic Relationship, Virulence Factors, Drug Resistance Profile and Biofilm Formation Ability of *Vibrio parahaemolyticus* Isolated from Mussel. *Frontiers in microbiology* 10:513.

Aslam B, Wang W, Arshad MI, Khurshid M, Muzammil S, Rasool MH, Nisar MA, Alvi RF, Aslam MA, Qamar MU, Salamat MKF, Baloch Z. 2018. Antibiotic Resistance: A Rundown of a Global Crisis. *Infection and drug resistance* 11:1645–1658.

Baker-Austin C, McArthur JV, Tuckfield RC, Najarro M, Lindell AH, Gooch J, Stepanauskas R. 2008. Antibiotic Resistance in the Shellfish Pathogen *Vibrio parahaemolyticus* Isolated from the Coastal Water and Sediment of Georgia and South Carolina, USA. *Journal of food protection* 71:2552–2558.

Bamford RA, Smith A, Metz J, Glover G, Titball RW, Pagliara S. 2017. Investigating the Physiology of Viable but Non-Culturable Bacteria by Microfluidics and Time-Lapse Microscopy. *BMC biology* 15:121.

Banerjee SK, Farber JM. 2018. Trend and Pattern of Antimicrobial Resistance in Molluscan *Vibrio* Species Sourced to Canadian Estuaries. *Antimicrobial agents and chemotherapy* 62:10.

Banks DJ, Beres SB, Musser JM. 2002. The Fundamental Contribution of Phages to GAS Evolution, Genome Diversification and Strain Emergence. *Trends in microbiology* 10:515–521.

Baquero F, Martinez J-L, Canto R. 2008. Antibiotics and Antibiotic Resistance in Water Environments. *Current Opinion in Biotechnology* 19:260–265.

Baret J-C. 2012. Surfactants in Droplet-Based Microfluidics. *Lab on a chip* 12:422–433.

Barille L, Prou J, Heral M, Raze D. 1997. Effects of High Natural Seston Concentrations on the feeding, Selection, and Absorption of the Oyster *Crassostrea gigas* (Thunberg). *Journal of experimental marine biology and ecology* 212:149–172.

Barr JJ, Auro R, Furlan M, Whiteson KL, Erb ML, Pogliano J, Stotland A, Wolkowicz R, Cutting AS, Doran KS, Salamon P, Youle M, Rohwer F. 2013. Bacteriophage Adhering to Mucus Provide a Non-Host-Derived Immunity. *Proceedings of the National Academy of Sciences of the United States of America* 110:10771–10776.

Barr JJ, Auro R, Sam-Soon N, Kassegne S, Peters G, Bonilla N, Hatay M, Mourtada S, Bailey B, Youle M, Felts B, Baljon A, Nulton J, Salamon P, Rohwer F. 2015. Subdiffusive Motion of Bacteriophage in Mucosal Surfaces Increases the Frequency of Bacterial Encounters. *Proceedings of the National Academy of Sciences of the United States of America* 112:13675–13680.

Beecham J. 2008. A Literature Review on Particle Assimilation by Molluscs and Crustaceans. Cefas.

Bernard FR. 1974. Particle Sorting and Labial Palp Function in the Pacific Oyster *Crassostrea gigas* (Thunberg). *The Biological bulletin* 146:1–10.

Bhattacharya M, Choudhury P, Kumar R. 2000. Antibiotic- and Metal-Resistant Strains of *Vibrio parahaemolyticus* Isolated from Shrimps. *Microbial drug resistance* 6:171–172.

Biller SJ, Berube PM, Dooley K, Williams M, Satinsky BM, Hackl T, Hogle SL, Coe A, Bergauer K, Bouman HA, Browning TJ, De Corte D, Hassler C, Hulston D, Jacquot JE, Maas EW, Reinthaler T, Sintes E, Yokokawa T, Chisholm SW. 2018. Marine Microbial Metagenomes Sampled Across Space and Time. *Scientific data* 5:180176.

Boggione DMG, Batalha LS, Gontijo MTP, Lopez MES, Teixeira AVNC, Santos IJB, Mendonça RCS. 2017. Evaluation of Microencapsulation of the UFV-AREG1 Bacteriophage in Alginate-Ca Microcapsules using Microfluidic Devices. *Colloids and surfaces. B, Biointerfaces* 158:182–189.

Bolger AM, Lohse M, Usadel B. 2014. Trimmomatic: A Flexible Trimmer for Illumina Sequence Data. *Bioinformatics* 30:2114–2120.

Bondy-Denomy J, Davidson AR. 2014. When a Virus is not a Parasite: The Beneficial Effects of Prophages on Bacterial Fitness. *Journal of microbiology* 52:235–242.

Boucher Y, Stokes HW. 2006. The Roles of Lateral Gene Transfer and Vertical Descent in *Vibrio* Evolution. In: Thompson FL, Austin B, Swings J eds. *The Biology of Vibrios*. American Society of Microbiology, 84–94.

Boyd EF, Brüssow H. 2002. Common Themes Among Bacteriophage-Encoded Virulence Factors and Diversity Among the Bacteriophages Involved. *Trends in microbiology* 10:521–529.

Brown MR, Camézuli S, Davenport RJ, Petelenz-Kurdziel E, Øvreås L, Curtis TP. 2015. Flow Cytometric Quantification of Viruses in Activated Sludge. *Water research* 68:414–422.

Brussaard CPD. 2009. Enumeration of Bacteriophages using Flow Cytometry. *Methods in molecular biology* 501:97–111.

Brussaard CPD, Wilhelm SW, Thingstad F, Weinbauer MG, Bratbak G, Heldal M, Kimmance SA, Middelboe M, Nagasaki K, Paul JH, Schroeder DC, Suttle CA, Vaqué D, Wommack KE. 2008. Global-Scale Processes with a

Nanoscale Drive: The Role of Marine Viruses. *The ISME journal* 2:575–578.
Brüssow H, Canchaya C, Hardt W-D. 2004. Phages and the Evolution of Bacterial Pathogens: From Genomic Rearrangements to Lysogenic Conversion. *Microbiology and molecular biology reviews: MMBR* 68:560–602.
Buchholz H. 2019. (*in prep*) Flow Cytometry for the High-throughput Isolation of Bacteriophage.
Calero-Cáceres W, Ye M, Balcázar JL. 2019. Bacteriophages as Environmental Reservoirs of Antibiotic Resistance. *Trends in microbiology* 27:570–577.
Canchaya C, Proux C, Fournous G, Bruttin A, Brüssow H. 2003. Prophage Genomics. *Microbiology and Molecular Biology Reviews: MMBR* 67:238–76.
Carlson-Jones JAP, Paterson JS, Newton K, Smith RJ, Dann LM, Speck P, Mitchell JG, Wormald P-J. 2016. Enumerating Virus-Like Particles and Bacterial Populations in the Sinuses of Chronic Rhinosinusitis Patients using Flow Cytometry. *PloS one* 11:e0155003.
Cartwright David Edgar, Edden Anne C., Spencer R., Vassie J. M., Charnock Henry. 1980. The Tides of the Northeast Atlantic Ocean. *Philosophical transactions of the Royal Society of London. Series A: Mathematical and physical sciences* 298:87–139.
Carvalho CM, Gannon BW, Halfhide DE, Santos SB, Hayes CM, Roe JM, Azeredo J. 2010. The *in vivo* Efficacy of Two Administration Routes of a Phage Cocktail to reduce Numbers of *Campylobacter coli* and *Campylobacter jejuni* in Chickens. *BMC microbiology* 10:232.
Casjens S. 2003. Prophages and Bacterial Genomics: What Have We Learned So Far? *Molecular microbiology* 49:277–300.
Castillo D, Kauffman K, Hussain F, Kalatzis P, Rørbo N, Polz MF, Middelboe M. 2018. Widespread Distribution of Prophage-Encoded Virulence Factors in Marine *Vibrio* Communities. *Scientific reports* 8:9973.
Cavin JF, Drici FZ, Prevost H, Divies C. 1991. Prophage Curing in *Leuconostoc oenos* by Mitomycin C Induction. *American Journal of Enology and Viticulture* 42.
Ceccarelli D, Hasan NA, Huq A, Colwell RR. 2013. Distribution and Dynamics of Epidemic and Pandemic V*ibrio parahaemolyticus* Virulence Factors. *Frontiers in cellular and infection microbiology* 3:97.
Centers for Disease Control and Prevention. 2013. *Antibiotic Resistance Threats in the United States, 2013*.
Chaipan C, Pryszlak A, Dean H, Poignard P, Benes V, Griffiths AD, Merten CA. 2017. Single-Virus Droplet Microfluidics for High-Throughput Screening of Neutralizing Epitopes on HIV Particles. *Cell chemical biology* 24:751–757.e3.
Cheetham BF, Katz ME. 1995. A Role for Bacteriophages in the Evolution and Transfer of Bacterial Virulence Determinants. *Molecular microbiology* 18:201–208.
Chen C-S, Breslauer DN, Luna JI, Grimes A, Chin W-C, Lee LP, Khine M. 2008. Shrinky-Dink Microfluidics: 3D Polystyrene Chips. *Lab on a chip* 8:622–624.
Chen I-MA, Chu K, Palaniappan K, Pillay M, Ratner A, Huang J, Huntemann M, Varghese N, White JR, Seshadri R, Smirnova T, Kirton E, Jungbluth SP, Woyke T, Eloe-Fadrosh EA, Ivanova NN, Kyrpides NC. 2019. IMG/M v.5.0: An Integrated Data Management and Comparative Analysis System for Microbial Genomes and Microbiomes. *Nucleic acids research* 47:D666–D677.
Chen W, Kim J-H, Zhang D, Lee K-H, Cangelosi GA, Soelberg SD, Furlong CE, Chung J-H, Shen AQ. 2013. Microfluidic One-Step Synthesis of Alginate

Microspheres Immobilized with Antibodies. *Journal of the Royal Society, Interface / the Royal Society* 10:20130566.
Chinnadurai S, Kripa V, Venkatesan V, Mohamed KS. 2013. Effect of Low Temperature on the Survival of Edible Oyster *Crassostrea madrasensis* during Transportation and Storage. *Journal of the Marine Biological Association of India* 55:83–86.
Chuah L-O, Effarizah ME, Goni AM, Rusul G. 2016. Antibiotic Application and Emergence of Multiple Antibiotic Resistance (MAR) in Global Catfish Aquaculture. *Current environmental health reports* 3:118–127.
Cinquerrui S, Mancuso F, Vladisavljević GT, Bakker SE, Malik DJ. 2018. Nanoencapsulation of Bacteriophages in Liposomes Prepared Using Microfluidic Hydrodynamic Flow Focusing. *Frontiers in microbiology* 9:2172.
Cloern JE. 2001. Our Evolving Conceptual Model of the Coastal Eutrophication Problem. *Marine ecology progress series* 210:223–253.
Clokie MR, Millard AD, Letarov AV, Heaphy S. 2011. Phages in Nature. *Bacteriophage* 1:31–45.
Cognie B, Barillé L, Massé G, Beninger PG. 2003. Selection and Processing of Large Suspended Algae in the Oyster *Crassostrea gigas*. *Marine ecology progress series* 250:145–152.
Colom J, Cano-Sarabia M, Otero J, Aríñez-Soriano J, Cortés P, Maspoch D, Llagostera M. 2017. Microencapsulation with Alginate/CaCO3: A Strategy for Improved Phage Therapy. *Scientific reports* 7:41441.
Comeau AM, Hatfull GF, Krisch HM, Lindell D, Mann NH, Prangishvili D. 2008. Exploring the Prokaryotic Virosphere. *Research in microbiology* 159:306–313.
Conchouso D, Castro D, Khan SA, Foulds IG. 2014. Three-Dimensional Parallelization of Microfluidic Droplet Generators for a Litre per Hour Volume Production of Single Emulsions. *Lab on a chip* 14:3011–3020.
Costanzo SD, Murby J, Bates J. 2005. Ecosystem Response to Antibiotics Entering the Aquatic Environment. *Marine pollution bulletin* 51:218–223.
Dale B, Edwards M, Reid PC. 2006. Climate Change and Harmful Algal Blooms. In: Granéli E, Turner JT eds. *Ecology of Harmful Algae*. Berlin, Heidelberg: Springer Berlin Heidelberg, 367–378.
Daramola BA, Williams R, Dixon RA. 2009. *In vitro* Antibiotic Susceptibility of *Vibrio parahaemolyticus* from Environmental Sources in Northern England. *International journal of antimicrobial agents* 34:499–500.
Dawood MAO, Koshio S. 2016. Recent Advances in the Role of Probiotics and Prebiotics in Carp Aquaculture: A Review. *Aquaculture* 454:243–251.
Dawson MP, Humphrey BA, Marshall KC. 1981. Adhesion: A Tactic in the Survival Strategy of a Marine *Vibrio* during Starvation. *Current microbiology* 6:195–199.
Deepanjali A, Sanath Kumar H, Karunasagar I, Karunasagar I. 2005. Seasonal Variation in Abundance of Total and Pathogenic *Vibrio parahaemolyticus* Bacteria in Oysters along the Southwest Coast of India. *Applied and environmental microbiology* 71:3575–3580.
DePaola A, Nordstrom JL, Bowers JC, Wells JG, Cook DW. 2003. Seasonal Abundance of Total and Pathogenic *Vibrio parahaemolyticus* in Alabama Oysters. *Applied and environmental microbiology* 69:1521–1526.
Destoumieux-Garzón, D. *et al.* (2005) The iron-siderophore transporter FhuA is the receptor for the antimicrobial peptide microcin J25: Role of the microcin Val11-Pro16 β-hairpin region in the recognition mechanism. *Biochemical Journal* 389:869–876.

Devadas S, Bhassu S, Soo TCC, Iqbal SNM, Yusoff FM, Shariff M. 2018. Draft Genome Sequence of a *Vibrio parahaemolyticus* Strain, KS17. S5-1, with Multiple Antibiotic Resistance Genes, Which Causes Acute Hepatopancreatic Necrosis Disease in Penaeus Monodon in the West Coast of Peninsular Malaysia. *Microbiol Resour Announc* 7:e00829–18.

Devadas S, Bhassu S, Soo TCC, Yusoff FM, Shariff M. 2019. A New 5-Plex PCR Detection Method for Acute Hepatopancreatic Necrosis Disease (AHPND)-Causing *Vibrio parahaemolyticus* Strains. *Aquaculture* 503:373–380.

Devi R, Surendran PK, Chakraborty K. 2009. Antibiotic Resistance and Plasmid Profiling of *Vibrio parahaemolyticus* Isolated from Shrimp Farms Along the Southwest Coast of India. *World journal of microbiology & biotechnology* 25:2005–2012.

d'Hérelle, F. 1917. Sur un microbe invisible antagoniste des bacilles dysentériques. *Comptes rendus de l'Académie des Sciences* 165: 373–375.

Dini C, Islan GA, de Urraza PJ, Castro GR. 2012. Novel Biopolymer Matrices for Microencapsulation of Phages: Enhanced Protection against Acidity and Protease Activity. *Macromolecular bioscience* 12:1200–1208.

Di DYW, Shin H, Han D, Unno T, Hur H-G. 2019. High Genetic Diversity of *Vibrio parahaemolyticus* Isolated from Tidal Water and Mud of Southern Coast of South Korea. *FEMS microbiology ecology* 95.

Done HY, Venkatesan AK, Halden RU. 2015. Does the Recent Growth of Aquaculture Create Antibiotic Resistance Threats Different from those Associated with Land Animal Production in Agriculture? *The AAPS journal* 17:513–524.

Doss J, Culbertson K, Hahn D, Camacho J, Barekzi N. 2017. A Review of Phage Therapy against Bacterial Pathogens of Aquatic and Terrestrial Organisms. *Viruses* 9.

Droplet Chips User Guide. Dolomite Microfluidics.

Dulvy NK, Rogers SI, Jennings S, Stelzenmller V, Dye SR, Skjoldal HR. 2008. Climate Change and Deepening of the North Sea Fish Assemblage: A Biotic Indicator of Warming Seas. *The Journal of applied ecology* 45:1029–1039.

Dupuy C, Le Gall S, Hartmann HJ, Breret M. 1999. Retention of Ciliates and Flagellates by the Oyster *Crassostrea gigas* in French Atlantic Coastal Ponds: Protists as a trophic Link between Bacterioplankton and Benthic Suspension-Feeders. *Marine Ecology Process Series* 177:165–175.

Ecdc EAE. 2017. ECDC/EFSA/EMA Second Joint Report on the Integrated Analysis of the Consumption of Antimicrobial Agents and Occurrence of Antimicrobial Resistance in Bacteria from Humans and Food-Producing Animals.

Eddings MA, Johnson MA, Gale BK. 2008. Determining the optimal PDMS–PDMS Bonding Technique for Microfluidic Devices. *Journal of micromechanics and microengineering: structures, devices, and systems* 18:067001.

Ehara M, Shimodori S, Kojima F, Ichinose Y, Hirayama T, Albert MJ, Supawat K, Honma Y, Iwanaga M, Amako K. 1997. Characterization of Filamentous Phages of *Vibrio cholerae* O139 and O1. *FEMS microbiology letters* 154:293–301.

Ellis T, Gardiner R, Gubbins M, Reese A, Smith D. 2012. Aquaculture Statistics for the UK, with a Focus on England and Wales 2012. Cefas.

Elmahdi S, Parveen S, Ossai S, DaSilva LV, Jahncke M, Bowers J, Jacobs J. 2018. *Vibrio parahaemolyticus* and *Vibrio vulnificus* Recovered from Oysters

during an Oyster Relay Study. *Applied and environmental microbiology* 84.
Ertesvåg H, Valla S. 1998. Biosynthesis and Applications of Alginates. *Polymer degradation and stability* 59:85–91.
Ervynck A, Van Neer W, Hüster-Plogmann H, Schibler J. 2003. Beyond Affluence: the Zooarchaeology of Luxury. *World archaeology* 34:428–441.
FAO. 2012. The State of World Fisheries and Aquaculture 2012. FAO.
FAO. 2016. The State of World Fisheries and Aquaculture: Contributing to Food Security and Nutrition for All. FAO.
FAO. 2018. The State of World Fisheries and Aquaculture 2018 - Meeting the Sustainable Development Goals. FAO.
Faruque SM, Mekalanos JJ. 2003. Pathogenicity Islands and Phages in *Vibrio cholerae* Evolution. *Trends in microbiology* 11:505–510.
Fleischmann RD, Adams MD, White O, Clayton RA, Kirkness EF, Kerlavage AR, Bult CJ, Tomb JF, Dougherty BA, Merrick JM. 1995. Whole-Genome Random Sequencing and Assembly of *Haemophilus influenzae* Rd. *Science* 269:496–512.
Folke C, Kautsky N. 1992. Aquaculture with its Environment: Prospects for Sustainability. *Ocean & coastal management* 17:5–24.
Forde A, Hill C. 2018. Phages of Life-the Path to Pharma. *British journal of pharmacology* 175:412–418.
Forrest BM, Keeley NB, Hopkins GA, Webb SC, Clement DM. 2009. Bivalve Aquaculture in Estuaries: Review and Synthesis of Oyster Cultivation Effects. *Aquaculture* 298:1–15.
Fortier L-C, Sekulovic O. 2013. Importance of Prophages to Evolution and Virulence of Bacterial Pathogens. *Virulence* 4:354–365.
Fortuna MA, Barbour MA, Zaman L, Hall AR, Buckling A, Bascompte J. 2019. Coevolutionary Dynamics Shape the Structure of Bacteria- Phage Infection Networks. *Evolution; international journal of organic evolution* 73:1001–1011.
Fujino T, Okuno Y, Nakada D, Aoyama A, Fukai K, Mukai T, Ueho T. 1953. On the Bacteriological Examination of Shirasu-Food Poisoning. *Medical Jounral of Osaka University* 4:299–304.
Gasson MJ, Davies FL. 1980. Prophage-Cured Derivatives of *Streptococcus lactis* and *Streptococcus cremoris*. *Applied and environmental microbiology* 40:964–966.
Gervais T, El-Ali J, Günther A, Jensen KF. 2006. Flow-Induced Deformation of Shallow Microfluidic Channels. *Lab on a chip* 6:500–507.
Ghenem L, Elhadi N. 2018. Isolation, Molecular Characterization, and Antibiotic Resistance Patterns of *Vibrio parahaemolyticus* Isolated from Coastal Water in the Eastern Province of Saudi Arabia. *Journal of water and health* 16:57–69.
González-Menéndez E, Fernández L, Gutiérrez D, Rodríguez A, Martínez B, García P. 2018. Comparative Analysis of Different Preservation Techniques for the Storage of *Staphylococcus* phages Aimed for the Industrial Development of Phage-Based Antimicrobial Products. *PloS one* 13:e0205728.
Gordillo Altamirano FL, Barr JJ. 2019. Phage Therapy in the Postantibiotic Era. *Clinical microbiology reviews* 32.
Gregory AC *et al*. 2019. Marine DNA Viral Macro- and Microdiversity from Pole to Pole. *Cell* 0.
Guo MT, Rotem A, Heyman JA, Weitz DA. 2012. Droplet Microfluidics for High-Throughput Biological Assays. *Lab on a chip* 12:2146–2155.

Hall CM, Sharples L. 2008. Food Events, Festivals and Farmers' Markets: An Introduction. *Food and wine festivals and events around the world*. Routledge, 20–39.
Hamdan RH, Peng TL, Ong BL, Suhana MYS, Hamid NH, Afifah MNF, Raina MS. 2018. Antibiotics Resistance of *Vibrio* spp. Isolated from Diseased Seabass and Tilapia in Cage Culture.
Han C, Tang H, Ren C, Zhu X, Han D. 2016. Sero-Prevalence and Genetic Diversity of Pandemic *V. parahaemolyticus* Strains Occurring at a Global Scale. *Frontiers in microbiology* 7:567.
Han F, Walker RD, Janes ME, Prinyawiwatkul W, Ge B. 2007. Antimicrobial Susceptibilities of *Vibrio parahaemolyticus* and *Vibrio vulnificus* Isolates from Louisiana Gulf and Retail Raw Oysters. *Applied and environmental microbiology* 73:7096–7098.
Hasman H, Hammerum AM, Hansen F, Hendriksen RS, Olesen B, Agersø Y, Zankari E, Leekitcharoenphon P, Stegger M, Kaas RS, Others. 2015. Detection of mcr-1 Encoding Plasmid-Mediated Colistin-Resistant *Escherichia coli* Isolates from Human Bloodstream Infection and Imported Chicken Meat, Denmark 2015. *Eurosurveillance (Online Edition)* 20:1–5.
Håti AG, Bassett DC, Ribe JM, Sikorski P, Weitz DA, Stokke BT. 2016. Versatile, Cell and Chip Friendly Method to Gel Alginate in Microfluidic Devices. *Lab on a chip* 16:3718–3727.
He Y, Jin L, Sun F, Hu Q, Chen L. 2016. Antibiotic and Heavy-Metal Resistance of V*ibrio parahaemolyticus* Isolated from Fresh Shrimps in Shanghai Fish Markets, China. *Environmental science and pollution research international* 23:15033–15040.
Herbert RJH, Roberts C, Humphreys J, Fletcher S. 2012. The Pacific Oyster *(Crassostrea gigas)* in the UK: Economic, Legal and Environmental Issues Associated with its Cultivation, Wild Establishment and Exploitation*. Report for the Shellfish Association of Great Britain*.
Huang K-S, Lai T-H, Lin Y-C. 2006. Manipulating the Generation of Ca-Alginate Microspheres using Microfluidic Channels as a Carrier of Gold Nanoparticles. *Lab on a chip* 6:954–957.
Huang K, Nitin N. 2019. Edible Bacteriophage Based Antimicrobial Coating on Fish Feed for Enhanced Treatment of Bacterial Infections in Aquaculture Industry. *Aquaculture* 502:18–25.
Humphreys J, Herbert RJH, Roberts C, Fletcher S. 2014. A Reappraisal of the History and Economics of the Pacific Oyster in Britain. *Aquaculture* 428-429:117–124.
Hyman P. 2019. Phages for Phage Therapy: Isolation, Characterization, and Host Range Breadth. *Pharmaceuticals* 12.
Hyman P, Abedon ST. 2010. Bacteriophage Host Range and Bacterial Resistance. *Advances in applied microbiology* 70:217–248.
Inoue T, Matsuzaki S, Tanaka S. 1995. A 26-kDa Outer Membrane Protein, OmpK, Common to *Vibrio* Species is the Receptor for a Broad-Host-Range Vibriophage, KVP40. *FEMS microbiology letters* 125:101–105.
IQ-TREE: Efficient Phylogenomic Software by Maximum Likelihood. *Available at http://www.iqtree.org/* (accessed June 7, 2019).
Jiang Y, Chu Y, Xie G, Li F, Wang L, Huang J, Zhai Y, Yao L. 2019. Antimicrobial Resistance, Virulence and Genetic Relationship of *Vibrio parahaemolyticus* in Seafood from Coasts of Bohai Sea and Yellow Sea, China. *International journal of food microbiology* 290:116–124.
Joensson HN, Andersson Svahn H. 2012. Droplet Microfluidics—A Tool for

Single-Cell Analysis. *Angewandte Chemie, International Edition* 51:12176–12192.
Johnson CN, Bowers JC, Griffitt KJ, Molina V, Clostio RW, Pei S, Laws E, Paranjpye RN, Strom MS, Chen A, Hasan NA, Huq A, Noriea NF 3rd, Grimes DJ, Colwell RR. 2012. Ecology of *Vibrio parahaemolyticus* and *Vibrio vulnificus* in the Coastal and Estuarine Waters of Louisiana, Maryland, Mississippi, and Washington (United States). *Applied and environmental microbiology* 78:7249–7257.
Jończyk E, Kłak M, Międzybrodzki R, Górski A. 2011. The Influence of External Factors on Bacteriophages-Review. *Folia microbiologica* 56:191–200.
Jun JW, Han JE, Tang KFJ, Lightner DV, Kim J, Seo SW, Park SC. 2016. Potential Application of Bacteriophage pVp-1: Agent Combating *Vibrio parahaemolyticus* Strains Associated with Acute Hepatopancreatic Necrosis Disease (AHPND) in Shrimp. *Aquaculture* 457:100–103.
Jun JW, Kim HJ, Yun SK, Chai JY, Park SC. 2014a. Eating Oysters Without Risk of Vibriosis: Application of a Bacteriophage against *Vibrio parahaemolyticus* in Oysters. *International journal of food microbiology* 188:31–35.
Jun JW, Shin TH, Kim JH, Shin SP, Han JE, Heo GJ, De Zoysa M, Shin GW, Chai JY, Park SC. 2014b. Bacteriophage Therapy of a *Vibrio parahaemolyticus* Infection caused by a Multiple-Antibiotic-Resistant O3:K6 Pandemic Clinical Strain. *The Journal of infectious diseases* 210:72–78.
Kalatzis PG, Castillo D, Katharios P, Middelboe M. 2018. Bacteriophage Interactions with Marine Pathogenic Vibrios: Implications for Phage Therapy. *Antibiotics (Basel, Switzerland)* 7.
Kalkan S. 2018. *Vibrio parahaemolyticus* ATCC 17802 Inactivation by Using Methylcellulose Films Containing Encapsulated Bacteriophages. *Turkish Journal of Veterinary and Animal Sciences* 42:480–485.
Kaminski TS, Scheler O, Garstecki P. 2016. Droplet Microfluidics for Microbiology: Techniques, Applications and Challenges. *Lab on a chip* 16:2168–2187.
Kang C-H, Shin Y, Yu H, Kim S, So J-S. 2018. Antibiotic and Heavy-Metal Resistance of *Vibrio parahaemolyticus* Isolated from Oysters in Korea. *Marine pollution bulletin* 135:69–74.
Karunasagar I, Karunasagar. 2018. Ecology, Virulence Factors and Global Spread of *Vibrio parahaemolyticus*. *Asian fisheries science* 31.
Kauffman KM, Polz MF. 2018. Streamlining Standard Bacteriophage Methods for Higher Throughput. *MethodsX* 5:159–172.
Kaushik AM, Hsieh K, Chen L, Shin DJ, Liao JC, Wang T-H. 2017. Accelerating Bacterial Growth Detection and Antimicrobial Susceptibility Assessment in Integrated Picoliter Droplet Platform. *Biosensors & bioelectronics* 97:260–266.
Kaushik AM, Hsieh K, Wang T-H. 2018. Droplet Microfluidics for High-Sensitivity and High-Throughput Detection and Screening Of Disease Biomarkers. *WIRE's Nanomedicine and Nanobiotechnology* 10.
Kawagishi I, Imagawa M, Imae Y, McCarter L, Homma M. 1996. The Sodium-Driven Polar Flagellar Motor of Marine *Vibrio* as the Mechanosensor that Regulates Lateral Flagellar Expression. *Molecular microbiology* 20:693–699.
Keen, EC. 2015. A Century of Phage Research: Bacteriophages and the Shaping of Modern Biology. *Bioassays* 37:6-9.
Khemayan K, Pasharawipas T, Puiprom O, Sriurairatana S, Suthienkul O, Flegel TW. 2006. Unstable Lysogeny and Pseudolysogeny in *Vibrio harveyi* Siphovirus-Like Phage 1. *Applied and environmental microbiology* 72:1355–

1363.
Kim Y, Lee S, Hwang I, Yoon K. 2012. Effect of Temperature on Growth of *Vibrio paraphemolyticus* and *Vibrio vulnificus* in Flounder, Salmon Sashimi and Oyster Meat. *International journal of environmental research and public health* 9:4662–4675.
King AH. 1983. Brown Seaweed Extracts (Alginates). *Food hydrocolloids* 2:115–188.
Koga T, Toyoshima S, Kawata T. 1982. Morphological Varieties and Host Ranges of *Vibrio parahaemolyticus* Bacteriophages Isolated from Seawater. *Applied and environmental microbiology* 44:466–470.
Kokkari C, Sarropoulou E, Bastias R, Mandalakis M, Katharios P. 2018. Isolation and Characterization of a Novel Bacteriophage Infecting *Vibrio alginolyticus*. *Archives of microbiology* 200:707–718.
Köster S, Angilè FE, Duan H, Agresti JJ, Wintner A, Schmitz C, Rowat AC, Merten CA, Pisignano D, Griffiths AD, Weitz DA. 2008. Drop-Based Microfluidic Devices for Encapsulation of Single Cells. *Lab on a chip* 8:1110–1115.
Kovalchuka NM, Roumpea E, Nowaka E, Chinaud M, Angeli P, Simmons MJH. 2018. Effect of Surfactant on Emulsification in Microchannels. *Chemical engineering science* 176.
Kutter E, De Vos D, Gvasalia G, Alavidze Z, Gogokhia L, Kuhl S, Abedon ST. 2010. Phage Therapy in Clinical Practice: Treatment of Human Infections. *Current pharmaceutical biotechnology* 11:69–86.
Labella A, Gennari M, Ghidini V, Trento I, Manfrin A, Borrego JJ, Lleo MM. 2013. High Incidence of Antibiotic Multi-Resistant Bacteria in Coastal Areas Dedicated to Fish Farming. *Marine pollution bulletin* 70:197–203.
Lafferty KD, Harvell CD, Conrad JM, Friedman CS, Kent ML, Kuris AM, Powell EN, Rondeau D, Saksida SM. 2015. Infectious Diseases Affect Marine Fisheries and Aquaculture Economics. *Annual review of marine science* 7:471–496.
Lai H-C, Ng TH, Ando M, Lee C-T, Chen I-T, J-C C, Mavichak R, Chang S-H, Yeh M-D, Chiang Y-A, Takeyama H, Hamaguchi H-O, Lo C-F, Aoki T, H-C W. 2015. Pathogenesis of Acute Hepatopancreatic Necrosis Disease (AHPND) in Shrimp. *Fish and Shellfish Immunology* 47.
Langmead B, Salzberg SL. 2012. Fast Gapped-Read Alignment with Bowtie 2. *Nature methods* 9:357–359.
Lan S-F, Huang C-H, Chang C-H, Liao W-C, Lin I-H, Jian W-N, Wu Y-G, Chen S-Y, Wong H-C. 2009. Characterization of a New Plasmid-Like Prophage in a Pandemic *Vibrio parahaemolyticus* O3:K6 Strain. *Applied and environmental microbiology* 75:2659–2667.
Lee Y, Choi Y, Lee S, Lee H, Kim S, Ha J, Lee J, Oh H, Kim Y, Yoon Y. 2019. Occurrence of Pathogenic *Vibrio parahaemolyticus* in Seafood Distribution Channels and their Antibiotic Resistance Profiles in S. Korea. *Letters in applied microbiology* 68:128–133.
Lee KY, Mooney DJ. 2012. Alginate: Properties and Biomedical Applications. *Progress in polymer science* 37:106–126.
Lee JN, Park C, Whitesides GM. 2003. Solvent Compatibility of Poly(Dimethylsiloxane)-Based Microfluidic Devices. *Analytical chemistry* 75:6544–6554.
Lenski RE. 1988. Experimental Studies of Pleiotropy and Epistasis in Escherichia Coli. I. Variation in Competitive Fitness among Mutants Resistant To Virus T4. *Evolution; international journal of organic evolution* 42:425–432.
Le Roux F, Wegner KM, Baker-Austin C, Vezzulli L, Osorio CR, Amaro C, Ritchie

JM, Defoirdt T, Destoumieux-Garzón D, Blokesch M, Mazel D, Jacq A, Cava F, Gram L, Wendling CC, Strauch E, Kirschner A, Huehn S. 2015. The Emergence of *Vibrio* pathogens in Europe: Ecology, Evolution, and Pathogenesis (Paris, 11-12th March 2015). *Frontiers in microbiology* 6:830.

Letchumanan V, Chan K-G, Lee L-H. 2014. *Vibrio parahaemolyticus*: A Review on the Pathogenesis, Prevalence, and Advance Molecular Identification Techniques. *Frontiers in microbiology* 5:705.

Letchumanan V, Pusparajah P, Tan LT-H, Yin W-F, Lee L-H, Chan K-G. 2015a. Occurrence and Antibiotic Resistance of *Vibrio parahaemolyticus* from Shellfish in Selangor, Malaysia. *Frontiers in microbiology* 6:1417.

Letchumanan V, Yin W-F, Lee L-H, Chan K-G. 2015b. Prevalence and Antimicrobial Susceptibility of *Vibrio parahaemolyticus* Isolated from Retail Shrimps in Malaysia. *Frontiers in microbiology* 6:33.

Letunic I. iTOL: Interactive Tree Of Life. *Available at https://itol.embl.de/* (accessed June 7, 2019).

Leung SSY, Morales S, Britton W, Kutter E, Chan H-K. 2018. Microfluidic-Assisted Bacteriophage Encapsulation into Liposomes. *International journal of pharmaceutics* 545:176–182.

Liao Q-Q, Zhao S-K, Cai B, He R-X, Rao L, Wu Y, Guo S-S, Liu Q-Y, Liu W, Zhao X-Z. 2018. Biocompatible fabrication of cell-laden calcium alginate microbeads using microfluidic double flow-focusing device. *Sensors and actuators. A, Physical* 279:313–320.

Lightner DV, Reman RM, Pantoja CR, Noble BL, Tran L. 2012. Early Mortality Syndrome Affects Shrimp In Asia. *Global Aquaculture Advocate*.

Li H, Handsaker B, Wysoker A, Fennell T, Ruan J, Homer N, Marth G, Abecasis G, Durbin R, 1000 Genome Project Data Processing Subgroup. 2009. The Sequence Alignment/Map Format and SAMtools. *Bioinformatics* 25:2078–2079.

Li D, Li X, Chen C, Zheng Z, Chang H. 2018. Monodisperse Water-in-Oil-in-Water Emulsions Generation for Synthesising Alginate Hydrogel Microspheres via Locally Hydrophobic Modification to PMMA Microchannels. *Sensors and actuators. B, Chemical* 255:1048–1056.

Liu Y, Tottori N, Nisisako T. 2018. Spherical Calcium Alginate Microgels Synthesized Using a Microfluidic Chip. *Proceedings of JSPE Semestrial Meeting* 2018S:487–488.

Liu Y-Y, Wang Y, Walsh TR, Yi L-X, Zhang R, Spencer J, Doi Y, Tian G, Dong B, Huang X, Yu L-F, Gu D, Ren H, Chen X, Lv L, He D, Zhou H, Liang Z, Liu J-H, Shen J. 2016. Emergence of Plasmid-Mediated Colistin Resistance Mechanism MCR-1 in Animals and Human Beings in China: A Microbiological and Molecular Biological Study. *The Lancet infectious diseases* 16:161–168.

Li J, Xue F, Yang Z, Zhang X, Zeng D, Chao G, Jiang Y, Li B. 2016. *Vibrio parahaemolyticus* Strains of Pandemic Serotypes Identified from Clinical and Environmental Samples from Jiangsu, China. *Frontiers in microbiology* 7:787.

Łobocka MB, Głowacka A, Golec P. 2018. Methods for Bacteriophage Preservation. In: Azeredo J, Sillankorva S eds. *Bacteriophage Therapy: From Lab to Clinical Practice*. New York, NY: Springer New York, 219–230.

Loizou K, Wong V-L, Hewakandamby B. 2018. Examining the Effect of Flow Rate Ratio on Droplet Generation and Regime Transition in a Microfluidic T-Junction at Constant Capillary Numbers. *Inventions* 3:54.

Lomelí-Ortega CO, Martínez-Díaz SF. 2014. Phage Therapy against *Vibrio*

parahaemolyticus Infection in the Whiteleg Shrimp (*Litopenaeus vannamei*) Larvae. *Aquaculture* 434:208–211.

Lopatek M, Wieczorek K, Osek J. 2015. Prevalence and Antimicrobial Resistance of *Vibrio parahaemolyticus* Isolated from Raw Shellfish in Poland. *Journal of food protection* 78:1029–1033.

Lopatek M, Wieczorek K, Osek J. 2018a. Characterization and Genetic Diversity of *Vibrio parahaemolyticus* Isolated from Seafoods. *Applied and environmental microbiology*.

Lopatek M, Wieczorek K, Osek J. 2018b. Antimicrobial Resistance, Virulence Factors, and Genetic Profiles of *Vibrio parahaemolyticus* from Seafood. *Applied and environmental microbiology* 84.

Lu, MJ and Henning, U. 1994. Superinfection Exclusion by T-Even-Type Coliphages. *Trends in Microbiology* 2:137–139.

Madhusudana Rao B, Lalitha KV. 2015. Bacteriophages for Aquaculture: Are they Beneficial or Inimical. *Aquaculture* 437:146–154.

Makino K, Oshima K, Kurokawa K, Yokoyama K, Uda T, Tagomori K, Iijima Y, Najima M, Nakano M, Yamashita A, Kubota Y, Kimura S, Yasunaga T, Honda T, Shinagawa H, Hattori M, Iida T. 2003. Genome Sequence of *Vibrio parahaemolyticus*: a Pathogenic Mechanism Distinct from that of *V. cholerae*. *The Lancet* 361:743–749.

Malik DJ, Sokolov IJ, Vinner GK, Mancuso F, Cinquerrui S, Vladisavljevic GT, Clokie MRJ, Garton NJ, Stapley AGF, Kirpichnikova A. 2017. Formulation, Stabilisation and Encapsulation of Bacteriophage for Phage Therapy. *Advances in colloid and interface science* 249:100–133.

Ma Y, Pacan JC, Wang Q, Sabour PM, Huang X, Xu Y. 2012. Enhanced Alginate Microspheres as Means of Oral Delivery of Bacteriophage for Reducing *Staphylococcus aureus* Intestinal Carriage. *Food hydrocolloids* 26:434–440.

Ma Y, Pacan JC, Wang Q, Xu Y, Huang X, Korenevsky A, Sabour PM. 2008. Microencapsulation of Bacteriophage Felix O1 into Chitosan-Alginate Microspheres for Oral Delivery. *Applied and environmental microbiology* 74:4799–4805.

Marcy Y, Ouverney C, Bik EM, Lösekann T, Ivanova N, Martin HG, Szeto E, Platt D, Hugenholtz P, Relman DA, Quake SR. 2007. Dissecting Biological “Dark Matter” with Single-Cell Genetic Analysis of Rare and Uncultivated TM7 Microbes from the Human Mouth. *Proceedings of the National Academy of Sciences of the United States of America* 104:11889–11894.

Marie D, Brussaard CPD, Thyrhaug R, Bratbak G, Vaulot D. 1999. Enumeration of Marine Viruses in Culture and Natural Samples by Flow Cytometry. *Applied and environmental microbiology* 65:45–52.

Martínez-Díaz SF, Hipólito-Morales A. 2013. Efficacy of Phage Therapy to Prevent Mortality during the Vibriosis of Brine Shrimp. *Aquaculture* 400-401:120–124.

Martinez CJ, Kim JW, Ye C, Ortiz I, Rowat AC, Marquez M, Weitz D. 2012. A Microfluidic Approach to Encapsulate Living Cells in Uniform Alginate Hydrogel Microparticles. *Macromolecular Bioscience* 12.

Martinez-Urtaza J, Blanco-Abad V, Rodriguez-Castro A, Ansede-Bermejo J, Miranda A, Rodriguez-Alvarez MX. 2012. Ecological Determinants of the Occurrence and Dynamics of *Vibrio parahaemolyticus* in Offshore Areas. *The ISME journal* 6:994–1006.

Martinez-Urtaza J, Bowers JC, Trinanes J, DePaola A. 2010. Climate Anomalies and the Increasing Risk of *Vibrio parahaemolyticus* and *Vibrio vulnificus* Illnesses. *Food research international* 43:1780–1790.

Martinez-Urtaza J, Trinanes J, Abanto M, Lozano-Leon A, Llovo-Taboada J, Garcia-Campello M, Pousa A, Powell A, Baker-Austin C, Gonzalez-Escalona N. 2018. Epidemic Dynamics of *Vibrio parahaemolyticus* Illness in a Hotspot of Disease Emergence, Galicia, Spain. *Emerging infectious diseases* 24:852–859.

Mateus L, Costa L, Silva YJ, Pereira C, Cunha A, Almeida A. 2014. Efficiency of Phage Cocktails in the Inactivation of *Vibrio* in Aquaculture. *Aquaculture* 424-425:167–173.

Matsuzaki S, Tanaka S, Koga T, Kawata T. 1992. A Broad-Host-Range Vibriophage, KVP40, Isolated from Sea Water. *Microbiology and immunology* 36:93–97.

McCallin S, Sarker SA, Sultana S, Oechslin F, Brüssow H. 2018. Metagenome Analysis of Russian and Georgian Pyophage Cocktails and a Placebo-Controlled Safety Trial of Single Phage versus Phage Cocktail in Healthy *Staphylococcus aureus* Carriers. *Environmental microbiology* 20:3278–3293.

Meselson, M, Yuan, R and Heywood, J. 1972. Restriction and Modification of DNA. *Annual Review of Biochemistry* 41:447–466.

Michelsen O, Cuesta-Dominguez A, Albrechtsen B, Jensen PR. 2007. Detection of Bacteriophage-Infected Cells of *Lactococcus lactis* by Using Flow Cytometry. *Applied and environmental microbiology* 73:7575–7581.

MicrobesNG - Unlock Your Microbial Genomes. *Available at https://microbesng.uk/* (accessed May 21, 2019).

Millard A. 2019. Unravelling the Vast Diversity of Vibriophages by Genomic and Metagenomic Analyses.

Moghtader F, Eğri S, Piskin E. 2017. Phages in Modified Alginate Beads. *Artificial cells, nanomedicine, and biotechnology* 45:357–363.

Morozova VV, Vlassov VV, Tikunova NV. 2018. Applications of Bacteriophages in the Treatment of Localized Infections in Humans. *Frontiers in microbiology* 9:1696.

Nair GB, Ramamurthy T, Bhattacharya SK, Dutta B, Takeda Y, Sack DA. 2007. Global Dissemination of *Vibrio parahaemolyticus* Serotype O3:K6 and its Serovariants. *Clinical microbiology reviews* 20:39–48.

Nasu H, Iida T, Sugahara T, Yamaichi Y, Park KS, Yokoyama K, Makino K, Shinagawa H, Honda T. 2000. A Filamentous Phage Associated with Recent Pandemic *Vibrio parahaemolyticus* O3:K6 Strains. *Journal of clinical microbiology* 38:2156–2161.

National Research Council (US) Committee on Metagenomics: Challenges, Applications F. 2007. *Why Metagenomics?* National Academies Press (US).

Neild R. 1996. [BOOK REVIEW] The English, the French and the Oyster. *Economist* 339:supp–14.

Nelapati S, Nelapati K, Chinnam BK. 2012. *Vibrio parahaemolyticus*- An Emerging Foodborne Pathogen. *Vet World* 5:48–63.

Newton A, Kendall M, Vugia DJ, Henao OL, Mahon BE. 2012. Increasing Rates of Vibriosis in the United States, 1996-2010: Review of Surveillance Data from 2 Systems. *Clinical infectious diseases: an official publication of the Infectious Diseases Society of America* 54 Suppl 5:S391–5.

Nilsson AS. 2014. Phage Therapy—Constraints and Possibilities. *Upsala Journal of Medical Sciences* 119:192-198.

Nordström, K and Forsgren, A. 1974. Effect of Protein A on Adsorption of Bacteriophages to *Staphylococcus aureus*. *Journal of virology* 14:198–202.

Nunan L, Lightner D, Pantoja C, Gomez-Jimenez S. 2014. Detection of Acute Hepatopancreatic Necrosis Disease (AHPND) in Mexico. *Diseases of aquatic organisms* 111:81–86.

Okoh AI, Igbinosa EO. 2010. Antibiotic Susceptibility Profiles of Some *Vibrio* Strains Isolated from Wastewater Final Effluents in a Rural Community of the Eastern Cape Province of South Africa. *BMC microbiology* 10:143.

Oliveira M, Viñas I, Colàs P, Anguera M, Usall J, Abadias M. 2014. Effectiveness of a Bacteriophage in Reducing *Listeria monocytogenes* on Fresh-Cut Fruits and Fruit Juices. *Food microbiology* 38:137–142.

Oxford Nanopore Technologies. 2018. *1D Native barcoding genomic DNA (With EXP-NBD103 and SQK-LSK108)*.

Oyinlola MA, Reygondeau G, Wabnitz CCC, Troell M, Cheung WWL. 2018. Global Estimation of Areas with Suitable Environmental Conditions for Mariculture Species. *PloS one* 13:e0191086.

Pales Espinosa E, Barillé L, Allam B. 2007. Use of Encapsulated Live Microalgae to Investigate Pre-Ingestive Selection in the Oyster *Crassostrea gigas*. *Journal of experimental marine biology and ecology* 343:118–126.

Paterson S, Vogwill T, Buckling A, Benmayor R, Spiers AJ, Thomson NR, Quail M, Smith F, Walker D, Libberton B, Fenton A, Hall N, Brockhurst MA. 2010. Antagonistic Coevolution Accelerates Molecular Evolution. *Nature* 464:275–278.

Paul JH. 2008. Prophages in Marine Bacteria: Dangerous Molecular Time Bombs or the Key to Survival in the Seas? *The ISME journal* 2:579–589.

Payne DJ, Gwynn MN, Holmes DJ, Pompliano DL. 2007. Drugs for Bad Bugs: Confronting the Challenges of Antibacterial Discovery. *Nature reviews. Drug discovery* 6:29–40.

Peng Y, Ding YJ, Lin H, Wang JX. 2013. Isolation, Identification and Lysis Properties Analysis of a *Vibrio parahaemolyticus* Phage VPp1. *Haiyang kexue = Marine sciences*.

Pesant S, Not F, Picheral M, Kandels-Lewis S, Le Bescot N, Gorsky G, Iudicone D, Karsenti E, Speich S, Troublé R, Dimier C, Searson S, Tara Oceans Consortium Coordinators. 2015. Open Science Resources for the Discovery and Analysis of Tara Oceans Data. *Scientific data* 2:150023.

Pingoud, A. *et al.* 2005. Type II Restriction Endonucleases: Structure and Mechanism. *Cellular and Molecular Life Sciences* 62:685–707.

Plaza N, Castillo D, Pérez-Reytor D, Higuera G, García K, Bastías R. 2018. Bacteriophages in the Control of Pathogenic *Vibrios*. *Electronic journal of biotechnology: EJB* 31:24–33.

Polz M. 2019. Phage-Bacteria Interaction in the Coastal Ocean. FEMS annual conference.

Powell A, Baker-Austin C, Wagley S, Bayley A, Hartnell R. 2013. Isolation of Pandemic *Vibrio parahaemolyticus* from UK Water and Shellfish Produce. *Microbial ecology* 65:924–927.

Prachumwat A, Taengchaiyaphum S, Mungkongwongsiri N, Aldama-Cano DJ, Flegel TW, Sritunyalucksana K. 2018. Update on Early Mortality Syndrome/Acute Hepatopancreatic Necrosis Disease by April 2018. *Journal of the World Aquaculture Society* 68:373.

Puapermpoonsiri U, Ford SJ, van der Walle CF. 2010. Stabilization of Bacteriophage During Freeze Drying. *International journal of pharmaceutics* 389:168–175.

Puapermpoonsiri U, Spencer J, van der Walle CF. 2009. A Freeze-Dried Formulation of Bacteriophage Encapsulated in Biodegradable Microspheres.

European journal of pharmaceutics and biopharmaceutics: official journal of Arbeitsgemeinschaft fur Pharmazeutische Verfahrenstechnik e.V 72:26–33.
Raissy M, Moumeni M, Ansari M, Rahimi E. 2012. Antibiotic Resistance Pattern of some Vibrio Strains Isolated from Seafood. *Iranian journal of fisheries sciences / Iranian Fisheries Research Organization* 11:618–626.
Ramirez K, Cazarez-Montoya C, Lopez-Moreno HS, Castro-Del Campo N. 2018. Bacteriophage Cocktail for Biocontrol of *Escherichia coli* O157:H7: Stability and Potential Allergenicity Study. *PloS one* 13:e0195023.
Reeve SM, Lombardo MN, Anderson AC. 2015. Understanding the Structural Mechanisms of Antibiotic Resistance Sets the Platform for New Discovery. *Future microbiology* 10:1727–1733.
Richards GP, Chintapenta LK, Watson MA, Abbott AG, Ozbay G, Uknalis J, Oyelade AA, Parveen S. 2019. Bacteriophages against Pathogenic *Vibrios* in Delaware Bay Oysters (*Crassostrea virginica*) During a Period of High Levels of Pathogenic *Vibrio parahaemolyticus*. *Food and environmental virology* 11:101–112.
Riede, I and Eschbach, ML. 1986. Evidence that TraT Interacts with OmpA of *Escherichia coli*. *FEBS Letters* 205:241–245.
Rohde C, Resch G, Pirnay J-P, Blasdel BG, Debarbieux L, Gelman D, Górski A, Hazan R, Huys I, Kakabadze E, Łobocka M, Maestri A, Almeida GM de F, Makalatia K, Malik DJ, Mašlaňová I, Merabishvili M, Pantucek R, Rose T, Štveráková D, Van Raemdonck H, Verbeken G, Chanishvili N. 2018. Expert Opinion on Three Phage Therapy Related Topics: Bacterial Phage Resistance, Phage Training and Prophages in Bacterial Production Strains. *Viruses* 10.
Rohde C, Wittmann J, Kutter E. 2018. Bacteriophages: A Therapy Concept against Multi-Drug-Resistant Bacteria. *Surgical infections* 19:737–744.
Romero J, Gloria C, Navarrete P. 2012. Antibiotics in Aquaculture – Use, Abuse and Alternatives. Carvalho E ed. *Health and Environment in Aquaculture*. InTech.
Rong R, Lin H, Wang J, Khan MN, Li M. 2014. Reductions of *Vibrio parahaemolyticus* in Oysters after Bacteriophage Application during Depuration. *Aquaculture* 418-419:171–176.
Roux S, Enault F, Hurwitz BL, Sullivan MB. 2015. VirSorter: Mining Viral Signal from Microbial Genomic Data. *PeerJ* 3:e985.
Roux S, Krupovic M, Daly RA, Borges AL, Nayfach S, Schulz F, Cheng J-F, Ivanova NN, Bondy-Denomy J, Wrighton KC, Woyke T, Visel A, Kyrpides N, Eloe-Fadrosh EA. 2019a. Cryptic Inoviruses are Pervasive in Bacteria and Archaea across Earth's Biomes. *bioRxiv*:548222.
Roux S, Krupovic M, Daly RA, Borges AL, Nayfach S, Schulz F, Sharrar A, Matheus Carnevali PB, Cheng J-F, Ivanova NN, Bondy-Denomy J, Wrighton KC, Woyke T, Visel A, Kyrpides NC, Eloe-Fadrosh EA. 2019b. Cryptic Inoviruses Revealed as Pervasive in Bacteria and Archaea across Earth's Biomes. *Nature microbiology*.
Rusch, DB, *et al*. 2007. The Sorcerer II Global Ocean Sampling Expedition: Northwest Atlantic through Eastern Tropical Pacific. *PLoS Biology* 5: e77-431.
Saez AC, Zhang J, Rostagno MH, Ebner PD. 2011. Direct Feeding of Microencapsulated Bacteriophages to Reduce *Salmonella* Colonization in Pigs. *Foodborne Pathogens and Disease* 8.
Sandmann FG, Jit M, Robotham JV, Deeny SR. 2017. Burden, Duration and Costs of Hospital Bed Closures due to Acute Gastroenteritis in England per

Winter, 2010/11-2015/16. *The Journal of hospital infection* 97:79–85.
Santos L, Ramos F. 2018. Antimicrobial Resistance in Aquaculture: Current Knowledge and Alternatives to Tackle the Problem. *International journal of antimicrobial agents* 52:135–143.
Schiller L, Bailey M, Jacquet J, Sala E. 2018. High Seas Fisheries Play a Negligible Role in Addressing Global Food Security. *Science advances* 4:eaat8351.
Schneider CA, Rasband WS, Eliceiri KW. 2012. NIH Image to ImageJ: 25 Years of Image Analysis. *Nature methods* 9:671–675.
Scott JR. 1974. A Turbid Plaque-Forming Mutant of Phage P1 that cannot Lysogenize *Escherichia coli*. *Virology* 62:344–349.
Serp D, Mueller M, Von Stockar U, Marison IW. 2002. Low-Temperature Electron Microscopy for the Study of Polysaccharide Ultrastructures in Hydrogels. II. Effect of Temperature on the Structure of Ca2+-Alginate Beads. *Biotechnology and bioengineering* 79:253–259.
Shakerian A, Barton MD, Akinbowale OL, Khamesipour F. 2018. Antimicrobial Resistance Profile and Resistance Genes of *Vibrio* Species Isolated from Giant Freshwater Prawn (*Macrobrachium rosenbergii*) Raised in Iran. *Journal of the Hellenic Veterinary Medical Society* 68:79–88.
Shapira A, Kohn A. 1974. The Effects of Freeze-Drying on Bacteriophage T4. *Cryobiology* 11:452–464.
Shimizu-Kadota M, Sakurai T. 1982. Prophage Curing in *Lactobacillus casei* by Isolation of a Thermoinducible Mutant. *Applied and environmental microbiology* 43:1284–1287.
Shivu MM, Rajeeva BC, Girisha SK, Karunasagar I, Krohne G, Karunasagar I. 2007. Molecular Characterization of *Vibrio harveyi* Bacteriophages Isolated from Aquaculture Environments along the Coast of India. *Environmental microbiology* 9:322–331.
Silva IP, Carneiro C de S, Saraiva MAF, Oliveira TAS de, Sousa OV de, Evangelista-Barreto NS. 2018. Antimicrobial Resistance and Potential Virulence of *Vibrio parahaemolyticus* Isolated from Water and Bivalve Molluscs from Bahia, Brazil. *Marine pollution bulletin* 131:757–762.
Silva YJ, Costa L, Pereira C, Mateus C, Cunha A, Calado R, Gomes NCM, Pardo MA, Hernandez I, Almeida A. 2014. Phage Therapy as an Approach to Prevent *Vibrio anguillarum* Infections in Fish Larvae Production. *PloS one* 9:e114197.
Silvester R, Alexander D, Ammanamveetil MHA. 2015. Prevalence, Antibiotic Resistance, Virulence and Plasmid Profiles of *Vibrio parahaemolyticus* from a Tropical Estuary and Adjoining Traditional Prawn Farm along the Southwest Coast of India. *Annals of microbiology* 65:2141–2149.
Skaradzińska A, Skaradziński G, Choińska-Pulit A, Śliwka P, Łaba W, Mituła P, Żaczek M, Weber-Dąbrowska B. 2018. Potential Application of Lyophilization in Commercial Use of Bacteriophage Preparations in Veterinary Medicine. *Slovenian veterinary research* 55.
Skurnik M, Strauch E. 2006. Phage Therapy: Facts and Fiction. *International journal of medical microbiology: IJMM* 296:5–14.
Śliwka P, Mituła P, Mituła A, Skaradziński G, Choińska-Pulit A, Niezgoda N, Weber-Dąbrowska B, Żaczek M, Skaradzińska A. 2019. Encapsulation of Bacteriophage T4 in Mannitol-Alginate Dry Macrospheres and Survival in Simulated Gastrointestinal Conditions. *LWT* 99:238–243.
Smith P. 2008. Antimicrobial Resistance in Aquaculture. *Revue scientifique et technique* 27:243–264.

Spencer BE. 2002. *Molluscan Shellfish Farming*. Wiley.
Spencer SJ, Tamminen MV, Preheim SP, Guo MT, Briggs AW, Brito IL, A Weitz D, Pitkänen LK, Vigneault F, Juhani Virta MP, Alm EJ. 2016. Massively Parallel Sequencing of Single Cells by epicPCR Links Functional Genes with Phylogenetic Markers. *The ISME journal* 10:427–436.
Stanford K, McAllister TA, Niu YD, Stephens TP, Mazzocco A, Waddell TE, Johnson RP. 2010. Oral Delivery Systems for Encapsulated Bacteriophages Targeted at *Escherichia coli* O157:H7 in Feedlot Cattle. *Journal of food protection* 73:1304–1312.
Steele PR, Davies JD, Greaves RI. 1969. Some Factors Affecting the Viability of Freeze-Thawed T4 Bacteriophage. *The Journal of hygiene* 67:107–114.
Storm DR, Rosenthal KS, Swanson PE. 1977. Polymyxin and Related Peptide Antibiotics. *Annual review of biochemistry* 46:723–763.
Sugano Y, Terada I, Arita M, Noma M, Matsumoto T. 1993. Purification and Characterization of a New Agarase from a Marine Bacterium, *Vibrio* sp. Strain JT0107. *Applied and environmental microbiology* 59:1549–1554.
Su Y-C, Liu C. 2007. *Vibrio parahaemolyticus*: A Concern of Seafood Safety. *Food microbiology* 24:549–558.
Summers WC. 2012. The Strange History of Phage Therapy. *Bacteriophage* 2:130–133.
Suttle CA. 2007. Marine Viruses—Major Players in the Global Ecosystem. *Nature reviews. Microbiology* 5:801.
Tagini F, Greub G. 2017. Bacterial Genome Sequencing in Clinical Microbiology: a Pathogen-Oriented Review. *European journal of clinical microbiology & infectious diseases: official publication of the European Society of Clinical Microbiology* 36:2007–2020.
Tamburri MN, Zimmer-Faust RK. 1996. Suspension Feeding: Basic Mechanisms Controlling Recognition and Ingestion of Larvae. *Limnology and Oceanography* 41.
Tang Z, Huang X, Baxi S, Chambers JR, Sabour PM, Wang Q. 2013. Whey Protein Improves Survival and Release Characteristics of Bacteriophage Felix O1 Encapsulated in Alginate Microspheres. *Food research international* 52:460–466.
Taniguchi H, Sato K, Ogawa M, Udou T, Mizuguchi Y. 1984. Isolation and Characterization of a Filamentous Phage, Vf33, Specific for *Vibrio parahaemolyticus*. *Microbiology and immunology* 28:327–337.
Tan W-H, Takeuchi S. 2007. Monodisperse Alginate Hydrogel Microbeads for Cell Encapsulation. *Advanced Materials* 19:2696–2701.
Teh S-Y, Lin R, Hung L-H, Lee AP. 2008. Droplet Microfluidics. *Lab on a chip* 8:198–220.
Tonin M, Descharmes N, Houdré R. 2016. Hybrid PDMS/Glass Microfluidics for High Resolution Imaging and Application to Sub-Wavelength Particle Trapping. *Lab on a chip* 16:465–470.
Tran L, Nunan L, Redman RM, Mohney LL, Pantoja CR, Fitzsimmons K, Lightner DV. 2013. Determination of the Infectious Nature of the Agent of Acute Hepatopancreatic Necrosis Syndrome Affecting Penaeid Shrimp. *Diseases of aquatic organisms* 105:45–55.
trimal [trimAl]. 2011. *Available at http://trimal.cgenomics.org/* (accessed June 7, 2019).
Trubl G, Roux S, Solonenko N, Li Y-F, Bolduc B, Rodríguez-Ramos J, Eloe-Fadrosh EA, Rich VI, Sullivan MB. 2019. Towards Optimized Viral Metagenomes for Double-Stranded and Single-Stranded DNA Viruses from

Challenging Soils. *PeerJ* 7:e7265.
Twort, FW. 1915. An Investigation on the Nature of Ultra-microscopic Viruses. *Lancet* 2:1241–1243.
UN DESA. 2017. *World Population Prospects: The 2017 Revision, Key Findings and Advance Tables*. UN.
USDA Foreign Agricultural Service. 2006. *Positive seafood report*.
Utech S, Prodanovic R, Mao AS, Ostafe R, Mooney DJ, Weitz DA. 2015. Microfluidic Generation of Monodisperse, Structurally Homogeneous Alginate Microgels for Cell Encapsulation and 3D Cell Culture. *Advanced healthcare materials* 4:1628–1633.
Utting SD, Spencer BE. 1992. Introductions of Marine Bivalve Molluscs into the United Kingdom for Commercial Culture - Case Histories. *ICES mar. Sei. Symp.* 194:84–91.
Varela A. 2018. Transmission of Bacterial Virulence Factors, a Real and Current Threat to Aquaculture Production, a Diagnostic Challenge. *Journal of Microbiology and Experimentation* 6.
Venkateswaran K, Kim SW, Nakano H, Onbé T, Hashimoto H. 1989. The Association of *Vibrio parahaemolyticus* Serotypes with Zooplankton and its Relationship with Bacterial Indicators of Pollution. *Systematic and applied microbiology* 11:194–201.
Vinner GK, Malik DJ. 2018. High Precision Microfluidic Microencapsulation of Bacteriophages for Enteric Delivery. *Research in microbiology* 169:522–530.
Vinner GK, Vladisavljević GT, Clokie MRJ, Malik DJ. 2017. Microencapsulation of *Clostridium difficile* Specific Bacteriophages using Microfluidic Glass Capillary Devices for Colon Delivery using Ph Triggered Release. *PloS one* 12:e0186239.
Vinod MG, Shivu MM, Umesha KR, Rajeeva BC, Krohne G, Karunasagar I, Karunasagar I. 2006. Isolation of *Vibrio harveyi* Bacteriophage with a Potential for Biocontrol of Luminous Vibriosis in Hatchery Environments. *Aquaculture* 255:117–124.
Vonasek EL, Choi AH, Sanchez J Jr, Nitin N. 2018. Incorporating Phage Therapy into WPI Dip Coatings for Applications on Fresh Whole and Cut Fruit and Vegetable Surfaces. *Journal of food science* 83:1871–1879.
Wagley S, Koofhethile K, Rangdale R. 2009. Prevalence and Potential Pathogenicity of *Vibrio parahaemolyticus* in Chinese Mitten Crabs (*Eriocheir sinensis*) Harvested from the River Thames Estuary, England. *Journal of food protection* 72:60–66.
Waldor MK, Mekalanos JJ. 1996. Lysogenic Conversion by a Filamentous Phage Encoding Cholera Toxin. *Science* 272:1910–1914.
Wang W, Li M, Lin H, Wang J, Mao X. 2016. The *Vibrio parahaemolyticus*-Infecting Bacteriophage qdvp001: Genome Sequence and Endolysin with a Modular Structure. *Archives of virology* 161:2645–2652.
Wang M, Liu P, Zhou Q, Tao W, Sun Y, Zeng Z. 2018. Estimating the Contribution of Bacteriophage to the Dissemination of Antibiotic Resistance Genes in Pig Feces. *Environmental pollution* 238:291–298.
Warwick-Dugdale J, Buchholz HH, Allen MJ, Temperton B. 2019a. Host-Hijacking and Planktonic Piracy: How Phages Command the Microbial High Seas. *Virology journal* 16:15.
Warwick-Dugdale J, Solonenko N, Moore K, Chittick L, Gregory AC, Allen MJ, Sullivan MB, Temperton B. 2019b. Long-Read Viral Metagenomics Captures Abundant and Microdiverse Viral Populations and their Niche-Defining Genomic Islands. *PeerJ* 7:e6800.

Watts JEM, Schreier HJ, Lanska L, Hale MS. 2017. The Rising Tide of Antimicrobial Resistance in Aquaculture: Sources, Sinks and Solutions. *Marine drugs* 15.

Wee S, Gombotz WR. 1998. Protein Release from Alginate Matrices. *Advanced drug delivery reviews* 31:267–285.

Weinbauer MG. 2004. Ecology of Prokaryotic Viruses. *FEMS microbiology reviews* 28:127–181.

Whitesides GM. 2006. The Origins and the Future of Microfluidics. *Nature* 442:368–373.

Wick RR, Judd LM, Gorrie CL, Holt KE. 2017. Unicycler: Resolving Bacterial Genome Assemblies from Short and Long Sequencing Reads. *PLoS computational biology* 13:e1005595.

Williams RC, Fraser D. 1953. Morphology of the Seven T-Bacteriophages. *Journal of bacteriology* 66:458–464.

Witherall L, Wagley S, Butler C, Tyler CR, Temperton B. 2019. Genome Sequences of Four *Vibrio parahaemolyticus* Strains Isolated from the English Channel and the River Thames. *Microbiology resource announcements* 8.

Wong HC, Wang P. 2004. Induction of Viable but Nonculturable State in *Vibrio parahaemolyticus* and its Susceptibility to Environmental Stresses. *Journal of applied microbiology* 96:359–366.

Wong H-C, Wang T-Y, Yang C-W, Tang C-T, Ying C, Wang C-H, Chang W-H. 2018. Characterization of a Lytic Vibriophage VP06 of *Vibrio parahaemolyticus*. *Research in microbiology*.

Xiao J, Liu L, Ke Y, Li X, Liu Y, Pan Y, Yan S, Wang Y. 2017. Shrimp AHPND-Causing Plasmids Encoding the PirAB Toxins as Mediated by pirAB-Tn903 are Prevalent in Various *Vibrio* Species. *Scientific reports* 7:42177.

Xu JH, Li SW, Tan J, Wang YJ, Luo GS. 2006. Controllable Preparation of Monodisperse O/W and W/O Emulsions in the Same Microfluidic Device. *Langmuir: the ACS journal of surfaces and colloids* 22:7943–7946.

Yang F, Shen C, Zheng X, Liu Y, El-Sayed Ahmed MAE-G, Zhao Z, Liao K, Shi Y, Guo X, Zhong R, Xu Z, Tian G-B. 2019. Plasmid-Mediated Colistin Resistance Gene mcr-1 in *Escherichia coli* and *Klebsiella pneumoniae* Isolated from Market Retail Fruits in Guangzhou, China. *Infection and drug resistance* 12:385–389.

Yin Y, Ni P 'en, Liu D, Yang S, Almeida A, Guo Q, Zhang Z, Deng L, Wang D. 2019. Bacteriophage Potential against *Vibrio parahaemolyticus* Biofilms. *Food control* 98:156–163.

Yoon KS, Min KJ, Jung YJ, Kwon KY, Lee JK, Oh SW. 2008. A Model of the Effect of Temperature on the Growth of Pathogenic and Nonpathogenic *Vibrio parahaemolyticus* Isolated from Oysters in Korea. *Food microbiology* 25:635–641.

Yu Y-P, Gong T, Jost G, Liu W-H, Ye D-Z, Luo Z-H. 2013. Isolation and Characterization of Five Lytic Bacteriophages Infecting a *Vibrio* Strain Closely Related to *Vibrio owensii*. *FEMS microbiology letters* 348:112–119.

Zanetti S, Spanu T, Deriu A, Romano L, Sechi LA, Fadda G. 2001. *In vitro* Susceptibility of *Vibrio* spp. Isolated from the Environment. *International journal of antimicrobial agents* 17:407–409.

Zhang Y, Hu L, Qiu Y, Osei-Adjei G, Tang H, Zhang Y, Zhang R, Sheng X, Xu S, Yang W, Yang H, Yin Z, Yang R, Huang X, Zhou D. 2019a. QsvR Integrates into Quorum Sensing Circuit to Control *Vibrio parahaemolyticus* Virulence. *Environmental microbiology*.

Zhang G, Sun K, Ai G, Li J, Tang N, Song Y, Wang C, Feng J. 2019b. A Novel Family of Intrinsic Chloramphenicol Acetyltransferase CATC in *Vibrio parahaemolyticus*: Naturally Occurring Variants Reveal Diverse Resistance Levels against Chloramphenicol. *International journal of antimicrobial agents*.

Zhang H, Yang Z, Zhou Y, Bao H, Wang R, Li T, Pang M, Sun L, Zhou X. 2018. Application of a Phage in Decontaminating *Vibrio parahaemolyticus* in Oysters. *International journal of food microbiology* 275:24–31.

Zhao Y, Temperton B, Thrash JC, Schwalbach MS, Vergin KL, Landry ZC, Ellisman M, Deerinck T, Sullivan MB, Giovannoni SJ. 2013. Abundant SAR11 Viruses in the Ocean. *Nature* 494:357–360.

Zilionis R, Nainys J, Veres A, Savova V, Zemmour D, Klein AM, Mazutis L. 2017. Single-Cell Barcoding and Sequencing using Droplet Microfluidics. *Nature protocols* 12:44–73.